THE AMBIENT ORGANIC AEROSOL SOLUBLE IN WATER: MEASUREMENTS, CHEMICAL CHARACTERIZATION, AND AN INVESTIGATION OF SOURCES

A Dissertation
Presented to
The Academic Faculty

By

Amy P. Sullivan

In Partial Fulfillment
Of the Requirements for the Degree
Doctor of Philosophy in Atmospheric Chemistry

Georgia Institute of Technology
August 2006

THE AMBIENT ORGANIC AEROSOL SOLUBLE IN WATER: MEASUREMENTS, CHEMICAL CHARACTERIZATION, AND AN INVESTIGATION OF SOURCES

Approved By:

Dr. Rodney J. Weber, Advisor
School of Earth and Atmospheric Sciences
Georgia Institute of Technology

Dr. Michael H. Bergin
School of Earth and Atmospheric Sciences and School of Civil and Environmental Engineering
Georgia Institute of Technology

Dr. L. Gregory Huey
School of Earth and Atmospheric Sciences
Georgia Institute of Technology

Dr. Martial Taillefert
School of Earth and Atmospheric Sciences
Georgia Institute of Technology

Dr. Paul H. Wine
School of Earth and Atmospheric Sciences and School of Chemistry and Biochemistry
Georgia Institute of Technology

Date Approved: April 19, 2006

ACKNOWLEDGEMENTS

First and foremost, I would like to thank my advisor Dr. Rodney J. Weber. It has been my pleasure to work for him during the past six years. Through my work with Rodney I have not only been able to learn from his expertise, but have been given many amazing opportunities to investigate in the lab and field. The experience has been invaluable in the development of my skills as a research scientist. But most importantly, I would like to thank him for always believing in me and encouraging me to push the limits.

I would also like to acknowledge a number of fellow colleagues in Earth and Atmospheric Sciences. I would like to thank Drs. Jason D. Ritchie and E. Michael Perdue for their insights regarding the XAD-8 and SEC columns and procedures, Drs. Poulomi Sannigrahi and Ellery D. Ingall for their help with the ^{13}C-NMR sample preparation and analysis, Akua Asa-Awuku and Dr. Athanasios Nenes for the surface tension measurements, Bo Yan, Dr. Mei Zheng, and Dr. Armistead Russell for the generous use of the Hi-Volume Samplers and help in collecting the paired experiment samples, and Dr. Karsten Baumann (now at RTI International) for providing the biomass burning samples. I would also like to thank my fellow past and present group members, especially Richard E. Peltier who helped run the PILS-TOC during the NEAQS/ITCT 2004 Study.

I would also like to acknowledge a number of people I worked with during various field campaigns. I thank Andrea L. Clements (now at the California Institute of Technology) and Dr. Jay R. Turner of Washington University in St. Louis for assistance

with the St. Louis – Midwest Supersite measurements, Drs. Min-Suk Bae (now at the University at Albany, State University of New York) and James J. Schauer of the University of Wisconsin–Madison for the St. Louis – Midwest Supersite OC data, Dr. Eric Edgerton of Atmospheric Research and Analysis, Inc. for his assistance in arranging the Yorkville sampling, and the NOAA WP-3D crew, support team, and collaborators during NEAQS/ITCT 2004, especially Drs. Charles A. Brock, Joost A. de Gouw, John S. Holloway, Carsten Warneke, and Adam G. Wollny of the Chemical Sciences Division at the NOAA Earth Systems Research Laboratory and Cooperative Institute for Research in Environmental Sciences and Dr. Elliot L. Atlas of the University of Miami.

I also thank the Air Quality System, Office of Air Quality Planning and Standards, U.S. EPA for the ozone, $PM_{2.5}$ mass, and PAMS VOC data. The interpretations based on this data are those solely of the author. I also gratefully acknowledge the NOAA Air Resources Laboratory (ARL) for the provision of the HYSPLIT transport and dispersion model and/or READY website (http://www.arl.noaa.gov/ready.html) used in this thesis.

TABLE OF CONTENTS

LIST OF TABLES

LIST OF FIGURES

LIST OF ABBREVIATIONS

^{13}C-NMR = ^{13}Carbon-Nuclear Magnetic Resonance

AMS = aerosol mass spectrometer

ARL = Air Resources Laboratory

CCN = cloud condensation nuclei

CO = carbon monoxide

CST = central standard time

DI Water = deionized water

EC = elemental carbon

EDT = eastern daylight time

EPA = Environmental Protection Agency

FTIR = Fourier transform infrared

GC = gas chromatography

GC/MS = gas chromatography/mass spectroscopy

GIT = Georgia Institute of Technology

HCl = hydrochloric acid

H-NMR = proton-nuclear magnetic resonance

HULIS = humic-like substances found in the aerosol

IC = ion chromatograph

ICARTT = International Consortium for Atmospheric Research on Transport and Transformation

LC/MS = liquid chromatography/mass spectroscopy

LOD = limit of detection

LTI = low turbulence inlet

MACR = methacrolein

MVK = methyl vinyl ketone

NaOH = sodium hydroxide

NEAQS/ITCT = New England Air Quality Study/Intercontinental Transport and Chemical Transformation

$(NH_4)_2S_2O_8$ = ammonium persulfate

NOAA = National Oceanic and Atmospheric Administration

NOM = natural organic matter

O_3 = ozone

OC = organic carbon

OPC = optical particle counter

PAMS = Photochemical Assessment Monitoring Stations

PEEK = polyetheretherketone

PILS = Particle-into-Liquid Sampler

PM_1 = particles with aerodynamic diameters less than 1 μm

$PM_{2.5}$ = particles with aerodynamic diameters less than 2.5 μm

PTR-MS = proton transfer reaction – mass spectrometer

SEC = size-exclusion chromatography

SOA = secondary organic aerosol

SO_2 = sulfur dioxide

SO_4^{-2} = sulfate

SPE = solid phase extraction

TOC = Total Organic Carbon (analyzer)

TOT = thermal/optical transmission

UTC = coordinated universal time

UV = ultraviolet (light)

VOC(s) = Volatile Organic Compound(s)

WIOC = water-insoluble organic carbon (calculated from OC – WSOC)

WSOC = water-soluble organic carbon

WSOCxp = hydrophilic water-soluble organic carbon, compounds that penetrate the XAD-8 column at pH 2 adjusted by 0.1 M HCl (measured with Total Organic Carbon (TOC) analyzer)

WSOCxp_a = hydrophilic aliphatic acids, includes mono-/di-/oxocarboxylic acids with less than 4 or 5 carbons (measured with TOC analyzer)

WSOCxp_b = hydrophilic bases (measured with TOC analyzer)

WSOCxp_n = hydrophilic neutrals, includes saccharides, polyols, and carbonyls with less than 4 or 5 carbons (measured with TOC analyzer)

WSOCxp_u = SEC unrecovered hydrophilic compounds (calculated from WSOCxp – WSOCxp_a – WSOCxp_n – WSOCxp_b)

WSOCxr = hydrophobic water-soluble organic carbon, compounds that are retained on the XAD-8 column (calculated from WSOC – WSOCxp)

WSOCxrr = recovered hydrophobic water-soluble organic carbon, compounds that are retained on the XAD-8 column and subsequently recovered from the XAD-8 using 0.1 M NaOH at pH 13 (measured with TOC analyzer)

WSOCxrr_a = recovered hydrophobic acids, includes aromatics with no O-H groups (i.e., no N/O substituted aromatic bonds) or other compounds with similar properties as determined by interactions with XAD-8 resin (measured with TOC analyzer)

WSOCxrr_n = recovered hydrophobic neutrals, includes aromatics with at least one N/O substituted aromatic bond, such as phenols, or other compounds with similar properties as determined by interactions with XAD-8 resin (measured with TOC analyzer)

WSOCxrr_u = SEC unrecovered hydrophobic compounds, includes non-ionizable compounds with large log K_{ow} (calculated from WSOCxrr – WSOCxrr_a – WSOCxrr_n)

WSOCxru = unrecovered hydrophobic water-soluble organic carbon, compounds that are retained on the XAD-8 column and are not recovered from the XAD-8 in the 0.1 M NaOH at pH 13, includes organic nitrates, cyclic acids, and mono- and dicarboxylic acids with greater than 3 or 4 carbons (calculated from WSOC – WSOCxp – WSOCxrr)

SUMMARY

This thesis characterizes the ambient fine organic carbon (OC) aerosol and investigates its sources through the development and deployment of new analytical measurement techniques. Recognizing that OC is highly chemically complex, the approach was to develop methods capable of quantitatively measuring a large chemical fraction of the aerosol instead of specific chemical speciation. The focus is on organic compounds that are soluble in water (WSOC) since little is known about its chemical nature. The results from this thesis show that WSOC has mainly two sources: biomass burning and secondary organic aerosol (SOA). In urban areas, WSOC increases with plume age, and tracks other photochemically produced compounds. Chemical analysis of WSOC suggests that in urban Atlanta, the SOA is mainly small-chain aliphatic compounds indirectly linked to vehicle emissions.

A method was first developed for quantitative on-line measurements of WSOC by extending the application of the Particle-into-Liquid Sampler (PILS) from inorganic to organic aerosol measurements. In this approach a PILS captures ambient particles into a flow of purified water, which is then forced through a liquid filter and the carbonaceous content quantified on-line by a Total Organic Carbon (TOC) analyzer. An instrument was first developed for ground-based measurements and then modified for airborne deployment.

Ground-based measurements at the St. Louis - Midwest Supersite during the summer of 2003 showed that the fraction of OC that is water-soluble can have a highly diurnal pattern with WSOC to OC ratios reaching 0.80 during the day and lows of 0.40

during the night. During extended periods under stagnation pollution events, this pattern was well correlated with ozone concentrations. The results are consistent with formation of SOA.

Airborne PILS-TOC measurements from the NOAA WP-3D during the New England Air Quality Study/Intercontinental Transport and Chemical Transformation (NEAQS/ITCT) 2004 program investigated WSOC sources over the northeastern U.S. and Canada. Two main sources were identified: biomass burning emissions from fires in the Alaska/Yukon region and emissions emanating from urban centers. Biomass burning WSOC was correlated with carbon monoxide (CO) and acetonitrile ($R^2 > 0.88$). Apart from the biomass burning influence, the highest concentrations were at low altitudes in distinct plumes of enhanced particle concentrations from urban centers. WSOC and CO were highly correlated ($R^2 > 0.78$) in these urban plumes. The ratio of the enhancement in WSOC relative to that of CO was found to be low (~ 3 μg C/m^3/ppmv) in plumes that had been in transit for a short time, and increased with plume age, but appeared to level off at ~32 μg C/m^3/ppmv after approximately one day of transport from the sources. The results suggest WSOC in fine particles is produced from compounds co-emitted with CO and that these emissions are rapidly converted to organic particulate matter within ~1 day following emission.

To further chemically investigate the organic constituents of WSOC, a method for group speciation of the WSOC into hydrophilic and hydrophobic fractions has been developed using a XAD-8 resin column. XAD-8 resin coupled with a TOC analyzer allows for direct quantification. Based on laboratory calibrations with atmospherically relevant standards and ^{13}C-NMR (^{13}Carbon-Nuclear Magnetic Resonance) analysis, the

hydrophilic fraction (compounds that penetrate the XAD-8 with near 100% efficiency at pH 2) is composed of short-chain carboxylic acids and carbonyls and saccharides. The fraction of WSOC retained by XAD-8, termed the hydrophobic fraction, includes aromatic acids, phenols, organic nitrates, cyclic acids, and carbonyls and mono-/dicarboxylic acids with greater than 3 or 4 carbons. Only aromatic compounds (or aromatic-like compounds with similar properties) can subsequently be extracted from XAD-8 with high efficiency and are referred to as the recovered hydrophobic fraction.

By coupling a PILS with this technique, on-line measurements of WSOC, hydrophilic WSOC, and hydrophobic WSOC are possible. Urban measurements from St. Louis and Atlanta, on a carbon mass basis, show an increase in the mean WSOC fraction from winter (51%) to summer (61%), due to increases in the hydrophilic WSOC to OC ratio from 0.25 to 0.35. During a summer Atlanta PM event, WSOC to OC was 0.75, driven largely by increases in the hydrophilic WSOC fraction. The results are consistent with the view that in the summer there are increased amounts of oxygenated polar compounds, that are mainly hydrophilic and possibly from SOA production. These compounds can account for an even larger fraction of OC during stagnation events.

The XAD-8 resin can also be used in the first step of a two-step off-line method to isolate chemical fractions of ambient organic aerosol based on acid, neutral, and basic functional groups. The second step is a newly developed method involving size-exclusion chromatography (SEC) to separate the hydrophilic WSOC and recovered hydrophobic WSOC compounds by organic functional group. Calibrations show that hydrophilic WSOC separates into short-chain aliphatic acids, neutrals (e.g. saccharides,

polyols, and short-chain carbonyls), and organic bases. The recovered hydrophobic compounds are separated into acids (e.g., aromatic) and neutrals (e.g., phenols).

Comparisons are made between XAD-8/SEC results from urban Atlanta summer and winter, and biomass burning samples. During the summer in Atlanta, approximately 20% of the OC (on a carbon mass basis) is due to hydrophilic aliphatic acids and recovered hydrophobic acids. The hydrophilic aliphatic acids are additionally the largest isolated fraction of Atlanta summer WSOC (29% μg C/μg C), suggesting aliphatic acids of less than C_4 or C_5 are the dominant SOA product, and are also correlated with the recovered hydrophobic acids ($R^2 = 0.74$), elemental carbon ($R^2 = 0.64$), CO ($R^2 = 0.73$), and VOCs (Volatile Organic Compounds) expected from mobile source emissions such as isopentane ($R^2 = 0.67$) and acetylene ($R^2 = 0.61$). Biomass burning samples, however, were dominated by the hydrophilic and recovered hydrophobic neutral compounds. In the winter, when the WSOC is much lower, the samples tended to be a combination of the other two sample types.

Combining the results of these various WSOC measurements over Atlanta and its surrounding regions, the data indicate that the source of WSOC is indirectly linked to vehicle emissions. Aircraft measurements show that WSOC is correlated with CO over large regions, and that the ratio of the metropolitan Atlanta ΔWSOC/ΔCO is similar to that in urban plumes in the northeastern U.S. Over a wide geographical region (~100 km) WSOC is comprised of three major chemical groups (> 70%) that increase in concentration under more polluted conditions, and appear to be linked to a similar source. The fraction of the organic aerosol that is water-soluble varies between roughly 0.40 and

0.75 depending on the location, with higher ratios in regions further from mobile source emissions.

CHAPTER 1
INTRODUCTION

1.1. Importance of Water-Soluble Organic Carbon

The carbonaceous component remains one of the least well-understood chemical fractions of ambient particles. These compounds are important because they can comprise a large fraction of the fine particle mass, 10 to 70% [*Andrews et al.*, 2000], and may influence atmospherically important properties of aerosol particles. Organic carbon (OC) is directly emitted from a wide range of sources including combustion of fossil fuels, direct injection of unburnt fuel and lubricants, industrial emissions, plant matter, biomass burning, and biogenic emissions [*Jacobson et al.*, 2000]. Studies suggest that under certain conditions a large fraction of the ambient OC can be produced from secondary organic aerosol (SOA) formation from biogenic emissions and combustion sources. The organic aerosol has been found to be highly chemically complex including compounds ranging from relatively water-soluble to insoluble.

Traditionally, chemical characterization of the organic aerosol has been performed on an individual compound basis. Although techniques such as gas chromatography/mass spectroscopy (GC/MS) can provide detailed information on a wide range of specific compounds, only a small fraction of these compounds have been characterized [*Schauer et al.*, 1996; *Hamilton et al.*, 2004]. For example, *Hamilton et al.* [2004] isolated 10,000 individual organic compounds with a wide range of chemical functionalities in the urban aerosol using thermal desorption coupled with gas chromatography (GC) and time of flight – mass spectroscopy. However, only a fraction of these compounds could be identified and quantification was not even attempted.

A potential solution to this problem is to isolate the organic aerosol into broad and comprehensive chemical fractions. This would simplify the complexity and provide samples for further analysis. One approach is to focus on the fraction of organic aerosol that is soluble in water. The water-soluble organic carbon (WSOC) fraction tends to be an operationally-defined quantity since solubility of some (although likely a small) fraction of the organic aerosol may depend on the solution concentrations, which are determined by the experimental procedure, and the pH of all protolyzable compounds. However, by employing a consistent extraction method, significant changes in the water-soluble fraction over time will provide evidence for changes in aerosol composition over time. WSOC in aerosol particles is not well understood in part because most previous organic carbon analyses have involved GC separation methods that are not readily applicable to polar compounds.

The water-soluble fraction is of interest for a number of reasons. WSOC can at times be a large fraction of the carbonaceous component. *Zappoli et al.* [1999] found, based on integrated filter measurements, that fine particle WSOC accounted for 77, 48, and 65% of the fine particle organic carbon in European background, rural, and polluted sites, respectively. A seasonal study of WSOC in the Po Valley, Italy found that WSOC in the summer and fall accounted for 50 and 47% of the fine particle organic carbon, respectively [*Decesari et al.*, 2001].

Water is an ubiquitous atmospheric component and its interaction with aerosols has significant and wide-ranging consequences. In liquid clouds, water-soluble organic compounds may contribute to or impede the ability of aerosol particles to act as cloud condensation nuclei (CCN) [*Novakov and Penner*, 1993; *Novakov and Corrigan*, 1996;

Facchini et al., 1999]. These compounds may also affect particles's hygroscopicity, the uptake of water vapor (or lack of) under sub-saturated conditions. *Saxena et al.* [1995] have provided evidence that particle-phase organics enhance water uptake by atmospheric particles in some locations and inhibit or retard water uptake in other locations. In a non-urban area (the Grand Canyon) the presence of organic compounds enhanced water absorption by particles and accounted for 25 to 40% of the total water uptake. In an urban area (Los Angeles) the presence of organic compounds inhibited water uptake by about 25 to 35%. These interactions between particle chemistry and water vapor can affect visibility and the global radiation budget. The hygroscopic nature of individual particles can also influence their life spans, which is often dictated by precipitation scavenging.

WSOC can have unique physical properties. For example, *Facchini et al.* [2000] have shown that the WSOC fraction can significantly depress the surface tension of aqueous solutions. This may be one way that organic compounds can affect ambient particles's hygroscopicity and their ability to serve as CCN as discussed above.

Finally, it is believed that one of the major sources of WSOC is through SOA formation [*Saxena and Hildemann*, 1996], a process that is not well understood. SOA generally refers to the organic compounds that partition from the gas-phase to the aerosol phase from products of gas-phase oxidation reactions of parent organic compounds. This occurs because gas-phase organic compounds can often undergo oxidation processes in the gas-phase. These processes will lead to low vapor pressure products which, in turn, are able to partition to the aerosol phase. Condensed-phase multifunctional organic products are expected from the oxidation of larger (carbons > 5) alkenes, cyclic alkenes,

and aromatic hydrocarbons [*Grosjean and Seinfeld*, 1989; *Grosjean*, 1992]. Often these SOA products are oxygenated, and hence water-soluble. WSOC compounds formed via these reactions can include dicarboxylic acids, oxocarboxylic acids, dicarbonyls, organic nitrates, and aromatic acids.

SOA formation is generally studied by running controlled smog chamber experiments. Organic gaseous precursors are mixed with oxidants such as ozone or the hydroxyl radical. The particle products formed can be analyzed off-line by collection of integrated filters or on-line using such techniques as a PTR-MS (Proton Transfer Reaction – Mass Spectrometer) or an AMS (Aerosol Mass Spectrometer). Although these smog chamber studies have provided useful information, often the conditions are not representative of the atmosphere. For example, precursor concentrations are generally considerably higher than what is typically found in the atmosphere so that reaction products can be detected [*Kanakidou et al.*, 2005].

SOA reactions, determined from smog chamber studies, which are likely to form water-soluble organic compounds are discussed below. Larger gaseous alkenes are mainly emitted to the atmosphere by anthropogenic sources, including motor vehicle exhaust and gasoline. Cyclic gaseous alkenes can also be emitted from motor vehicle exhaust and gasoline. These larger alkenes can form via oxidation processes straight-chain aldehydes, monocarboxylic acids, and lactones [*Forstner et al.*, 1997a]. Whereas the cycloalkenes can form straight-chain dicarboxylic acids, oxocarboxylic acids, and dialdehydes. The transformation of the aerosol in the particle phase is likely to be dialdehyde to oxocarboxylic acid to dicarboxylic acid [*Hatakeyama et al.*, 1987].

Cyclic gaseous alkenes also include terpenes and sesquiterpenes, which are emitted from biogenic sources. These terpenes and sesquiterpenes also produce dicarboxylic acids, oxocarboxylic acids, and aldehydes, although the aerosols produced via oxidation from these biogenic hydrocarbons are often in their cyclic form [*Glasius et al.*, 2000]. Until recently it was believed non-cyclic biogenic alkenes, such as isoprene, at low concentrations lead to insignificant SOA production [*Pandis et al.*, 1991; *Edney et al.*, 2005]. However, under high-NO_x conditions it may be significant [*Kroll et al.*, 2005].

Aromatic gaseous hydrocarbons are generally derived from anthropogenic sources. These include gasoline and engine oil vapors, and automobile exhaust. Of particular importance is the oxidation of benzene, toluene, xylenes, ethylbenzene, and 1,2,4-trimethylbenzene, the dominant aromatic hydrocarbons in ambient air. SOA reactions of aromatic hydrocarbons can produce ring-retaining products (aromatic and non-aromatic) as well as ring opening products. The aromatic ring retaining products can include acids, multifunctional phenols, and nitrogen containing compounds. Lactones and cyclohexenes are likely non-aromatic ring reserved products. Ring opening products identified have included carbonyls, hydroxy-carbonyls, and oxocarboxylic acids [*Forstner et al.*, 1997b; *Jang and Kamens*, 2001].

1.2. Current Methods and the Need for Real-time Measurements

The most widely used WSOC sampling technique involves collection of aerosol particles on pre-baked quartz fiber filters followed by manual extraction and analysis. However, in order to obtain sufficient mass for analysis of organic carbon, sampling

times on the order of hours or greater are typical. These long sampling times limit investigations into the WSOC sources and the processes that affect ambient concentrations since concentrations cannot be followed over time. Additionally, extended sampling periods can also lead to positive artifacts since collected gas-phase carbonaceous material is analyzed with the particulate matter. Negative artifacts are caused by the loss of semi-volatile organic material collected on a filter during sampling. Long sampling periods tend to enhance these losses by exposing collected particles to wider ranges of ambient conditions during the sampling period [*McDow and Huntzicker*, 1990].

There is a need for real-time measurements of WSOC to alleviate the tedious work and much of the uncertainties associated with making manual filter measurements. Also atmospheric processes that affect fine particulate carbon concentrations usually have a time scale of minutes to hours. A faster time resolution measurement would allow transient events to be detected, which filter measurements often miss. Near real-time measurements could provide information relevant to human exposure and acute health effects. Additionally, quantitative airborne measurements of the carbonaceous fraction can be of significant value since it would provide information on spatial distributions and facilitate the study of aerosol plume chemical evolution.

Generally, airborne measurements of organic carbon are scarce. Measurements were made over the east coast of the United States [*Novakov et al.*, 1997], the Indian Ocean [*Mayol-Bracero et al.*, 2002a], over southern Africa during the dry biomass burning season [*Kirchstetter et al.*, 2003], and in Asian outflow [*Huebert et al.*, 2004]. In all cases particles were collected onto pre-baked quartz filters. *Huebert et al.* [2004] used

an off-line Sunset Labs thermal/optical analyzer for the carbon analysis (Forest Grove, Oregon), whereas the other three studies used evolved gas analysis. *Maria et al.* [2002, 2003] have made airborne measurements of organic carbon functional groups with Fourier transform infrared (FTIR) analysis of solvent extracted filters. *Kawamura et al.* [2003] measured specific water-soluble dicarboxylic acids over east Asia and the western North Pacific using GC/MS analysis of quartz filter extracts. These methods were generally limited by long sampling times leading to few data points and poor spatial resolution. Detection limits were typically poor and artifacts a significant issue.

Measurements based on mass spectrometers have recently been used to quantitatively measure carbonaceous aerosol on-line from aircraft [*Bahreini et al.*, 2003]. These methods provide unique size-resolved data of the volatile fraction of the aerosol particles, and chemically group the carbonaceous material by their mass spectra and not by specific compound or physical property. For 1 minute averaged organic data a detection limit of 11.7 $\mu g/m^3$ was reported.

In the research presented in this dissertation, a new method has been developed for quantitative semi-continuous on-line measurements of WSOC both on the ground and airborne. The approach is an extension of the method used for on-line measurements of water-soluble inorganic compounds involving a Particle-into-Liquid Sampler (PILS) coupled directly to ion chromatographs (IC) [*Weber et al.*, 2001; *Orsini et al.*, 2003]. For this new technique, however, the PILS is connected to a Total Organic Carbon (TOC) Analyzer. A detailed description of the components of this method will be provided in chapter 2. Results showing its capabilities both on the ground in St. Louis and airborne during the New England Air Quality Study/Intercontinental Transport and Chemical

Transformation (NEAQS/ITCT) 2004 mission conducted in the northeastern U.S. will be presented in chapters 3 and 4 respectively.

1.3. WSOC Composition and Speciation

Studies have shown that WSOC is composed of compounds such as aliphatic and aromatic carboxylic acids, carbonyls, polyols, organic nitrates, and amines. WSOC is likely mainly oxygenated compounds with functional groups such as COOH, COH, C=O, COC, $CONO_2$, CNO_2, and CNH_2 [*Saxena and Hildemann*, 1996, and references within].

There are many known primary and secondary sources, biogenic as well as anthropogenic, for these compounds. Motor vehicle emissions can directly produce aliphatic and aromatic acids and aldehydes. Aliphatic acids and aldehydes can also be directly emitted from vegetation. Emitted gaseous aliphatic and aromatic anthropogenic hydrocarbons can produce aliphatic and aromatic carboxylic acids and aldehydes via SOA formation [*Kawamura et al.*, 1985; *Khwaja*, 1995; *Forstner et al.*, 1997b; *Seinfeld and Pandis*, 1998; *Finlayson-Pitts and Pitts*, 2000]. Biogenic volatile organic compounds (VOCs), such as pinene, can produce cyclic acids and long-chain aldehydes as SOA products [*Seinfeld and Pandis*, 1998; *Glasius et al.*, 2000].

In particular, many biomass burning compounds have been found to be water-soluble [*Novakov and Corrigan*, 1996; *Narukawa et al.*, 1999; *Graham et al.*, 2002; *Mayol-Bracero et al.*, 2002b]. Biomass burning WSOC has been shown to be predominately aliphatic, composed mainly of oxygenated compounds [*Graham et al.*, 2002]. A minor content of aromatic compounds containing carboxylic acids and phenols has also been observed.

A variety of different off-line methods have been developed to try to characterize these various compounds and functional groups within the WSOC. *Decesari et al.* [2000] developed a technique involving chromatographic separation of the WSOC using an anion exchange diethylaminoethyl (DEAE)-TSK gel column to give three groups: FR1 (Fraction 1, neutral and/or basic compounds), FR2 (Fraction 2, mono- and dicarboxylic acids), and FR3 (Fraction 3, polyacidic compounds). Proton-Nuclear Magnetic Resonance (H-NMR) suggested that FR1 was composed of polyols or polyethers, FR2 hydroxylated aliphatic acids, and FR3 unsaturated polyacidic compounds of predominately aliphatic character, with minor content of hydroxyl-groups. Though some compounds may not be separated into their expected groups [*Chang et al.*, 2005]. Using this method it has been observed in the Po Valley, Italy, that the polycarboxylic acids were the most abundant in all seasons, except for the summer when the mono- and dicarboxylic acids dominated [*Decesari et al.*, 2001].

Krivácsy et al. [2001] have developed a two-step SPE (solid phase extraction) technique using Merck LiChrolut RP-18 SPE columns to give three fractions: Fraction I (slightly hydrophilic, partly acidic, highly polyconjugated), Fraction II (moderately hydrophilic, acidic, moderately polyconjugated), and Fraction III (very hydrophilic, neutral, slightly polyconjugated). This study found that there were two main fractions in ambient fine particles, highly polyconjugated weak polyacids (or humic-like substances, often referred to as HULIS) and slightly polyconjugated, very hydrophilic, neutral compounds, that were each approximately 50% of WSOC.

A one-step SPE on a Waters Oasis HLB column to separate the WSOC into moderately hydrophilic (retained on the column) and strongly hydrophilic (passed

through the column) was developed by *Kiss et al.* [2002]. They observed that the hydrophilic fraction that passed through the column contained more polar functional groups than the fraction retained on the column and lacked polyconjugated structures, suggesting a composition of short-chain carboxylic acids, hydroxy-acids, or polyhydroxy compounds.

These speciation methods of *Decesari et al.* [2000], *Krivácsy et al.* [2001], and *Kiss et al.* [2002] have all suggested the presence of HULIS in the WSOC aerosol, apparently associated with the hydrophobic WSOC fraction. These compounds are of interest since they have unique properties, including light absorption and surface activity [*Havers et al.*, 1998; *Facchini et al.*, 2000]. HULIS has been found in biomass burning [*Mukai and Ambe*, 1986; *Mayol-Bracero et al.*, 2002b], soot oxidation [*Decesari et al.*, 2002], secondary aerosol formation via heterogeneous reaction of isoprenoid and terpenoid compounds catalyzed by sulfuric acid aerosols particles [*Limbeck et al.*, 2003], and photooxidation of aromatics that leads to polyacids after ~20 hours [*Kalberer et al.*, 2004]. Therefore HULIS can be both primary and secondary in nature.

These methods have provided unique quantitative information, however, the main sources of these compounds have not been identified and important atmospheric processes that may alter chemical and physical properties remains unknown. In this study, new methodologies to group speciate the water-soluble organic carbon aerosol using XAD-8 resin and size-exclusion chromatography (SEC) have been developed. First, an on-line quantitative method that couples a PILS-TOC with a XAD-8 column in order to group speciate the WSOC into its hydrophilic and hydrophobic fractions is described in chapter 5. Ambient results from urban sites are presented as well. Second,

an off-line method that uses SEC to further separate samples by functional group, which have first been fractionated by the XAD-8, is described in chapter 6. Results from samples collected from urban Atlanta during the summer and winter are compared to biomass burning samples collected in rural Georgia in a region of prescribed burning. The goals are to assess these methods, chemically identify a large portion of the ambient fine particle organic aerosol in urban environments, and investigate possible sources.

As previously mentioned since the organic aerosol is so complex the sources of WSOC have not been well understood. Therefore, in chapter 7 all the information gained by these techniques to analyze and speciate WSOC will be used to better characterize the sources of WSOC in the southeastern U.S.

CHAPTER 2
INSTRUMENT DESIGN

This chapter provides a detailed description of the components of the Particle-into Liquid Sampler – Total Organic Carbon (PILS-TOC) system. This instrument can be used to make quantitative semi-continuous on-line measurements of WSOC both on the ground and when airborne.

2.1. Particle Collection Method

The PILS [*Weber et al.*, 2001; *Orsini et al.*, 2003] is an approach that combines two proven aerosol technologies: particle growth in a mixing condensation particle counter and droplet collection by a single jet inertial impactor. Ambient particles smaller than 1 μm or 2.5 μm aerodynamic diameter are collected with the PILS by rapidly mixing saturated water vapor with ambient aerosol, which is collected at a flowrate of 15 L/min. (Note, generally a 1 μm size cut MOUDI impactor is used for airborne measurements and a 2.5 μm sharp cut URG cyclone is used for ground-based measurements.) The resulting supersaturated water vapor condenses on all ambient particles larger than approximately 10 to 30 nm. Activated particles grow to a size of roughly 1 to 5 μm diameter, which are then easily collected by an inertial impactor. An accurately metered and adjustable flow of deionized water (DI Water) is pumped over the top of the impaction plate, flows around its perimeter, and merges with the liquid from the droplets. This produces a continuous liquid sample that can be analyzed and quantified by an on-line technique.

The PILS has been used extensively to measure the inorganic aerosol particle bulk composition by coupling it to ion chromatographs (IC) [e.g., *Orsini et al.*, 2003]. In

order to adapt the PILS for a WSOC measurement, minor modifications were made to the PILS-IC method. This included different denuders to remove organic gases, a method for on-line and frequent background measurements, syringe pumps for delivery of the liquid sample, and an in-line liquid filter. A schematic of the system is shown in Figure 2.1.

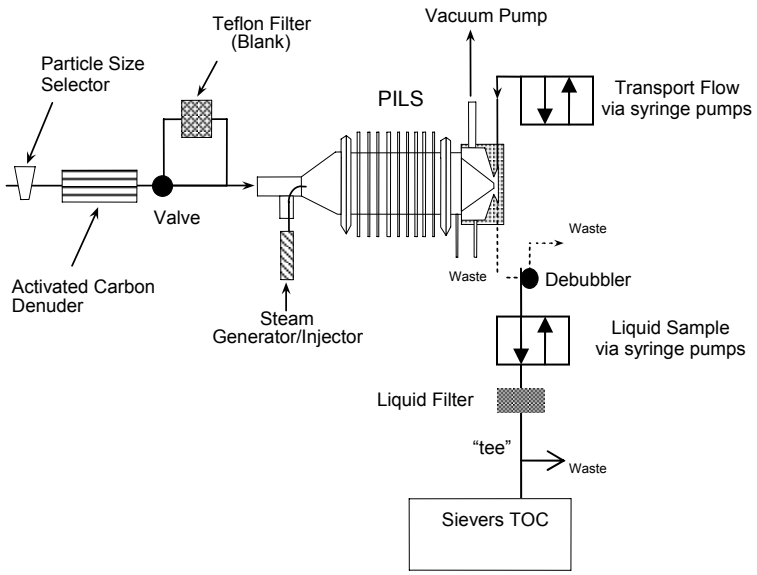

Figure 2.1. Schematic of the Particle-into-Liquid Sampler coupled to a Total Organic Carbon analyzer for measurement of bulk fine particle (PM_1 or $PM_{2.5}$) water-soluble organic carbon.

2.2. Removal of Organic Gases

The removal of some portion of gaseous organic carbon interferences was done by placing a denuder in-line before the PILS-TOC. A denuder removes gas-phase

organics by diffusion to an absorbent surface. For removal of organic gases typically activated carbon is used for the absorbent surface.

Both Eatough parallel plate carbon denuders [*Eatough et al.*, 1993] and MAST monolith carbon denuders (MAST Carbon Ltd., Surrey, UK) have been tested. A 12 inch long Eatough parallel plate activated carbon denuder is used in the PILS-TOC system. The MAST denuders were found to produce artifacts through catalytic cracking, which occurs when larger molecular weight organics are broken down to lower molecular weight organics. Because gaseous lower molecular weight organics are often water-soluble unlike their larger molecular weight counterparts, the carbon monolith denuder results in an increase in background concentrations and poorer measurement sensitivity.

2.3. Instrument Background Interferences

A number of issues must be resolved for making quantitative measurements of WSOC. This includes minimizing and measuring interferences from background carbonaceous material in the sampling system. Background organic carbon in the PILS-TOC system comes from the organic carbon found in DI Water, organic carbon that can desorb from the walls of the liquid sample lines, and any organic gases not removed by the denuder. To determine the concentration of only particulate organic carbon, the real background was determined using a dynamic blank and subtracted from the ambient measurement. This is similar to approaches used in other on-line carbonaceous measurements [*Lim et al.*, 2003]. A normally opened actuated value was periodically closed, via an external timer (ground-based) or computer with appropriate interface (airborne), forcing the sample air flow through a Teflon filter (Zefluor, 47 mm diameter,

2 μm pore size). Other studies [*McDow and Huntzicker*, 1990; *Turpin et al.*, 1994] have suggested that Teflon is an appropriate choice since it efficiently removes particles but not the interfering gases that could effect the WSOC measurement.

For ground-based studies, a background measurement was made every 4 hours for a half hour, whereas for airborne operation a background measurement was made every two hours for 10 minutes. Liquid concentrations from ambient ground-based measurements made at the St. Louis – Midwest Supersite during June 2003 are shown in Figure 2.2a. The difference between the measured (or ambient) and filtered air (background) was interpreted as the ambient aerosol particle WSOC concentration. (Note, the equation used to calculate the WSOC concentration can be found in Appendix A.1.2.) Periodically injecting DI Water directly into the TOC analyzer, independent of the PILS, produced the same background as the filtered air measurements. This indicates that the organic carbon in the DI Water apparently controls the background, and not the absorption of gases. Additionally, no changes were observed in the background when the denuder was removed (not shown). This suggested that positive artifacts due to absorption of gases within the PILS during the aerosol particle measurement were likely minimal in the WSOC measurements.

In the case of airborne measurements, Figure 2.2b shows liquid carbon concentrations for ambient and background measurements from a flight conducted on 27 July 2004 during the NEAQS/ITCT 2004 experiment. As with ground measurements, there was a clear background that was different from the measured signal. There was no evidence for an altitude dependence on background concentrations, and the background measurements within a single flight were fairly steady. At 18:10 UTC (14:10 EDT) a

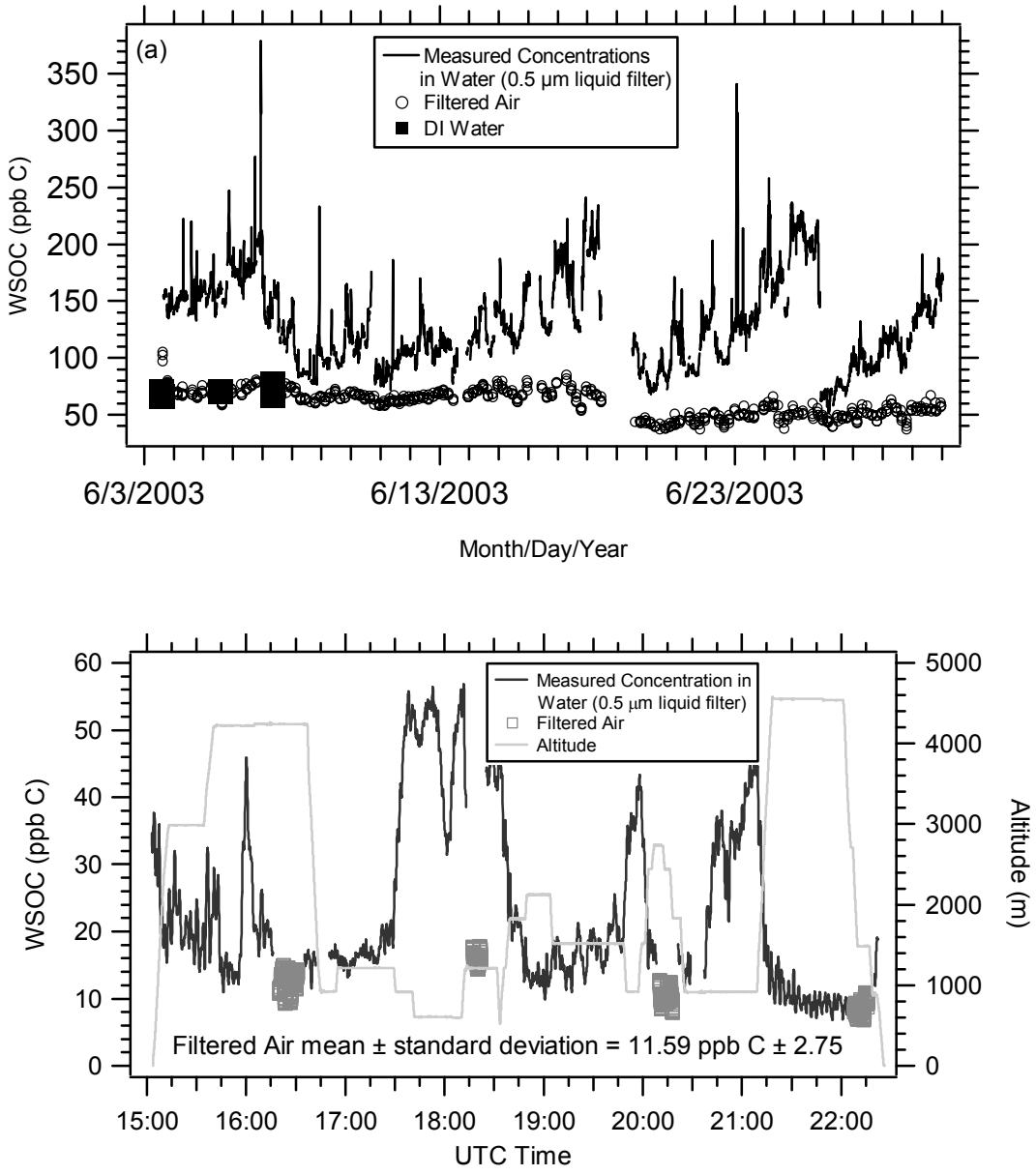

Figure 2.2. Measured TOC liquid concentrations of ambient fine particle WSOC and on-line background measurements (filtered air) for (a) ground-based measurements conducted in June 2003 in St. Louis and (b) airborne measurements from a flight conducted on 27 July 2004. The difference between these curves was the carbon associated with the ambient aerosol. In 2.2a DI water periodically injected directly into the TOC analyzer is also shown. The data gap was due to routine instrument maintenance and replenishing of the water used to operate the instrument. This resulted in a drop in the filtered air due to water with lower organic carbon concentrations. In 2.2b aircraft altitude for the WP-3D is also shown and local time is EDT = UTC – 4 hours.

background measurement that was made in an urban plume where ambient WSOC concentrations were high, is only slightly higher than backgrounds made in clean conditions (~5 ppb C higher than average of other background measurements within that flight). These results are consistent with the ground-based measurements that most background was from interferences in the purified water employed in the PILS system. Greatest background variation was found between flights due to differences in the DI Water purity.

2.4. Liquid Handling System

The liquid sample obtained from the PILS was filtered in-line prior to TOC measurement to remove any insoluble particles. Both 0.5 μm PEEK (polyetheretherketone) and 0.22 μm polypropylene filters have been tested. Little difference was observed between the two filter sizes. Therefore, all the work previous to the speciation measurements (chapters 5 and 6) was conducted with a 0.5 μm filter. During summer ground-based urban continuous measurements, a 0.5 μm filter required daily changes to limit pressure drops across the filter. During the airborne experiment the 0.5 μm filter was changed every second or third flight.

Employing a liquid filter requires that the liquid sample be pressurized to force it through the filter. A continuous flow of liquid sample was pushed through the liquid filter and delivered to the TOC analyzer using two Kloehn Versa 3 syringe pumps (Las Vegas, NV) in "handshaking" mode. (For ground-based measurements all syringes used were 1 ml and for airborne measurements 2.5 ml syringes were used.) In addition, two

similar pumps were used to supply the transport DI Water to the top of the PILS impaction plate.

Use of glass syringe pumps versus a peristaltic pump with polymer tubing appears to also help reduce background WSOC. Two different types of peristaltic pump tubing were tested: Tygon and Santoprene. Santoprene is a non-toxic medical grade rubber. It was found to have a background about half of that of Tygon tubing and was about 20 to 40 ppb C higher than the organic carbon naturally found in DI Water.

All liquid sample lines were narrow bore (0.5 mm ID) PEEK tubing. PEEK is a flexible tubing that is biocompatible and chemically inert. It is used in place of stainless steel, which is the preferred tubing for organic aerosol sampling, for most analytical systems. Unlike Teflon, PEEK was found not to absorb organic compounds.

2.5. TOC Analyzer

A Sievers Model 800 Turbo TOC analyzer (Boulder, CO) was used to determine the organic carbon in the aqueous samples containing the soluble components of the ambient aerosol. The TOC analyzer measures the organic carbon content of a liquid sample by on-line conversion of organic carbonaceous material to carbon dioxide using chemical oxidation via a combination of ultraviolet (UV) light and ammonium persulfate ($(NH_4)_2S_2O_8$). The carbon dioxide formed diffuses through a semi-permeable membrane into a flow of DI Water and is quantified by conductivity detection. The increase in conductivity of the DI Water is proportional to the concentration of aqueous carbon dioxide in the DI Water stream, which is proportional to the concentration of aqueous carbon dioxide formed from the sample. The instrument has two separate channels to

compute total organic carbon by the difference in total carbon (channel where oxidation takes place) and total inorganic carbon (unaltered channel). The analyzer allows for a six minute integrated measurement when run in on-line mode and a 3 s measurement when run in Turbo mode. This persulfate-ultraviolet oxidation method produces similar results as methods employing combustion conversion to carbon dioxide gas with infrared detection. However, unlike the combustion method the persulfate-ultraviolet oxidation approach is suitable for concentrations less than 1 ppm C [*Clesceri et al.*, 1989]. The TOC analyzer runs off of an internal calibration performed in the factory. This calibration was periodically verified with an oxalic acid standard. The oxalic acid calibration was typically found to be within 5% of the factory calibration (example data: slope = 1.04 ± 0.06 ppb C/ppb C, intercept = 59 ± 18 ppb C (± is one standard deviation). Note, the intercept is due to the previously mentioned organic carbon that naturally occurs in DI Water.)

TOC Analyzer Coupling to PILS:

A continuous liquid sample flow is drawn into the TOC analyzer by an internal peristaltic pump for analysis. Since syringe pumps are used to force the liquid sample through a filter, and exact flow matching is not possible, the liquid sample line cannot be directly coupled to the TOC. As shown in Figure 2.1, a "tee" was added downstream of the liquid filter prior to the TOC analyzer with one leg going to waste. Additionally, this means during airborne measurements the liquid sample is near cabin pressure prior to entering the TOC analyzer. This enables the TOC analyzer to operate in its normal mode and to control the sample flow by its internal pump. The transport flow is adjusted so that the "tee's" waste leg flowrate is minor (less than 0.1 ml/min) and the TOC never

draws air. The debubbler and "tee" were constructed of Pyrex with an internal volume of 0.05 ml or less.

2.6. Artifacts, Limit of Detection, and Measurement Uncertainty

The use of denuders and background corrections will minimize positive artifacts due to absorption of gases. As previously discussed and shown, positive artifacts due to absorption of gases within the PILS during the aerosol particle measurements are likely minimal in the WSOC measurements.

Negative artifacts associated with evaporation of semi-volatile organics using this method have not been systematically assessed. Elevated temperature in the droplets formed, and on collection surfaces in the PILS, could lead to volatility losses of organic compounds. For airborne measurements, evaporation of semi-volatile organic material may happen due to ram heating at the inlet or due to heat transfer in the sample lines between the inlet and the instrument. (Measurements of sample temperature at the PILS inlet indicate that sample air was typically 12 K higher than ambient for measurements at altitudes up to 2 km, and 30 K for measurements between 3 and 4 km. These are the altitudes where WSOC concentrations are investigated in most detail in chapter 4.) Not accounting for negative artifacts, if they do exist, would lead to systematic under measurement of WSOC.

Based on three times the background standard deviation, the limit of detection (LOD) for this system is estimated to be about 1 μg C/m^3. However, through comparisons with other aerosol measurements, such as particle volume, useful WSOC data are available down to 0.1 μg C/m^3. Thus, data down to 0.1 μg C/m^3 are included,

but it is recognized that concentrations between 0.1 and 1 μg C/m^3 are much more uncertain.

The uncertainty associated with the WSOC measurement can be estimated by combining the uncertainties in the method for determining the liquid concentration, uncertainties due to background variability, and uncertainties in various flowrates. For measurements of ionic aerosol composition with the PILS-IC system, dilution due to added liquid from collected drops and wall condensate to the impactor plate was accurately determined by spiking the transport flow with lithium. Recording the change in lithium measured upstream and downstream of the impactor provided a measure of dilution. A similar approach cannot be used in the PILS-TOC for measurement of WSOC. Therefore, a constant dilution factor of 1.17 is assumed, which is based on experiments where a PILS-IC was operated identically to the PILS-TOC. The uncertainty in assuming a constant value is estimated to be ± 4%. Since the background is assumed to be constant between consecutive background measurements, variability in backgrounds can lead to uncertainty. This component of the uncertainty is estimated to be typically ± 5% (or ± 0.3 μg C/m^3). The overall measurement uncertainty, based on combining the known uncertainties, is estimated to be approximately 10% (5% flows, 4% dilution, 5% background, and 5% TOC calibration). The true uncertainty due to unknown factors is likely to be higher. For concentrations between 0.1 and 1 μg C/m^3, where backgrounds are a larger fraction of the measured value, uncertainties are estimated to be at least ± 20%.

2.7. Modified Liquid Flowrates to Improve Response Times

As previously mentioned, the PILS-TOC can be deployed for either ground-based or airborne measurements. However, for aircraft measurements a rapid sampling rate is desired since the aircraft can cover a large sampling area in a short time, which often results in encountering quick changes in the various air masses sampled. As will be discussed in more detail below, to improve system response times and permit TOC operation at a faster sampling rate, the liquid flowrates were increased. The major operational differences for a system run for 3 s (airborne) or 6 minutes (ground-based) are summarized in Table 2.1.

Table 2.1. Summary of the operational differences for ground-based and airborne PILS-TOC measurements.

	Ground-Based	Airborne
Flowrate of Transport Water over impactor (ml/min)	0.6	1.4
Flowrate of sample out of the impactor and through the liquid filter (ml/min)	0.5	1.3
TOC analyzer sample flowrate (ml/min)	0.4	1.2
TOC analyzer sample mode and integrated sample time	On-line 6 minutes	Turbo 3 seconds
Duration of background measurement	30 minutes	10 minutes

Liquid-based systems may respond slowly to rapidly changing concentrations due to mixing in the various components that transmit the collected sample to the detector,

and within the detector itself [*Sorooshain et al.*, 2005]. Improved response times can be achieved in the liquid transport components by minimizing volumes. For example using narrow bore tubing, and small volume syringe pumps, debubblers, and liquid filters could help.

For the TOC analyzer, higher flowrates are the only feasible way to improve response times and help alleviate smearing of the measured concentrations that could occur when sampling inside and outside of a plume. By injecting an oxalic acid standard into the TOC analyzer to simulate a concentration change, experiments on TOC response time were performed to determine optimal liquid sample flowrates. The resulting change in measured concentration was recorded and the response time for a concentration change from 10% to 90% of the step increase (B minus A in Figure 2.3) determined. It was found that the TOC analyzer response time was approximately inversely proportional to the sample flowrate. Doubling the specified Turbo mode flowrate of the TOC analyzer from 0.6 to 1.2 ml/min improved the response time of our analyzer to approximately 1 minute (see Figure 2.3). The higher liquid flowrate improves the responsiveness of the complete system, however, this also results in a more dilute sample.

To assess response time of the complete system, comparisons were made between a 1 s measurement of carbon monoxide (CO) and the 3 s WSOC. Based on an analysis of two plumes with sharp edge transitions (the plumes shown in Figures 4.3 and 4.6b and discussed in chapter 4) the response time is estimated to be in the range 45 to 65 s. Slow response is believed to be mainly from mixing in the syringe pumps.

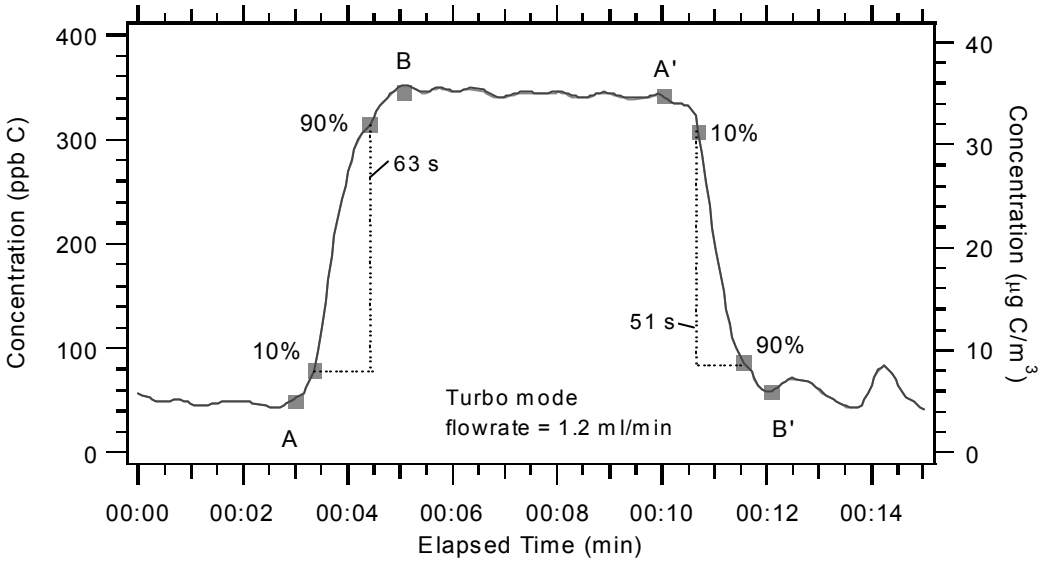

Figure 2.3. Response time of the TOC analyzer in Turbo mode for an optimized sample flowrate of 1.2 ml/min. A and B are the average initial and final concentrations, respectively.

CHAPTER 3
GROUND-BASED RESULTS

Results of near real-time measurements of WSOC obtained at the St. Louis - Midwest Supersite during the summer and autumn of 2003 are presented.

3.1. Site Details

The PILS-TOC was deployed at the St. Louis - Midwest Supersite from June 2003 through April 2004. (This chapter will focus on the data from June through October 2003. The data from March 2004 will be discussed later in chapter 5.) This urban site is located in East St. Louis, IL approximately 3 km to the east of the city of St. Louis, MO central business district. It is in a residential area with light commercial activity and is periodically impacted by industrial sources within a few kilometers to the south.

Along with the PILS-TOC, hourly-integrated $PM_{2.5}$ (Sunset Labs cyclone) OC and elemental carbon (EC) were measured for alternate hours using a field ECOC analyzer (Sunset Laboratory Inc., Forest Grove, Oregon). This instrument quantifies OC and EC using the thermal/optical transmission (TOT) method [*Birch and Cary*, 1996]. It was run following the method of *Bae et al.* [2004]. In order to minimize positive artifacts, the ECOC measurements used the same type of denuder as the PILS-TOC [*Bae et al.*, 2004].

3.2. Carbonaceous Aerosol Seasonal Trends, June to October

Monthly means of EC, OC, WSOC, and the ratio of WSOC to OC for June, August, and October are summarized in Table 3.1. Mean OC concentrations were fairly

Table 3.1. Mean and standard deviations (in parenthesis) of $PM_{2.5}$ EC, OC, WSOC, and the WSOC/OC ratio for June, August, and October 2003 at the St. Louis - Midwest Supersite. Concentrations are reported in μg C/m^3.

Month	EC	OC	WSOC	WSOC/OC
June	0.80 (0.57)	4.76 (2.53)	2.87 (1.41)	0.64 (0.13)
August*	0.62 (0.51)	4.04 (1.75)	2.40 (0.78)	0.61 (0.16)
October	1.11 (1.01)	4.55 (3.62)	1.33 (0.75)	0.31 (0.11)

*Measurements averaged over only August 1 to 17.

similar during these three months. Although based on standard deviations the mean WSOC concentration changed significantly. Compared to June and August, in October the WSOC was approximately 50% lower, and thus the ratio of WSOC to OC was also about 50% lower. This is consistent with the view that much of the WSOC may be from SOA formation, a process that would be less vigorous in the fall when actinic fluxes to drive photochemical activity are lower.

3.3. Diurnal Trends in the WSOC to OC Ratio

For the majority of the time, in St. Louis the WSOC tracks OC (e.g., for June, hourly-integrated OC regressed on hourly-averaged WSOC yields a $R^2 = 0.81$). To further demonstrate this behavior, Figure 3.1 shows the OC and WSOC concentrations, WSOC to OC ratio, and ozone (O_3) concentrations for 14 day periods in June and August 2003. A number of interesting features were observed both within and between these periods.

The time series for OC revealed a 3-to-7 day trend with a diurnal cycle superimposed. Although not shown, the EC trends were qualitatively similar to OC

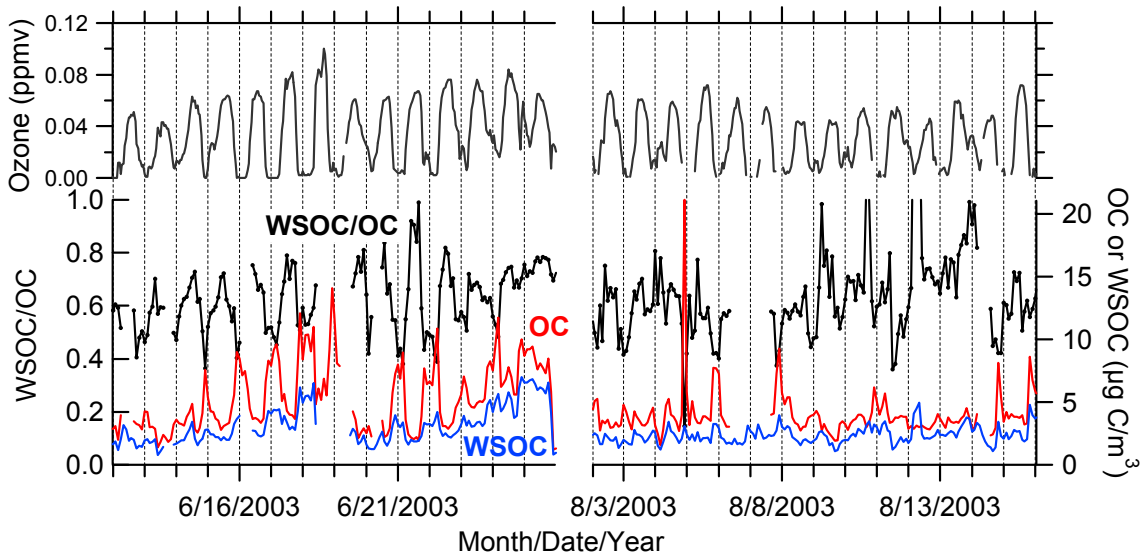

Figure 3.1. Time series of $PM_{2.5}$ OC, WSOC, the fraction of OC that was water-soluble, and O_3 concentration for two 14 day periods (June and August 2003). Dashed vertical lines represent midnight CST.

trends. The longer-term trend was dictated by precipitation events. Over the multi-day period following a precipitation event (e.g. 6/13/03 and 6/19/03 in Figure 3.1), the OC increased from approximately 1-4 µg C/m^3 up to about 10-15 µg C/m^3; subsequently, the OC concentrations rapidly dropped back to approximately 1-4 µg C/m^3 apparently due to precipitation scavenging (or washing out) of the aerosol. The steady increase in OC concentrations would resume again after the rain event. This cycle was observed three times in June 2003. In addition to this multi-day pattern the OC concentrations exhibited a distinct diurnal profile with a minimum during the day and maximum during the night. These trends are often observed in urban regions and interpreted as a result of continuous sources (day and night) combined with limited dispersion at night due to a nocturnal temperature inversion and thermally-driven daytime mixing. In contrast, for the period of

August 1-17, 2003 there was no discernable day-to-day buildup in the OC concentration and therefore the aforementioned diurnal profiles were only weakly discernible. October featured a combination of the trends observed for the June and August periods.

WSOC/OC trends also differed between June and August. In June there was a large and consistent variation in the daily WSOC/OC. For extended periods in June, often associated with the diurnal OC trends but ~12 hours out of phase, there was a clear temporal pattern in WSOC/OC with levels reaching ~0.80 during the day and dropping to near 0.40 at night. In several instances the water-insoluble fraction (WIOC) dominated at night (WIOC = OC - WSOC and thus WIOC/OC = 1 - WSOC/OC). As previously mentioned, in the past most WSOC measurements have been made using 24 hour integrated filter measurements that are incapable of resolving diurnal variability. The elucidation of subdaily WSOC patterns and its coupling to OC and other parameters represents a unique observation for an urban site and demonstrates the insights gained from near real-time measurements.

This site was also periodically influenced by strong local point sources. One such event can be seen in Figure 3.1 just prior to midnight on 8/5/03. The hourly-averaged OC concentration spiked to over 20 μg C/m^3, yet the WSOC concentration did not significantly increase. Thus the WSOC to OC ratio was very low (i.e., the WIOC fraction was high) suggesting that most of the carbonaceous aerosol was likely fresh primary OC.

During the periods of persistent diurnal trends in June, the WSOC to OC ratio was fairly well correlated with O_3. Table 3.2 summarizes linear regression results for the entire month of June, and for each period of OC concentration buildup observed between

Table 3.2. Number of data points (N), slope and intercept (both with 95% confidence limits), and R^2 value for linear regressions of the WSOC/OC ratio versus O_3 concentration for various periods during June 2003 in St. Louis.

Period in June	N	Slope*	Intercept	R^2
Entire Month	328	3.52 ± 0.26	0.53 ± 0.01	0.41
June 15 – 18	47	2.60 ± 0.30	0.53 ± 0.01	0.72
June 21 – 25	59	4.09 ± 0.50	0.48 ± 0.02	0.54
June 27 – 30	39	3.57 ± 0.51	0.57 ± 0.02	0.57

*Units are ppm^{-1}.

precipitation events. WSOC/OC to ozone correlations may suggest that a significant fraction of the June daytime WSOC was associated with SOA. In contrast, diurnal trends in OC and WSOC/OC were not as prominent in August and no correlation was found between WSOC/OC and O_3 ($R^2 = 0.02$). The observed contrasts between June and August could be due to a number of factors, including different atmospheric chemical and meteorological processes, and emissions. Thus, significant chemical differences may exist between the WSOC measured in June and August. (Note, measurements of species which could potentially reveal more about the chemistry of June versus August, such as the hydroxyl radical or VOCs, were not made at this site.)

3.4. Summary

Overall, these results show that on-line measurements of aerosol water-soluble organic carbon, coupled with equally rapid measurements of aerosol organic carbon, provided unique information into the sources and atmospheric processing of fine particulate organic compounds soluble in water. These results also suggest that at an urban site WSOC may, under certain conditions, be mainly from SOA formation. If so,

then these data indicate that SOA is often a large fraction (up to 80%) of the ambient OC. In the next chapter, the on-line WSOC measurements are extended to airborne measurements.

CHAPTER 4
AIRBORNE RESULTS

Results from ground-based studies of WSOC are expanded through airborne experiments, which provide new insights into sources and spatial distributions of WSOC and its evolution in distinct plumes.

4.1. Results during NEAQS/ITCT 2004

The National Oceanic and Atmospheric Administration (NOAA) sponsored NEAQS/ITCT 2004 airborne mission was part of the larger International Consortium for Atmospheric Research on Transport and Transformation (ICARTT). The NOAA WP-3D aircraft was operated out of Portsmouth, NH from 9 July to 15 August 2004. As part of this multi-investigator field study, measurements were made of a suite of aerosol particle physical and chemical properties, and of several reactive and trace gases. The aerosol measurements included bulk concentrations of the ionic constituents and WSOC (reported at 1 atmosphere and 293 K) of particles with aerodynamic diameters < 1.0 μm (PM_1) using the PILS-IC and TOC systems, respectively. Several flights focused on investigating sources, transport, mixing, and chemical transformations of anthropogenic emissions from the Boston/New York corridor. A map of the flight paths is shown in Figure 4.1a.

The PILS-TOC sampled from a Low Turbulence Inlet (LTI) [*Wilson et al.*, 2004], as did the PILS-IC system, the AMS, and a coarse mode optical particle counter. The PILS-IC, PILS-WSOC, and AMS shared a sample line running from the LTI through a non-rotating MOUDI impactor [*Marple et al.*, 1991] with 50% transmission efficiency at

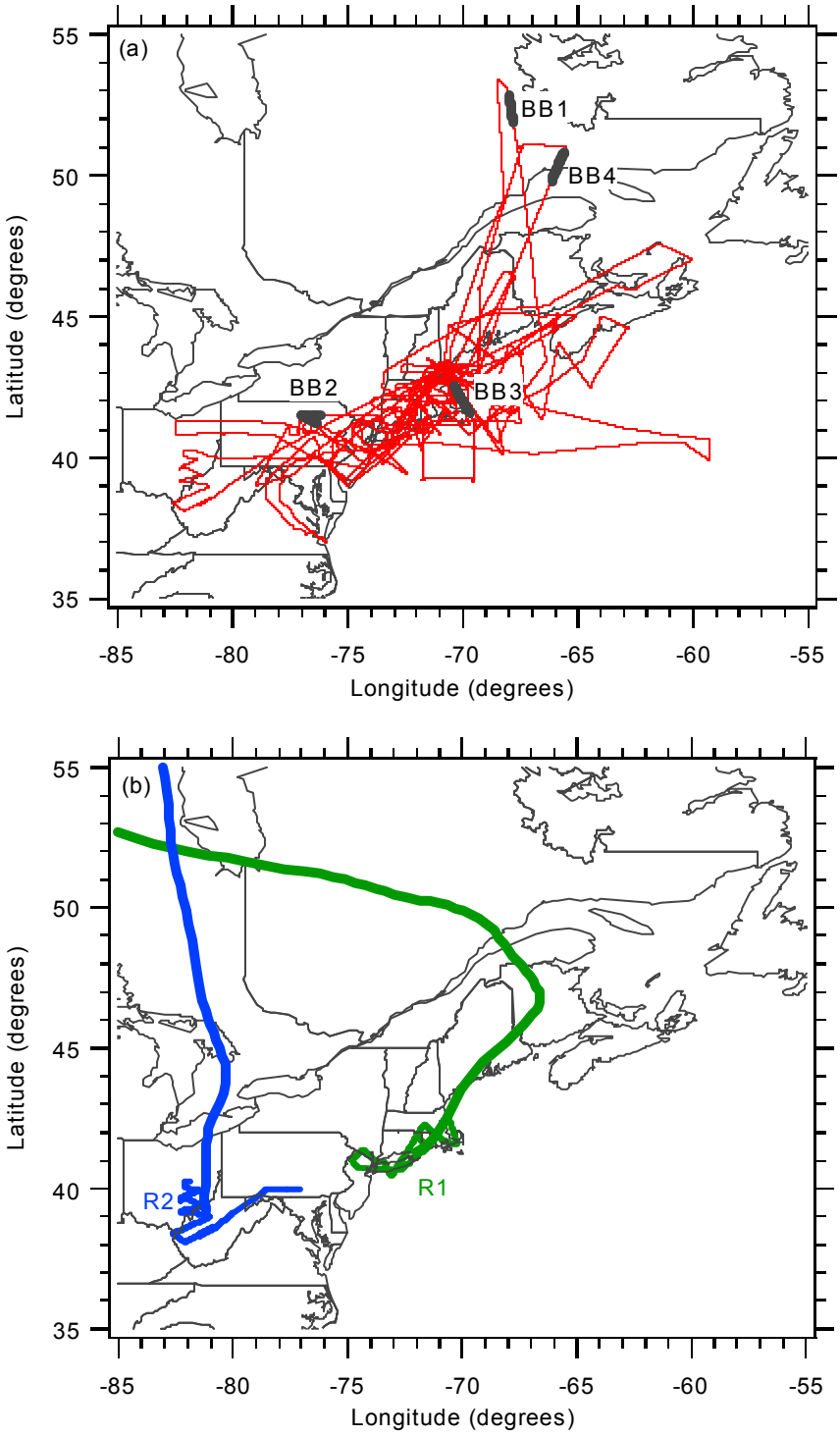

Figure 4.1. (a) Map of the aircraft flight paths during NEAQS/ITCT 2004. Identified are the various biomass burning (BB1 through BB4) plumes discussed in the analysis. (b) Back trajectory for rural plumes (R1, R2) discussed in the analysis. The back trajectories are based on the NOAA ARL HYSPLIT Trajectory Model.

1.0 μm at 1 atmosphere ambient pressure. The combined flow to these instruments was 30.5 L/min.

The focus of the following analysis is on the sources of submicron WSOC during the experiment. Additional measurements used in the analysis include gaseous organic compounds measured by a PTR-MS approximately every 18 s [*de Gouw et al.*, 2003a], 1 s CO [*Holloway et al.*, 2000], and PM_1 volume with 1 s resolution (determined from integrating particle number distributions measured by combining a 5-channel condensation particle counter, a modified LasAir 1001A laser optical particle counter (OPC), and a white light OPC [*Brock et al.*, 2000, 2004]).

During this study, substantially enhanced WSOC concentrations were associated with biomass burning plumes and plumes emanating from urban centers. Figures 4.2a and 4.2b show the measured WSOC concentration as a function of altitude, delineated into biomass and non-biomass influenced air masses. Acetonitrile was used as a unique biomass burning tracer [*de Gouw et al.*, 2003b]. Air masses with a biomass burning influence were identified when acetonitrile concentrations were above 250 pptv, assuming 250 pptv and below are background acetonitrile concentrations. It cannot be completely excluded that some biomass burning influence may persist in the data with below 250 pptv acetonitrile, but it is likely to play a very minor role. Figure 4.2a shows that most concentrated biomass plumes were detected in layers generally between altitudes of 3 and 4 km, however, evidence of a biomass influence (based on acetonitrile above 250 pptv) was observed over all measured altitudes. For non-biomass burning data, WSOC concentrations were highest near the surface and decreased with altitude, similar to sulfate, the other major aerosol chemical constituent during this study.

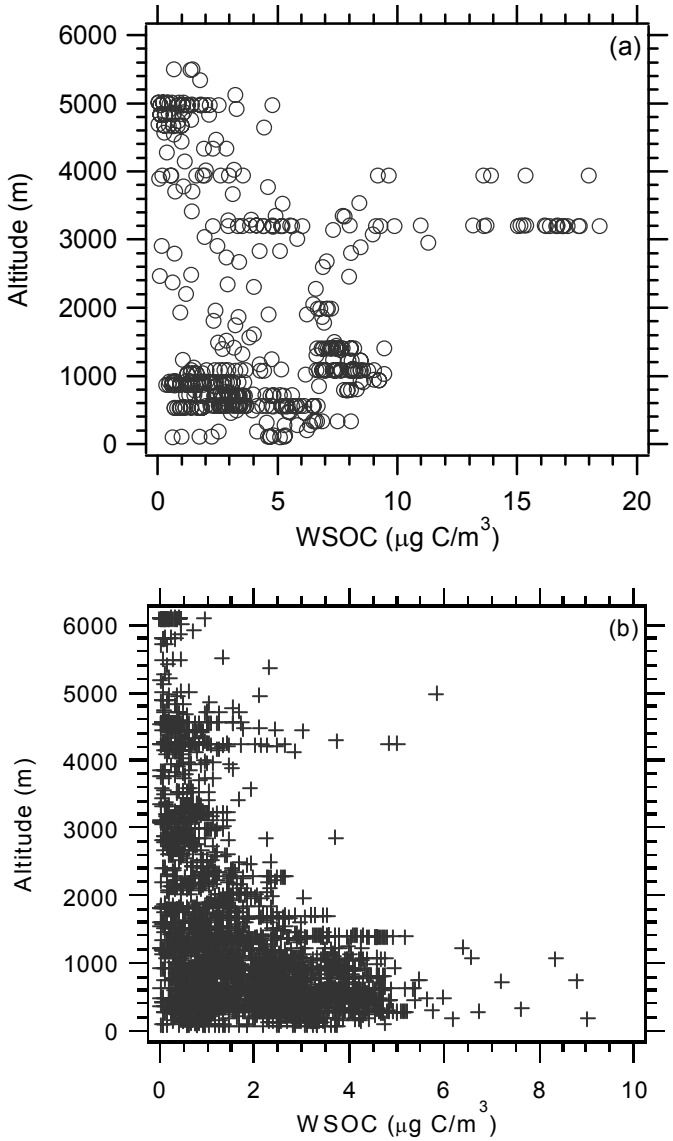

Figure 4.2. One minute averaged PM_1 WSOC concentrations as a function of altitude for all data collected during the experiment. Data are separated into (a) biomass burning (acetonitrile > 250 pptv) and (b) non-biomass burning (acetonitrile < 250 pptv) WSOC.

4.2. Biomass Burning WSOC

A variety of studies report that significant fractions of biomass burning smoke particles have carbonaceous components that are soluble in water [*Novakov and Corrigan*, 1996; *Narukawa et al.*, 1999; *Graham et al.*, 2002; *Mayol-Bracero et al.*, 2002b]. A similar result was observed in this experiment; measured WSOC was highly correlated with fine particle volume and known gaseous biomass burning emissions, such as acetonitrile and carbon monoxide.

The locations of four large and distinct biomass plumes are given in Table 4.1 and identified on the map in Figure 4.1a. These plumes were all intercepted within layers between 3 and 4 km altitude (see Figure 4.2a). A Lagrangian air particle dispersion model (FLEXPART, [*Stohl et al.*, 2002]) indicated that these plumes were from biomass burning in the Alaska/Yukon region and transported to the point of measurement over periods ranging from 4 to 10 days. In all cases the WSOC was highly correlated with acetonitrile and CO, with R^2 ranging between 0.88 and 0.96 (see Table 4.1). An exception was the biomass plume intercepted on 21 July 2004 (BB3) over Boston with a lower WSOC-CO R^2 of 0.71. Overall, these biomass plumes contained the highest concentrations of WSOC and PM_1 volume observed throughout the entire airborne experiment.

As an example of a specific biomass plume interception, Figure 4.3 shows the time series of the WSOC, fine particle volume, CO, and acetonitrile for the biomass plume intercepted on 9 July 2004 (BB1, Table 4.1 and Figure 4.1a). It can be seen that all four of these measurements are highly correlated within the plume and that the WSOC represented approximately 10% ($\mu g\ C/m^3$)/($\mu m^3/cm^3$) of the fine particle volume. This

Table 4.1. Characteristics of four major biomass plumes intercepted by the WP-3D. Included are the mean, in parenthesis the maximum and minimum values, and in brackets the average concentration increase within the plume relative to local background (all based on 1 minute averaged data). Date is given as month/date/year and local time is EDT = UTC – 4 hours.

	07/09/04 20:06 to 20:20 UTC (BB1)*	07/20/04 17:22 to 17:37 UTC (BB2)	07/21/04 19:51 to 20:03 UTC (BB3)	07/28/04 16:42 to 16:56 UTC (BB4)
WSOC (μg C/m^3)	8.13 (0.57, 18.00) [7.76]	14.54 (5.83,18.45) [11.36]	12.56 (5.54, 16.70) [11.58]	13.24 (6.04, 17.63) [10.42]
CO (ppbv)	362 (110, 633) [11]	325 (216, 410) [164]	278 (136, 419) [111]	299 (177, 363) [197]
Acetonitrile (pptv)	844 (279, 1491) [469]	775 (278, 904) [463]	709 (292, 947) [447]	555 (372, 627) [344]
PM_1 Volume ($\mu m^3/cm^3$)	80.6 (3.47, 181) [74.4]	70.3 (9.58, 91.8) [63.0]	65.1 (19.5, 103) [59.6]	78.1 (14.1, 104) [68.0]
Transport Time** (days)	6 to 8	8 to 10	8 to 10	4 to 5
Latitude (degrees)	52.32	41.42	41.98	50.32
Longitude (degrees)	-67.90	-76.71	-69.99	-65.87
Altitude (m)	3936	3161	3200	3197
WSOC-Acetonitrile R^2	0.95	0.92	0.93	0.89
WSOC-CO R^2	0.96	0.92	0.71	0.89
ΔWSOC/ΔCO*** (μg C/m^3/ppmv)	39.4	69.4	125.6	78.7

*BB1, BB2, BB3, and BB4 are used to identify the specific biomass plumes in Figure 4.1a.

**Calculated based on the FLEXPART Model.

***This ratio is the change in WSOC relative to CO within the plume above the local background concentrations. Background concentrations were determined from measurements at roughly the same altitude near each plume.

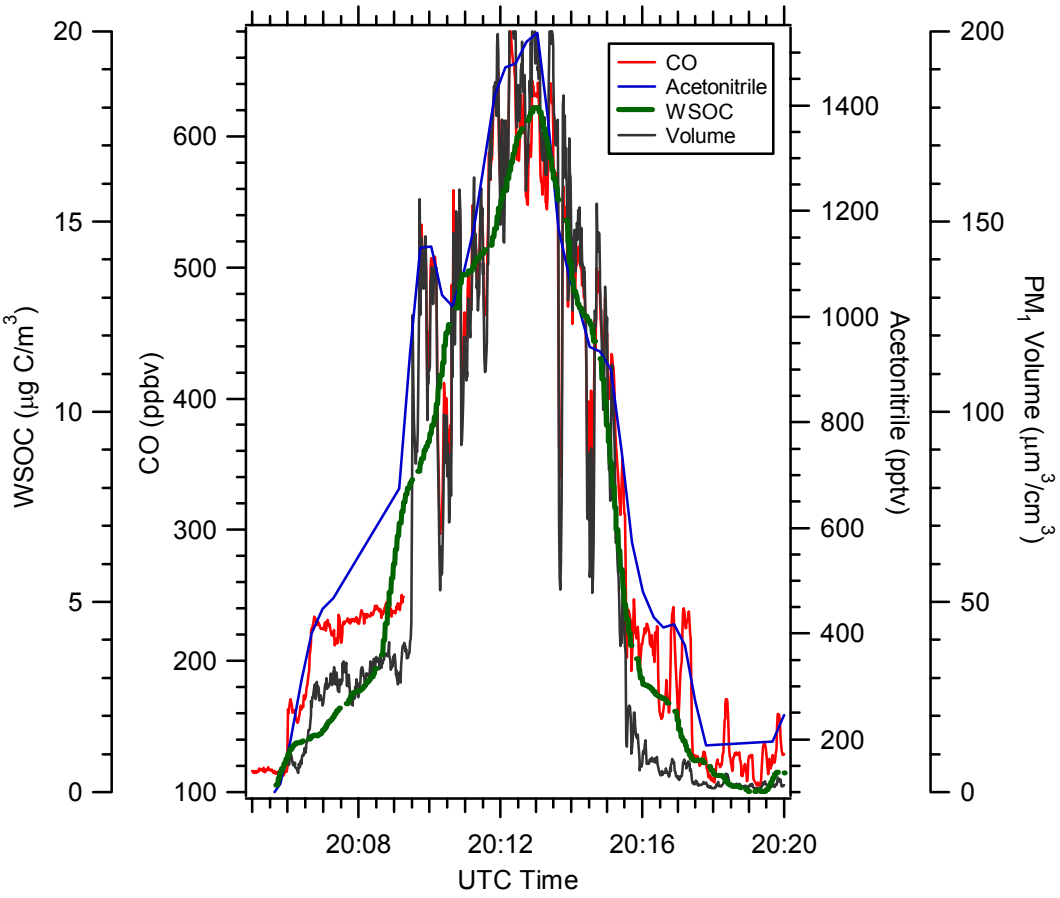

Figure 4.3. Time series of 3 s WSOC, fine particle volume, carbon monoxide, and acetonitrile recorded in the biomass plume BB1 (identified in Figure 4.1a) on 9 July 2004. Local time is EDT = UTC – 4 hours.

ratio ranged between ~10 and 22% for the large biomass plumes detected in this study (can be inferred from Table 4.1).

Other less distinct biomass burning plumes were also present throughout the study. Some were observed at lower altitudes and mixed with local anthropogenic sources. Back trajectory analysis [*Stohl et al.*, 2002] suggests all of these air masses were from the Alaska/Yukon fires. Although the aircraft did not measure down to the surface, other analysis shows that these emissions influenced ground-level local air quality during the period of the measurement campaign [*R.B. Pierce and J. Szykman*, personal communication].

4.3. Non-Biomass Burning WSOC

Although biomass plumes occasionally led to greatly enhanced WSOC concentrations throughout the study domain, as previously discussed, other known major sources of WSOC are secondary and possibly primary organic compounds from biogenic emissions and mobile sources. The St. Louis ground-based results suggest a source of WSOC is urban settings. To investigate these other non-biomass burning sources of WSOC, the biomass burning events were removed by considering only data for which acetonitrile was below 250 pptv (see Figure 4.2b). Apart from biomass burning emissions, SOA from biogenic and anthropogenic precursors will both lead to WSOC. Emission inventories for biogenic compounds, such as isoprene and terpenes, suggest that significant sources exist in the northeastern states, especially the northern part of Maine, and northern regions of Ontario and Quebec (http://map.ngdc.noaa.gov/website/al/emissions/viewer.htm). Air masses from these

regions were sampled during this experiment. In the following analysis only measurements made below 2 km altitude are analyzed to investigate these biogenic and anthropogenic surface sources for WSOC.

4.3.1. WSOC-CO Correlation

As in the biomass burning plumes, WSOC was also found to be correlated with CO. This correlation was found to be driven by emissions from urban plumes without a biomass burning influence. For all data measured when altitude was below 2 km and acetonitrile less than 250 pptv, WSOC and CO are positively correlated ($R^2 = 0.55$, see Figure 4.4). A number of individual plumes from urban centers, such as New York City, Boston, and Philadelphia, were intercepted at various times during the experiment. The measurement locations for 9 different plumes are shown in Figure 4.5 and the WSOC and CO concentration time series for three selected plumes are shown in Figure 4.6. WSOC and CO were well correlated in these specific urban plumes ($R^2 > 0.78$) and have higher correlations than the combined mission data set (see Table 4.3, which will be discussed in more detail in section 4.3.3, for a summary). Since CO in urban centers is mainly from vehicle emissions [*EPA*, 1997], these data suggest that mobile sources are linked to the observed WSOC.

4.3.2. Urban versus Background Rural

To contrast the urban WSOC concentrations to more rural background air masses, the FLEXPART Lagrangian air particle dispersion model [*Stohl et al.*, 2002] was used to identify air masses lacking significant influences from urban CO sources. As an

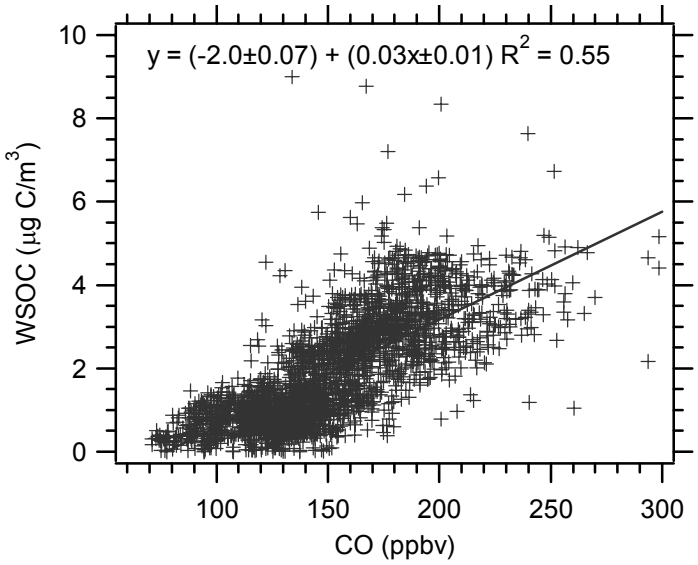

Figure 4.4. Correlation between one minute averaged WSOC and CO for all non-biomass burning influenced measurements (acetonitrile < 250 pptv) recorded below 2 km altitude during the experiment. Uncertainties associated with the least squares regression are one standard deviation.

example, concentrations measured in two air masses are shown in Table 4.2. The air masses were sampled during two flights, 25 July 2004 and 6 August 2004. The locations where they were encountered and representative air mass back trajectories are shown in Figure 4.1b. These air masses had passed over Canada and the Great Lakes, or Canada and New England, at altitudes between 800 and 1800 m within two days of the measurement.

Emission inventories for the regions where these air masses had recently advected over show significant biogenic VOC sources. Estimated relative emission levels are between ~50-173 (moles of isoprene)/(km^2 hr) or ~0.68-11.50 (moles of terpenes)/(km^2 hr) (http://www.epa.gov/asmdnerl/biogen.html). It is likely that the air masses contain

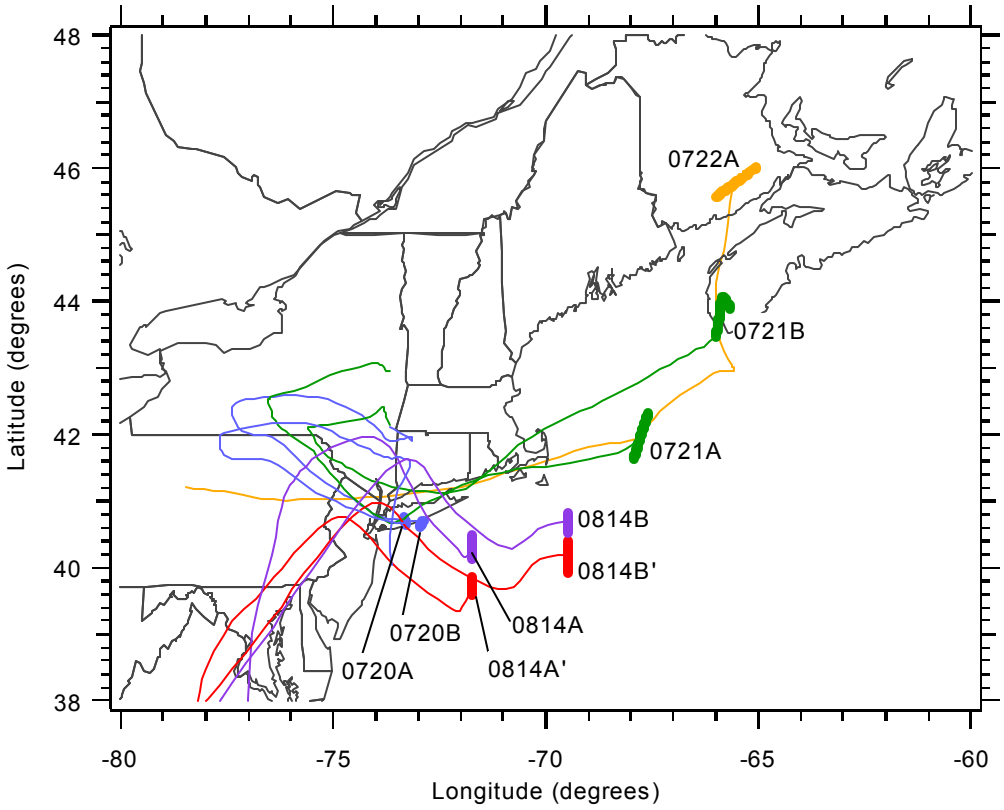

Figure 4.5. Characteristic air mass back trajectories for each of the 9 urban plumes discussed in the analysis. The back trajectories are based on the NOAA ARL HYSPLIT Trajectory Model.

aerosol particles that are representative of the background aerosol found in the northeastern U.S. and Canada, with potentially a significant biogenic influence. These rural air masses were found to have some of the lowest low altitude (< 2 km) CO and WSOC concentrations of the mission (see Table 4.2). The CO ranged from 99 to 177 ppbv. The 25 percentile for CO was 117 ppbv. For WSOC the range was from 0.43 to 2.13 μg C/m^3, with the WSOC 25 percentile at 0.72 μg C/m^3.

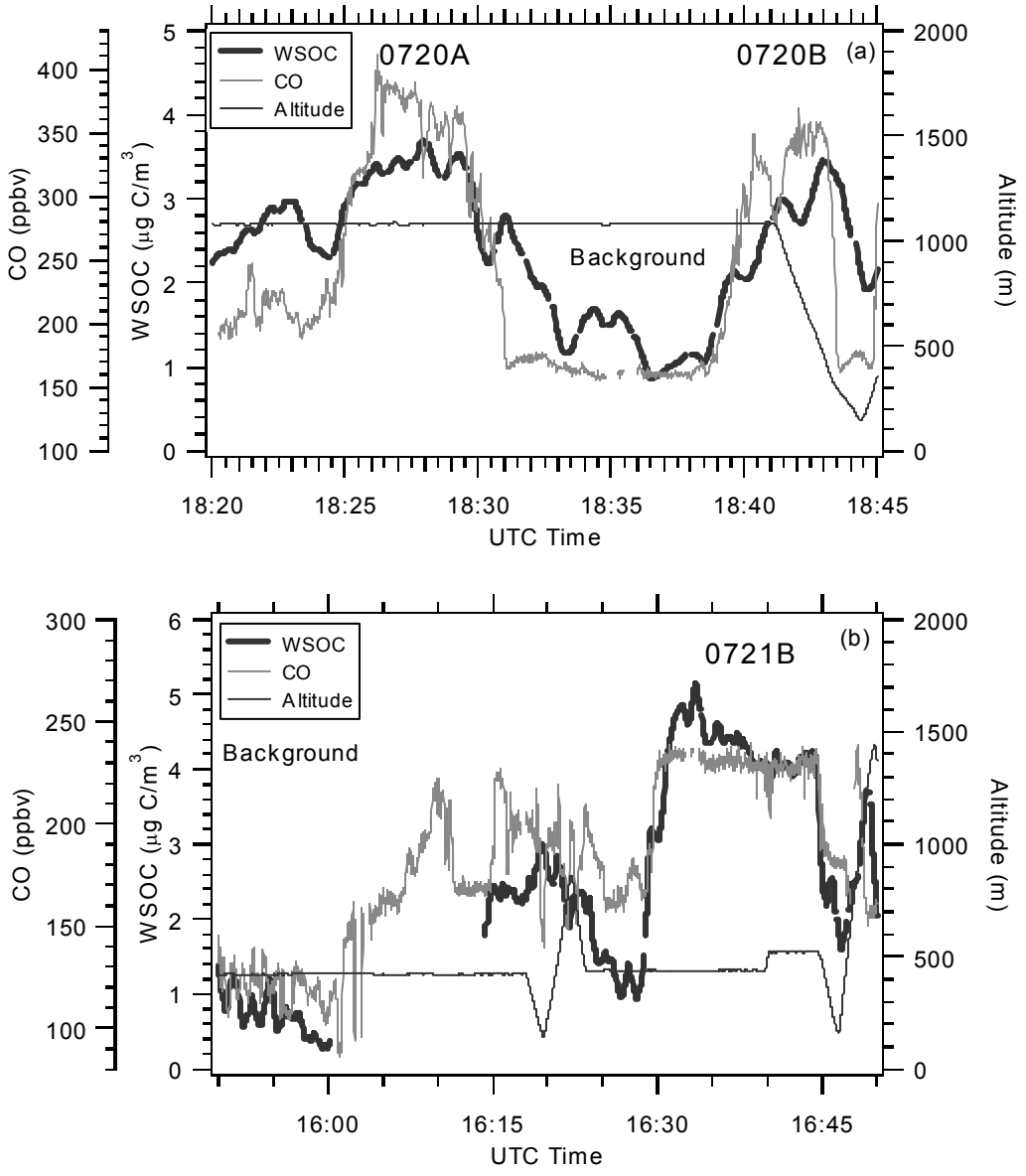

Figure 4.6. Time series of 3 s WSOC, carbon monoxide, and altitude for (a) two urban plumes intercepted on 20 July 2004 and (b) one urban plume on 21 July 2004 identified in Figure 4.5. Local time is EDT = UTC – 4 hours.

Table 4.2. WSOC and CO concentrations in two selected rural air masses. Mean concentrations, with maximum in parenthesis, are shown for both air masses. All data have been merged to a one minute average. Date is given as month/day/year and local time is EDT = UTC – 4 hours.

Air Mass*	Measurement Date and UTC Time	WSOC ($\mu g\ C/m^3$)	CO (ppbv)
New England/Canada (R1)**	07/25/04 14:30 to 16:30, 20:55 to 21:30	1.32 (2.13)	133 (177)
Great Lakes/Canada (R2)	08/06/04 16:30 to 20:25	0.85 (1.70)	120 (141)

*FLEXPART and NOAA ARL HYSPLIT Trajectory Model indicate that the air mass originates from or passed through the given locations within two days of the measurement.

**R1 and R2 are used to identify the rural plumes in Figure 4.1b.

4.3.3. WSOC Evolution in an Urban Plume

As was shown during NEAQS/ITCT 2004, urban centers were a major source of WSOC with concentrations factors of 2 to 3 times higher than background air masses (compare Tables 4.2 and 4.3). The range of WSOC concentrations observed for the urban influenced air during this study is comparable to the concentrations previously presented for ground-based measurements in urban St. Louis (chapter 3), which had typical summer concentrations from 2 to 4 $\mu g\ C/m^3$.

Secondary organic aerosol formation is expected to produce WSOC, and thus WSOC to CO ratios may be expected to increase with plume age. To investigate relative changes in CO and WSOC within these urban plumes, an estimate of the background concentrations of CO and WSOC is required. Analysis of rural air masses advecting toward the urban regions suggest background concentrations of the order of 125 ppbv for

CO and 1 μg C/m^3 for WSOC. Background concentrations can also be estimated from measurements made near the various plumes. For example, in Figure 4.6b regions of low CO likely representative of background conditions are recorded near the identified urban plumes. Background conditions near the urban plumes were near 141 ppbv for CO and 1.28 μg C/m^3 for WSOC, similar to values in the rural air mass R1 that was intercepted near the urban centers along the east coast. Since in some cases the urban plumes do not have as clear an increase from the background conditions as those in Figure 4.6b, the background concentrations shown in Figure 4.6b (CO 121 ppbv, WSOC 0.75 μg C/m^3) will be used for the remainder of the analysis.

The changes in WSOC concentration relative to CO above background levels (i.e., ΔWSOC/ΔCO) are summarized in Table 4.3, where the background WSOC and CO was assumed to be the same in all cases. The influence of assuming a constant background concentration on ΔWSOC/ΔCO is small. For example, based on the standard deviation on what are considered background concentrations measured at various locations, the variability in ΔWSOC/ΔCO is ± 1.2 μg C/m^3/ppmv. The variability in ΔWSOC/ΔCO given in Table 4.3 is the standard deviation of the ratio in the plume, assuming constant background. Variability in the plume is higher than the assumption of constant backgrounds, however, both are relatively small. (Note that ΔWSOC/ΔCO can also be determined from the slope of WSOC versus CO for data recorded within and in the vicinity of a specific plume. The two methods lead to similar ΔWSOC/ΔCO ratios. This will be demonstrated later in chapter 7.)

Table 4.3. Results for WSOC evolution in urban plumes. Concentrations are mean concentrations within the plume based on 3 s data. As an indicator of variability the ± standard deviation is shown. Date is given as month/day/year and local time is EDT = UTC – 4 hours. N/A = not applicable*

Plume ID	Measurement Date and UTC Time	Advection Time from Urban Center (hours)**	Altitude (m)	WSOC ($\mu g\ C/m^3$)	CO (ppbv)	ΔWSOC/ΔCO ($\mu g\ C/m^3$/ppmv)	WSOC-CO R^2
0720A	7/20/04 18:27 to 18:29	1 ± 0	1078	3.46 ± 0.35	362 ± 21	11.3 ± 4.1	0.92
0720B	7/20/04 18:40 to 18:42	3 ± 1	1010	2.59 ± 0.13	316 ± 17	8.5 ± 1.2	0.81
0814A	8/14/04 16:29 to 16:35	13 ± 1	85	1.08 ± 0.12	233 ± 20	3.1 ± 1.1	0.83
0814A'	8/14/04 16:40 to 16:45	13 ± 1	86	1.44 ± 0.45	201 ± 6	7.2 ± 5.0	N/A
0814B'	8/14/04 19:21 to 19:29	18 ± 1	72	2.29 ± 0.50	195 ± 14	19.5 ± 5.0	0.89
0814B	8/14/04 19:31 to 19:36	20 ± 0	73	3.50 ± 0.16	249 ± 17	21.8 ± 2.7	0.86
0721A	7/21/04 15:17 to 15:29	26 ± 1	279	4.98 ± 0.71	272 ± 27	28.8 ± 6.8	N/A
0721B	7/21/04 16:29 to 16:43	33 ± 3	456	4.20 ± 0.51	227 ± 11	31.8 ± 4.1	0.89
0722A	7/22/04 18:34 to 18:50	55 ± 1	742	3.21 ± 0.32	199 ± 9	32.0 ± 4.1	0.78

*A background was made either during the rise into or fall out of the plume.

** Calculated based on the average of NOAA ARL HYSPLIT back trajectories run at the beginning, in the middle, and at the end of each plume.

Based on estimates of plume transport age calculated from the NOAA Air Resources Laboratory (ARL) HYSPLIT Trajectory Model [*Draxler and Rolph*, 2003; *Rolph*, 2003], a general trend in ΔWSOC/ΔCO is observed. Figure 4.7a shows ΔWSOC/ΔCO versus an estimate of the advection time of the plume from the urban region to the measurement site. All plumes were measured during the day, however, because some advection times are longer than one day, they will include periods of low photochemical activity. Figure 4.7a shows a number of interesting features. First, for this data set, ΔWSOC/ΔCO ranged from approximately 3 to 32 μg C/m^3/ppmv. The observations that lowest ratios were generally observed in fresher plumes in measurement regions closer to the urban center, and that these ratios tended to approach zero, suggest that much of the WSOC is a secondary product from compounds co-emitted with CO (e.g., vehicles). Results from other experiments involving measurements next to highways (i.e., source) also indicate that this ratio should approach zero. In a more recent study, which will be discussed in more detail in chapter 7, WSOC measured within ~1 m of a major expressway was found to be similar to that of the background air, leading to a ΔWSOC of approximately zero. Moreover, ΔOC/ΔCO measured in the Caldecott Tunnel was also approximately zero, due to extremely high CO concentrations relative to primary OC [*Kirchstetter et al.*, 1999]. In contrast to the fresh plumes, Figure 4.7a shows that in the more aged and distant plumes from the city, after approximately one day of advection time, ΔWSOC/ΔCO appears to level out approaching a constant value of about 32 μg C/m^3/ppmv, possibly due to a depletion of SOA precursors. As an interesting contrast to the WSOC behavior, fine particle sulfate (SO_4^{-2}) continued to increase in these regions. For example, plumes 0721A and 0721B also contained significant

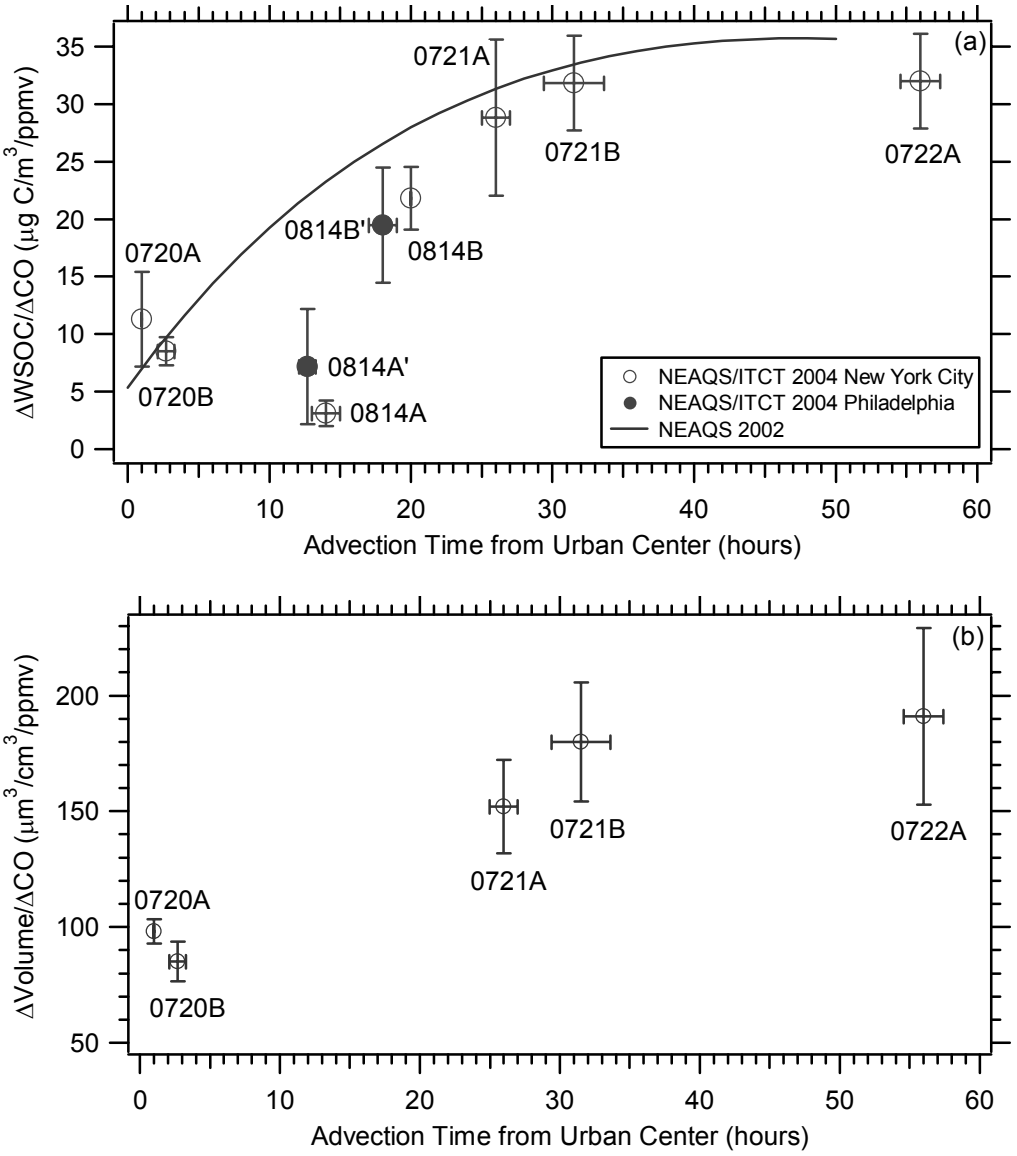

Figure 4.7. Ratio of (a) ΔWSOC to ΔCO and (b) ΔVolume to ΔCO as a function of estimated advection time from the urban center to the measurement site for the plumes identified in Figure 4.5 and Table 4.3. The advection time was calculated from the NOAA ARL HYSPLIT Trajectory Model. Based on the FLEXPART Model, two of the plumes (solid circles) were apparently influenced by Philadelphia whereas the other seven (open circles) were influenced primarily by New York City. Uncertainties are the ± standard deviation of the ratios calculated from variability within the plume (y-axis) and of the advection time calculated from variability in back trajectories calculated at the start, in the middle, and at the end of each of the nine plumes (x-axis). Included in (a) for comparison, is the ΔOC/ΔCO ratio calculated as a function of photochemical age (solid line) during the NEAQS 2002 study from *de Gouw et al.* [2005] (note, units are the same as ΔWSOC/ΔCO).

concentrations of sulfur dioxide (SO_2) and sulfate aerosol. For plumes 0721A and 0721B, $\Delta SO_4^{-2}/\Delta CO$ increased from 89 to 116 $\mu g/m^3/ppmv$, respectively (assuming for this simple analysis that background sulfate is zero), whereas $\Delta WSOC/\Delta CO$ only increased from 29 to 32 $\mu g\ C/m^3/ppmv$. Thus unlike SOA formation, which rapidly depleted precursors, secondary formation of SO_4^{-2} could continue for long periods due to ample supply of the critical precursor, SO_2.

For comparison with a previous study in this region, Figure 4.7a also shows the ΔOC to ΔCO ratio calculated as a function of photochemical age during the NEAQS 2002 experiment [*de Gouw et al.*, 2005]. ($\Delta OC/\Delta CO$ was calculated from the data presented in Figure 14b of *de Gouw et al.* [2005] multiplied by the ratio of acetylene to CO to permit a direct comparison with the results from the above analysis.) It is noteworthy that the results from the above analysis are consistent with those of *de Gouw et al.* [2005], which employed different measurement techniques and method of analysis. Note that a systematically larger ΔOC to ΔCO ratio compared to $\Delta WSOC/\Delta CO$ may be expected due to contributions from primary OC that are not included in the WSOC measurement.

Formation of SOA should lead to increased aerosol volume. Figure 4.7b shows the $\Delta Volume/\Delta CO$ for the same plumes in which $\Delta WSOC/\Delta CO$ was evaluated and volume data were available. (A constant volume background of 7.15 $\mu m^3/cm^3$ was assumed and obtained from the background period identified in Figure 4.6b.) The similar trends in $\Delta WSOC/\Delta CO$ and $\Delta Volume/\Delta CO$ in Figures 4.7a and 4.7b, especially the inflection point at about 25 to 30 hours advection time, suggest that the increase in WSOC with plume age was due to gas-to-particle conversion and not solely conversion

of primary OC to WSOC. As previously discussed, the $\Delta SO_4^{-2}/\Delta CO$ continued to increase with advection time, which would account for a continued increase in ΔVolume/ΔCO past 30 hours (note larger variability in ΔVolume/ΔCO with plume age).

4.4. Summary

Two main sources for WSOC were identified: biomass burning from long-range transport and emissions from populated regions. Both sources were correlated with CO.

Distinct biomass plumes were intercepted between 3 to 4 km altitude over eastern U.S. and Canada. Back trajectory analysis indicates that all large biomass plumes encountered during the mission were from fires in the Alaska/Yukon region. WSOC was highly correlated with CO and acetonitrile (R^2 typically > 0.88), and the highest fine particle volume and WSOC concentrations were recorded in these plumes. WSOC typically comprised from ~10 to 22% ($\mu g\ C/m^3$)/($\mu m^3/cm^3$) of the fine particle volume.

For air masses not influenced by biomass burning, highest concentrations of WSOC were recorded at lower altitudes, generally below 1000 m, and typically ranged from 2 to 6 $\mu g\ C/m^3$. WSOC showed a rapid concentration decrease with increasing altitude over the entire measurement domain with concentrations typically less than 1 $\mu g\ C/m^3$ above 3 km. Highest WSOC concentrations were observed in distinct plumes emanating from urban centers. In these plumes WSOC was highly correlated with CO with coefficients of correlation (R^2) larger than 0.78. Rural air masses had WSOC concentrations from the lower detection limit of ~0.1 to about 2 $\mu g\ C/m^3$; significantly less than those measured in urban emissions. In some cases inventories suggest significant biogenic emissions associated with these rural air masses.

Changes in ΔWSOC/ΔCO as a function of plume transport time from urban centers showed that the ratio was generally lower (~ 3 μg C/m^3/ppmv) for fresh plumes, increased with increasing plume age, and leveled off to about 32 μg C/m^3/ppmv after approximately one day. The data suggests that the WSOC associated with PM_1 particles measured in this mission was likely produced from compounds co-emitted with CO, such as could be found in motor vehicle emissions, and that these emissions were rapidly converted to secondary aerosol particle products within approximately one day. No evidence was found for a strong biogenic source for PM_1 WSOC.

Thus far, the results from both the ground-based and airborne measurements suggest WSOC can be produced by SOA. The aircraft study also shows that biomass burning can be a source of WSOC. Therefore, in the next two chapters to further investigate whether WSOC is produced by SOA, methods for chemically speciating WSOC are presented.

CHAPTER 5
ISOLATION OF HYDROPHILIC AND HYDROPHOBIC FRACTIONS WITH A XAD-8 RESIN

In this and the following chapter, methods for comprehensive speciation of WSOC are developed and presented. These methods are used to investigate the major chemical components of urban WSOC.

5.1. XAD-8 Separation Method

Group separation of WSOC can be performed by solid phase extraction (SPE) with direct TOC analysis, if no carbonaceous eluents are employed. The SPE method employed here involves the partitioning of organic solutes from the polar mobile phase (i.e., aqueous sample with dissolved aerosol components) into a XAD-8 resin, the non-polar solid phase. This resin's primary partitioning force is hydrophobic interactions. Therefore, the organic compounds retained are the most hydrophobic components of the ambient WSOC. Organic compounds not retained and that penetrate the column are the more hydrophilic fraction. XAD-8 resin is an uncharged but slightly polar resin comprised of polymerized methyl ester of polyacrylic acid. It is used extensively by geochemists for extraction of humic substances from natural waters by separating inorganic substances from the humic material [*Thurman and Malcolm*, 1981].

For this application a 6 mm ID x 10 cm long glass column hand-packed with resin and fitted on each end with 25 μm polyethylene frits is used. The column is prepared between sample runs via a 1 hour equilibrium period in which no eluent is run over the column, followed by 1 hour of 0.1 M NaOH (sodium hydroxide) and then 15 minutes of

0.1 M HCl (hydrochloric acid), both at a flowrate of 1.2 ml/min. (When performing on-line measurements, this regeneration cycle is typically performed after 3.5 hours of operation since under the current operating conditions the maximum sample volume that can be passed over the column before regeneration is necessary is 4 hours.) A 10-port actuated valve in combination with syringe pumps performed this regeneration automatically.

When the column is separating samples, a liquid sample is passed over the XAD-8 at a flowrate of 1.2 ml/min. Just prior to sample loading, the pH of the sample is adjusted to 2 by adding in 0.1 ml/min of 0.1 M HCl via a peristaltic pump. This is done to neutralize most organic compounds so that they are not in their ionic form (i.e., not deprotonated) and able to interact with the neutral XAD-8 resin. The result is that hydrophobic acid and "neutral" compounds are adsorbed to the resin, whereas hydrophobic bases are not. Adsorbed compounds are referred to as the hydrophobic fraction. On the other hand, the compounds that penetrate (or elute from) the XAD-8 column and are measured directly with the TOC analyzer are composed of hydrophobic bases and all hydrophilic compounds (acids, bases, and neutrals). Here, these compounds are referred to as the hydrophilic fraction. (Note that experiments to further speciate these fractions, which will be discussed in chapter 6, show that the contribution of organic bases to the hydrophilic fraction is typically very small (<1%), thus hydrophobic bases have little influence on the hydrophilic fraction.)

Some of the hydrophobic components retained on the XAD-8 resin can additionally be extracted by passing a pH 13 eluent of 0.1 M NaOH over the column at 1.2 ml/min for 15 minutes. Practically all compounds that are desorbed are recovered in

the first 5 minutes of the extraction procedure. Some fraction of the hydrophobic material remains adsorbed to the resin and cannot be recovered by this method. Experiments show that for this particular column (6 mm ID x 10 cm long glass column) at least 25 μg C must be loaded onto the column in order to achieve near 100% recovery with pH 13 eluent. Backflushing the column did not improve or change the recovery and therefore was not employed.

To characterize the performance of the XAD-8 resin, penetration and recovery tests were performed with a variety of different water-soluble organic compounds relevant to atmospheric aerosols. Table 5.1 summarizes these results. Three sets of chemical groups are separated by this method. They include hydrophilic compounds in the WSOC that pass through the column at pH 2 (WSOCxp), recovered hydrophobic compounds, which are compounds that are retained on the column at pH 2 and subsequently recovered with pH 13 eluent (WSOCxrr), and unrecovered hydrophobic compounds, compounds that are retained on the column at pH 2 but not recovered with high efficiency with pH 13 eluent (WSOCxru). In general the hydrophobic compounds were less soluble than the hydrophilic compounds, which often instantaneously dissolved in water.

These experiments showed that for the series of mono- and dicarboxylic acids and carbonyls, the transition from hydrophilic to hydrophobic occurs for compounds with approximately 4 to 5 carbons in the chain (see upper part of Table 5.1). Based on our limited calibrations, also included in this hydrophilic group are oxocarboxylic acids, amines, polyols, and all saccharides.

Table 5.1. Results of the XAD-8 penetration and recovery tests for a variety of water-soluble organic compounds listed by functional groups, where WSOCxp=hydrophilic, WSOCxrr=hydrophobic recovered, and WSOCxru=hydrophobic unrecovered. Listed in parenthesis is the number of carbon atoms per molecule for the series of mono- and dicarboxylic acids and carbonyls. Fractions that were not measured are left blank.

Functional Group	Compound	Initial Concentration (μg C/L)	Penetration (%)	Recovered in NaOH wash (%)	Comment
Monocarboxylic acid	Formic Acid (1)	51, 100, 131	110, 117, 112		WSOCxp
	Acetic Acid (2)	45, 55, 82, 84	102, 107, 116, 101		WSOCxp
	Butyric acid (4)	70	0		WSOCxru
	Caproic acid (6)	87	0	15	WSOCxru
Dicarboxylic acid	Oxalic Acid (2)	23, 105, 148, 149, 150	100, 102, 103, 98, 100		WSOCxp
	Malonic Acid (3)	58, 69, 76	114, 101, 104		WSOCxp
	Succinic Acid (4)	29, 46	124, 102		WSOCxp
	Maleic acid (4)	77	100		WSOCxp
	Fumaric acid (4)	2120	0		WSOCxru
	Glutaric acid (5)	87	0		WSOCxru
	Adipic acid (6)	2220	0		WSOCxru
	Pimelic acid (7)	88	0		WSOCxru
	Azelaic acid (9)	80	0	21	WSOCxru
Carbonyls	Glyoxal (2)	98	100		WSOCxp
	Methyl glyoxal (3)	74	100		WSOCxp
	Propanal (3)	91	112		WSOCxp
	Butanal (4)	58	0	16	WSOCxru
Oxocarboxylic acid	Glyoxylic acid	2055	102		WSOCxp
Amines	Ethanolamine	39, 41, 73, 79	133, 102, 100, 96		WSOCxp

Table 5.1. Continued.

Polyols	1,2-Ethanediol	40, 67	117, 108		WSOCxp
Saccharides	Levoglucosan	45, 86	101, 104		WSOCxp
	Inositol	1860	103		WSOCxp
	Sucrose	2070	100		WSOCxp
Phenols	Catechol	90	0	70	WSOCxrr
	Vanillin	97	0	78	WSOCxrr
	Syringaldehyde	91	0	66	WSOCxrr
	Salicylic acid	2100	0		WSOCxrr
	3-Hydroxybenzoic acid	107	0	99	WSOCxrr
Aromatic Acids	Benzoic acid	1540, 2000	0, 0	80	WSOCxrr
	Phthalic acid	1960	0	87	WSOCxrr
Cyclic Acids	Pinic acid	1960	0	25	WSOCxru
	cis-Pinonic acid	1980	0	20	WSOCxru
Humic-Like	Suwannee River Fulvic	99,176,220,1577	0, 0, 0, 0	93	WSOCxrr
	Suwannee River Humic	45, 95, 208, 235, 1477	0, 0, 0, 0, 0	88	WSOCxrr
Organic Nitrates	Isobutyl nitrate	980	0	10	WSOCxru
	Isopropyl nitrate	1270	0	8	WSOCxru

The lower part of Table 5.1 shows organic functional groups that are water-soluble but were completely retained at pH 2 (hydrophobic). Some functional groups are subsequently recovered in the pH 13 eluent and some not. Approximately 80% of the phenolic compounds could be recovered, 85% of the aromatic acids, and 90% of the humic substances. These recovered hydrophobic compounds are identified as WSOCxrr in Table 5.1. Unrecovered hydrophobic compounds, identified as WSOCxru in Table 5.1, include mono- and dicarboxylic acids and carbonyls with greater than ~3 to 4 carbons, organic nitrates, and cyclic acids, since only approximately 20% or less could be recovered in the pH 13 eluent. It must be kept in mind that these calibration results should only be viewed as a guide to the types of compounds in the ambient aerosol that will be separated into these three fractions, since much of the WSOC in organic aerosols remains unidentified.

The results of these experiments suggest that all aromatic-containing compounds are in the WSOCxrr fraction. This is consistent with results obtained from solid-state ^{13}C-NMR (^{13}Carbon-Nuclear Magnetic Resonance) performed on ambient aerosol total WSOC, WSOCxp, and WSOCxrr fractions obtained from integrated filter samples. Aromatic carbon was only identified in the WSOC and WSOCxrr fraction, whereas the WSOCxp fraction showed no evidence for aromatic carbon peaks [*Sannigrahi et al.*, 2006]. The ambient WSOCxrr fraction may, however, contain other aromatic-like compounds with similar properties as determined by the interactions with XAD-8 resin. More discussion on the comparisons with ^{13}C-NMR can be found in section 6.2.3.

The uncertainty for the reported WSOCxp and WSOCxrr fractions is estimated at ± 10%, obtained by calculating the propagation of all known quantifiable errors.

Interestingly for on-line XAD-8 measurements (as will be discussed below), this is similar to what was reported for the uncertainty in the WSOC measurements from the PILS-TOC. The additional flowrate of sample over the column and sample dilution volume cause minimal effects because of the high precision syringe pumps employed.

5.2. WSOC Speciation Results from Urban Sites

The on-line PILS-TOC system previously discussed in chapter 2 was coupled to a XAD-8 column. Therefore, WSOC and the WSOCxp could be sequentially measured by either passing the PILS liquid sample containing the dissolved carbonaceous material directly to the TOC or first through the XAD-8 column to strip out the hydrophobic fraction (WSOCxr). A valve was programmed to switch between these measurements to give 4 complete cycles per day, where a cycle was 2.5 hours of WSOC measurements followed by 3.5 hours of column measurements. During WSOC measurements, the XAD-8 column was regenerated. For this system, blank measurements were performed for 30 minutes every 3 hours so two background measurements would be made per cycle, one for WSOC and one for WSOCxp. A schematic of the modified system can be seen in Figure 5.1.

For a period in the summer of 2004, dual PILS-TOC systems were operated in parallel, one dedicated to measurement of WSOC (no XAD-8 column), the other measuring WSOCxp (XAD-8 column in-line). In the following analysis, for both set-ups, the XAD-8 column was not recovered (i.e., no data obtained for WSOCxrr and WSOCxru) because the loaded concentrations were insufficient for efficient recovery

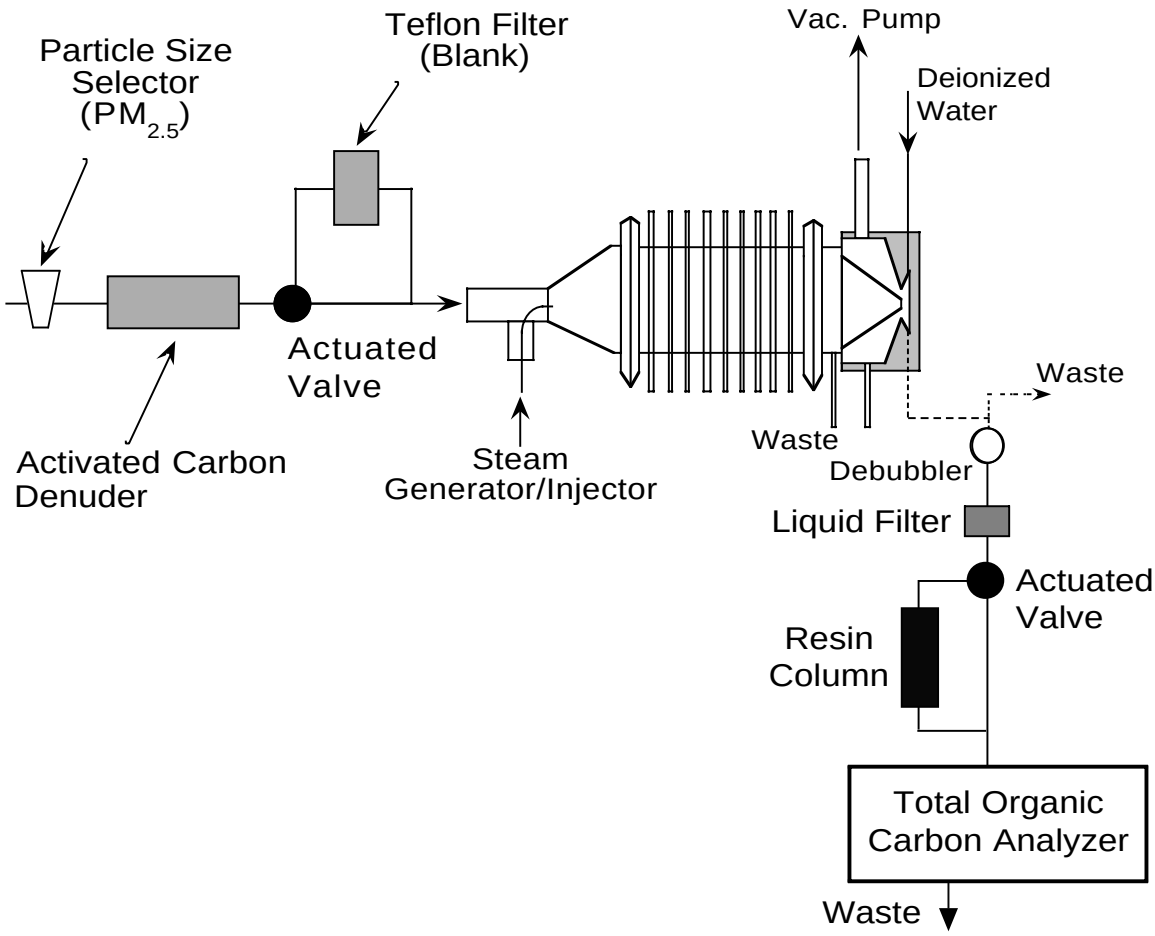

Figure 5.1. Schematic of the PILS-TOC system coupled with a XAD-8 resin column for sequential on-line WSOC and WSOCxp measurements. Dynamic blanks are performed every three hours for one-half hour via a programmed actuated valve that directs sample air through a Teflon filter prior to sampling. Liquid containing the ambient aerosol is pumped through a 0.22 μm liquid filter and then can either be measured directly by the TOC analyzer for a measurement of WSOC or first conducted through the XAD-8 resin column for a measurement of the WSOCxp fraction.

(see XAD-8 Separation Method above). Therefore, reported here are the measured WSOC, WSOCxp, and the difference in WSOC and WSOCxp to calculate WSOCxr. (Note, the equations used to calculate these concentrations can be found in Appendix A.1.) However, results from integrated filter samples where the WSOCxr fraction is further divided into WSOCxrr and WSOCxru will be presented in chapter 6.

Measurements were made during March 2004 at the St. Louis – Midwest Supersite and then the instrumentation moved to the Environmental Science and Technology Building rooftop laboratory at the Georgia Institute of Technology located in metro Atlanta, where it was operated April through September 2004. Measurements from both cities have been included to provide a greater seasonal contrast; from beginning of March to mid-September. As previously discussed in section 3.1, in St. Louis hourly-integrated $PM_{2.5}$ OC was measured using a field Sunset Labs ECOC analyzer. In Atlanta, this instrument was also used. The set-up was similar with the exception that 45 minute integrated OC was determined starting at the beginning of every hour.

A comparison of the OC, WSOC, WSOCxp, and WSOCxr is made for four periods in these urban environments: winter, a winter event, summer, and a summer event. Both the winter and summer events were chosen based on the presence of stationary high-pressure systems residing over the urban regions, making them times when local emissions likely play a larger role in the measured aerosols compared to other periods. These events also provide a contrast to the average conditions during each season. This is especially true for the summer event. Although Atlanta's summer of 2004 was atypically clean, from about July 19 to 24 a persistent stagnation condition

existed resulting in a buildup of ozone and $PM_{2.5}$. Peak $PM_{2.5}$ levels reached concentrations of 50-60 $\mu g/m^3$ in early morning hours, at least twice that measured for most of the summer. As shown in Table 5.2, during this period the highest $PM_{2.5}$, ozone, and temperature were recorded for the entire summer.

The discussion is based on the following analysis. Time series showing diurnal variability of the organic aerosol and isolated fractions are shown in Figure 5.2. Pie charts of the WSOCxp, WSOCxr, and water-insoluble fractions of OC (WIOC) based on means for each period are provided in Figure 5.3, and more details of these statistical results, based on the medians for these periods, are given in Table 5.3. Scatter plots with linear regression fits for data collected during these periods are shown in Figure 5.4. Note that in all cases these results are based on measurements of OC, WSOC, and WSOCxp. Calculated values include: WSOCxr = WSOC – WSOCxp and WIOC = OC – WSOC. Also, for the measurements from a single PILS-TOC, WSOC data were linearly interpolated since in this case the WSOC and WSOCxp measurements were made sequentially, not simultaneously.

The time series plots of Figure 5.2 show clear differences between winter and summer diurnal profiles in OC, WSOC, and WSOCxp. In winter, a prominent feature is the nighttime OC peaks, likely a result of reduced dispersion of emissions due to shallow nocturnal wintertime boundary layers. These nocturnal OC peaks often occurred near midnight (Figure 5.2a). In the typical summer period of 2004 (Figure 5.2b) much of this structure is less distinct, but it is clearly visible again in Figure 5.2c. In this summer event the OC peaks alternatively tend to occur early in the morning, coinciding with rush-

Table 5.2. Comparison between typical Atlanta summer 2004 and summer 2004 poor air quality event due to a stationary high-pressure system. The table contains the mean with ± standard deviation (as a measure of the variability), and in parenthesis the peak value measured during the time period. All ratios are based on carbon mass.

	OC ($\mu g\ C/m^3$)	WSOC ($\mu g\ C/m^3$)	$\frac{WSOC}{OC}$	$PM_{2.5}$ ($\mu g/m^3$)	Ozone* (ppbv)	Temperature (^oC)
Typical Summer	3.22±1.12	1.98±1.00	0.60±0.13	12.54±6.30	22.4±18.4	25.6±4.0
June 13-27	(8.23)	(6.52)	(0.89)	(31.71)	(75)	(32.9)
Summer Event	6.78±2.41	4.76±1.97	0.74±0.08	34.35±14.88	35.1±38.0	28.9±5.2
July 19-24	(11.71)	(9.30)	(0.91)	(65.20)	(136)	(39.8)

*Ozone data is from a Georgia EPA site in South DeKalb in Atlanta, approximately 20 km southeast of the aerosol measurements.

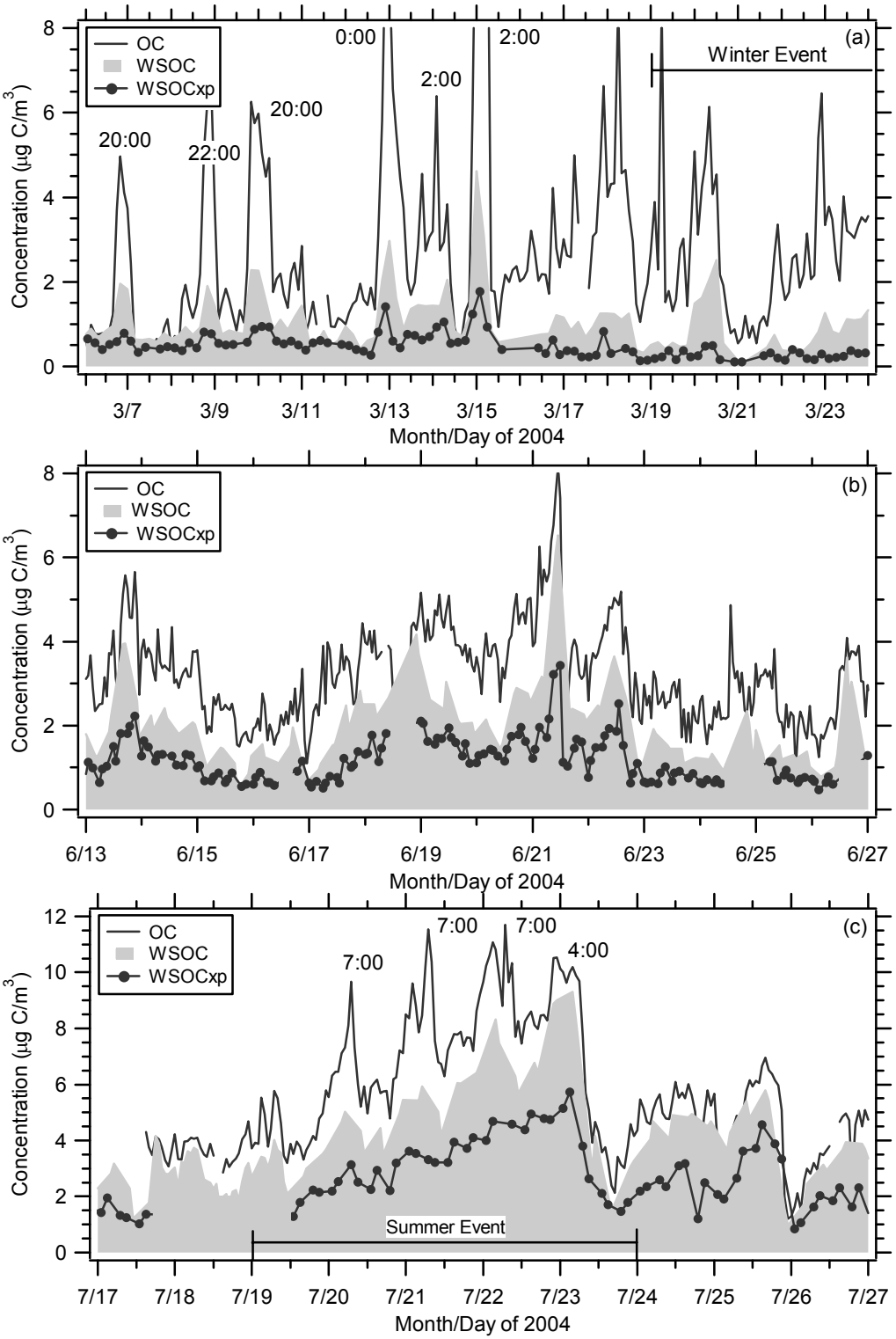

Figure 5.2. Time series of the OC, WSOC, and WSOCxp for (a) typical winter in St. Louis (March 6-18) and a winter event (March 19-24), (b) typical summer in Atlanta, and (c) a summer event in Atlanta. The WSOCxr is equal to the shaded area bounded by the WSOC and WSOCxp (i.e., WSOCxr = WSOC - WSOCxp).

hour traffic. (Note, OC peaks are generally only associated with morning rush hour since this occurs before the boundary layer breaks-up and mixing occurs.)

The WSOC to OC ratio (based on carbon mass) is generally lower in the winter than summer, but the more averaged data tends not to deviate too significantly from a 50:50 split. In March the medians and standard deviation of the WSOC to OC ratio was 0.56 ± 0.18 compared to June values of 0.58 ± 0.14. The mean winter and summer WSOC to OC ratios were 0.51 and 0.61 respectively. The nighttime values associated with the peaks in Figure 5.2a had somewhat lower WSOC to OC ratios, ranging from 0.30 to 0.40 (0.60 to 0.70 WIOC/OC). Although there was only a modest increase in WSOC/OC from March versus June 2004, for the winter and summer events a dramatic difference is seen in this ratio; in the winter event the mean WSOC to OC ratio was 0.36 compared to 0.75 in the summer event.

The winter WSOCxp and WSOCxr fractions were highly variable but on average about evenly split. (See Table 5.3 for WSOCxp to WSOCxr ratios and the pie charts of Figure 5.3. All ratios are based on carbon mass.) However, during the winter event when WSOC/OC was lowest, the WSOCxr fraction was nearly twice the WSOCxp fraction (Figure 5.3b). In the summer as WSOC/OC increased, the WSOCxp fraction becomes the more dominant component and a larger fraction of the fine particle OC. As shown in Figure 5.3d, this trend continued into the summer event when the WSOCxp fraction was nearly twice the WSOCxr fraction and comprised nearly 50% of the OC. These observations are likely due to the fact, as the calibrations also suggest, the WSOCxp fraction contains the small-chain species that are more likely produced via SOA, a process that is more important during the summer. More insights into these

Table 5.3. Comparisons of median ratios with the ± standard deviation for typical winter 2004 in St. Louis, winter event in St. Louis, typical summer 2004 in Atlanta, and summer event in Atlanta. All ratios are based on carbon mass.

Event	$\frac{WSOC}{OC}$	$\frac{WSOCxp}{WSOC}$	$\frac{WSOCxr}{WSOC}$	$\frac{WSOCxp}{WSOCxr}$
Typical Winter March 6-18	0.56±0.18	0.49±0.13	0.51±0.13	0.98±0.67
Winter Event March 19-24	0.36±0.11	0.32±0.21	0.68±0.21	0.47±1.41
Typical Summer June 13-27	0.58±0.14	0.61±0.13	0.39±0.13	1.53±1.37
Summer Event July 19-24	0.75±0.08	0.65±0.08	0.35±0.08	1.83±0.65

observations will be provided in chapter 6. An interesting observation seen in Figure 5.3 is that for this data, the mean WSOCxr fractions of OC were similar in all four cases studied, at approximately 25% of the OC.

Scatter plots showing ambient concentrations and linear regressions for WSOC versus OC, and WSOCxp and WSOCxr versus WSOC are shown in Figure 5.4. This linear regression analysis produces similar results to those discussed above based on means and medians. The WSOC and OC are highly correlated for all four cases. The lowest WSOC to OC slopes are associated with the winter event, and during this time the WSOCxr component dominated. The WSOCxr fraction is also more highly correlated with WSOC than the WSOCxp fraction. In contrast, during the summer event, the period of highest OC, WSOC, and WSOCxp concentrations, the WSOC to OC slope and fraction of WSOC that was WSOCxp were highest.

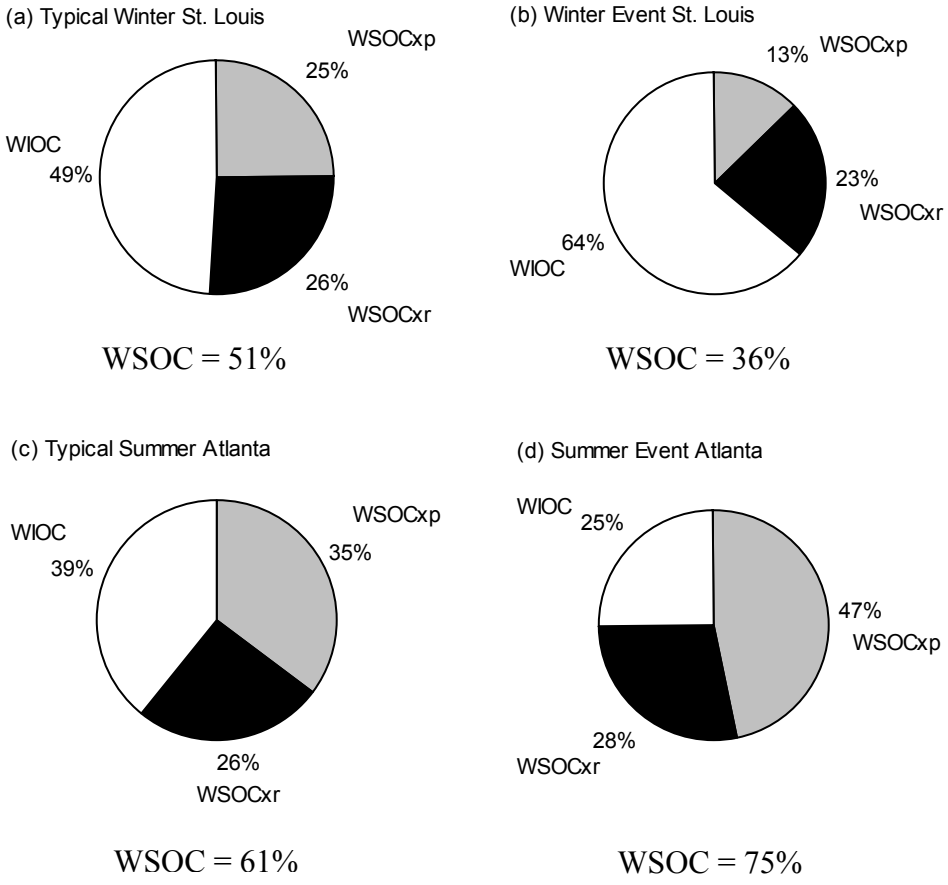

Figure 5.3. Percentage in carbon mass each fraction contributes to total OC, based on means, for the four periods shown in Figure 5.2. WIOC=water-insoluble OC (i.e. WIOC = OC – WSOC and WSOC is the sum of WSOCxp and WSOCxr).

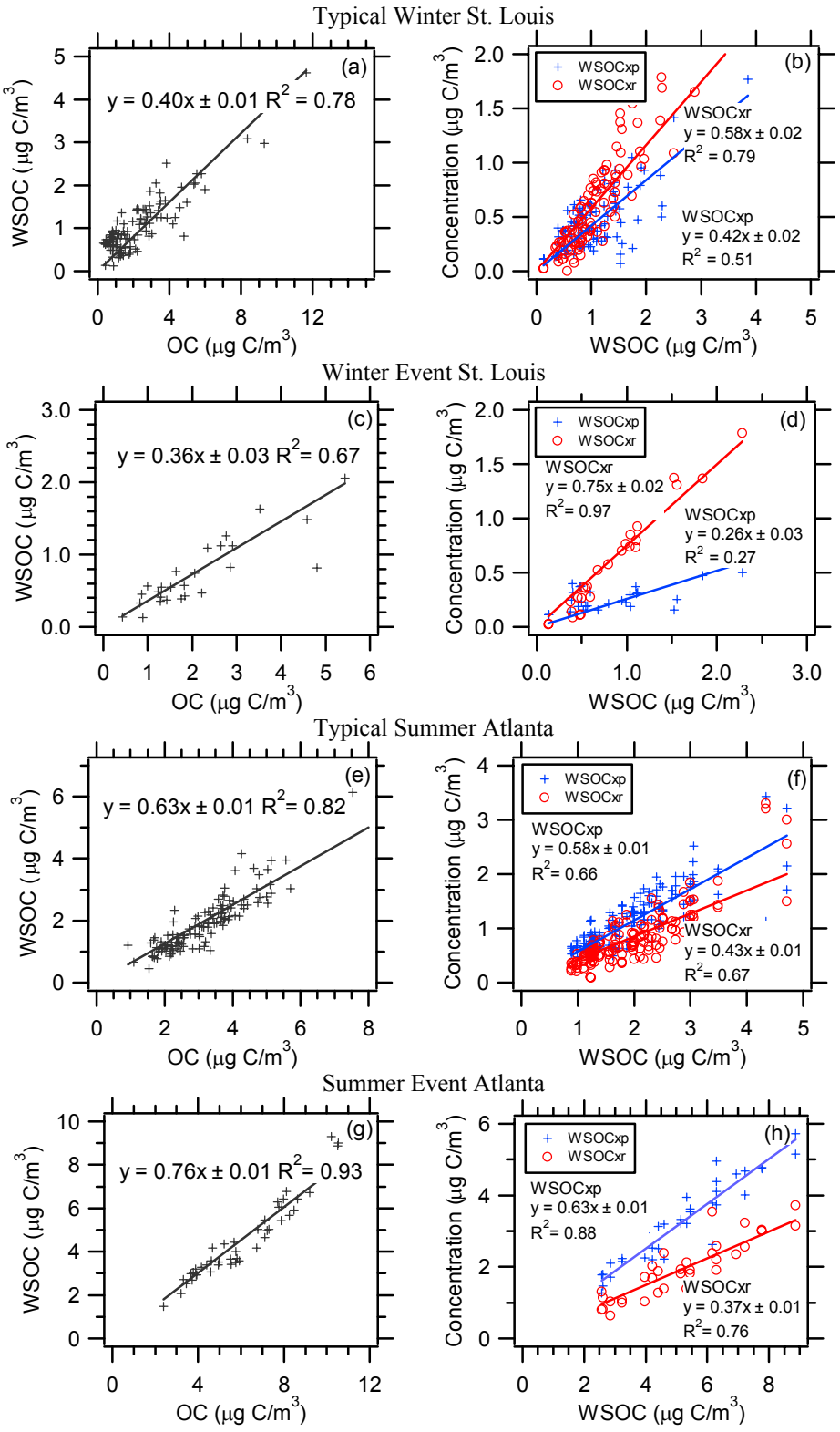

Figure 5.4. WSOC versus OC concentrations, and WSOCxp and WSOCxr fractions versus WSOC concentrations, for the four periods shown in Figure 5.2.

The seasonal progression in the changing dominance of the WSOCxr to WSOCxp fraction from late winter through summer and into early fall, using combined St. Louis and Atlanta data, is shown in Figure 5.5. The short periods analyzed and discussed above fit with the general seasonal trend observed in this figure. The WSOCxr fraction dominated in the winter, but starting roughly in April, the WSOCxp fraction increased relative to the WSOCxr fraction. The fractions were in equal proportions sometime in May, and then the WSOCxp fraction dominated throughout the summer. In late August, the WSOCxp fraction began to steadily decrease relative to the WSOCxr fraction and by September the fractions were back to 50:50 again. Even though there is an apparent

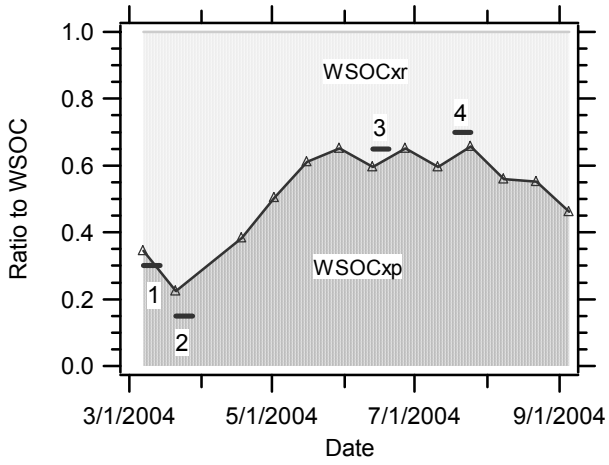

Figure 5.5. Seasonal trends in the WSOCxp and WSOCxr fractions based on carbon mass. Data were grouped into 14 day periods and the ratio determined by linear regression with zero intercept. All data are from urban Atlanta, except for the month of March, where measurements were made in St. Louis. The time periods shown in Figure 5.2 correspond to 1=typical winter, 2=winter event, 3=typical summer, and 4=summer event.

seasonality, no correlation with temperature for any of the fractions was observed. The observed seasonal trends may depend largely on changes in the dominant sources for each season.

Although the summer of 2004 in Atlanta was unusually clean with only 11 poor air quality days compared to typically 37 (summer averaged from 1987 to 2004), these data do provide evidence for a general shift in fine organic particle sources from winter to summer, and suggest that processes, such as SOA formation, which is likely more vigorous in the summer, produce significant levels of hydrophilic compounds that add substantially to the fine particle fraction of the organic aerosol. Because semi-volatile SOA compounds may not be efficiently measured with this approach (as previously mentioned this has not been tested), and they are likely to be small hydrophilic species, the WSOCxp fraction of OC may be even more significant during periods of active SOA production. In chapter 6, further chemical speciation of the WSOCxp and WSOCxr fractions provides insights into the sources of these compounds, including a more thorough discussion on SOA reactions and their likely products.

5.3. Summary

Aqueous extracts of the water-soluble organic fraction of atmospheric aerosols can be isolated into WSOCxp and WSOCxr fractions by XAD-8 resin. Because no organic eluents are employed, carbon mass can be quantified directly with a Total Organic Carbon analyzer, without intermediate isolation steps, and can be performed on-line with systems that collect particles into water, such as the PILS-TOC.

Laboratory calibrations suggest that WSOCxp is composed of compounds that include saccharides and amines as well as carbonyls and aliphatic mono-/dicarboxylic acids with less than 4 or 5 carbons. WSOCxr compounds are composed of aromatic acids and phenols, as well as organic nitrates, cyclic acids, and carbonyls and mono-/dicarboxylic acids with greater than 3 or 4 carbons. However, only aromatic compounds (or aromatic-like compounds with similar properties) can be extracted from the XAD-8 with high efficiency in the pH 13 eluent (WSOCxrr). For the most part, the remaining compounds (WSOCxru; organic nitrates, cyclic acids, and carbonyls and mono-/dicarboxylic acids with greater than 3 or 4 carbons) are not recovered. This method allows for a comprehensive and quantitative separation of the organic aerosol into distinct fractions from which a range of atmospherically relevant properties could be gained by applying additional analytical techniques.

Urban measurements showed both diurnal and seasonal changes in the WSOC and WSOCxp fractions of OC (on a carbon mass basis) between winter and summer. Overall, there is a general progression of increasing ratios of WSOC to OC and WSOCxp to OC from winter to summer, with highest ratios observed during a summer stagnation event. Mean ratios of WSOC to OC in winter versus a summer PM event were 0.36 and 0.75, respectively, and mean WSOCxp/OC for these two periods were 0.13 and 0.47. However, the WSOCxr fraction showed only a slight increase from 0.23 in winter to 0.28 during the summer event. It follows that the sources for the WSOC fraction of OC, and especially the WSOCxp fraction of OC, are strongest in the summer and a large contributor to the OC during pollution in urban Atlanta PM events. One possible explanation is SOA production, either from biogenic or anthropogenic emissions, or both.

This seems possible since, as the data and chapter 1 alluded to, SOA reactions often produce water-soluble organic compounds that are small-chains and based on the XAD-8 calibrations are part of the WSOCxp group.

This XAD-8 technique alone, however, cannot determine which groups of compounds that comprise the hydrophilic and hydrophobic WSOC fractions are responsible for the observed trends. In the next chapter, a method to further group speciate the hydrophilic and hydrophobic WSOC fractions using size-exclusion chromatography is presented.

CHAPTER 6
ISOLATION OF ACID, NEUTRAL, AND BASIC FRACTIONS BY MODIFIED SIZE-EXCLUSION CHROMATOGRAPHY

To further investigate the chemical nature and possible sources of WSOC, the hydrophilic and hydrophobic fractions of WSOC isolated with XAD-8 resin are each further divided into acid, neutral, and basic groups. The approach involves a newly developed method based on size-exclusion chromatography.

6.1. METHODS

6.1.1. Particulate Collection

A Thermo Anderson Hi-Volume Air Sampler was used to collect ambient particles on quartz filters for off-line analysis. Twenty-four hour integrated samples starting at midnight were collected during the summer (June and August 2004) and winter (December 2004 through February 2005) in Atlanta, GA. Samplers were located approximately 25 m above ground level on the rooftop of the Environmental Science and Technology Building on the Georgia Institute of Technology campus. Situated in the center of urban Atlanta, the site is heavily impacted by light-duty vehicle emissions due to close proximity (~400 m) to a major transportation corridor through the city center that prohibits most diesel-truck traffic. Two hour integrated samples were also collected directly within regions of prescribed burning conducted in Georgia at Fort Gordon and Fort Benning during April 2004. Shorter integration times were used for these samples due to much higher OC content.

The Hi-Volume sampler draws ambient air at nominally 1.13 m^3/min through a two-filter assembly to isolate and collect size fractions of the ambient aerosol. An impactor in combination with a slit filter collects PM_{10} particles, followed by a 20.3 cm x 25.4 cm filter to collect the $PM_{2.5}$. The quartz filters were wrapped in aluminum foil and pre-baked in an oven where the temperature was ramped up to 550^oC over a 12 hour cycle and then cooled naturally for an additional 24 hours to prevent the filters from absorbing water vapor. These pre-baked filters were stored in plastic bags in a sealed box until loaded into the filter holder. The filter holder was cleaned with isopropanol before filter loading. Only the $PM_{2.5}$ filter was analyzed. One quarter of the $PM_{2.5}$ filter was extracted in 125 ml of DI Water in a Nalgene Amber HDPE bottle, sonicated with heat [*Baumann et al.*, 2003] for 1.25 hours, and then filtered using a 0.45 μm PTFE syringe filter to remove any quartz filter fibers. Similar to the on-line system described in chapter 5, the liquid extracts were passed through a 0.22 μm pore liquid filter as part of the analysis procedure to remove insoluble particles.

Hi-Volume samples are not denuded making them susceptible to positive artifacts from organic vapor absorption to the collected aerosol particles and quartz filter fibers. Comparisons to denuded on-line measurements may provide some measure of the extent of this artifact. Figure 6.1 compares the summertime OC and WSOC from the Hi-Volume filter samples to the co-located on-line denuded measurements of OC and WSOC presented in chapter 5. Observed differences in OC and WSOC between these methods can be due to a host of variables including particle losses in sampling trains, sample flowrates, $PM_{2.5}$ cut sizes, and positive/negative artifacts. Figure 6.1 shows that based on linear regression slopes forced through zero, the Hi-Volume samplers are

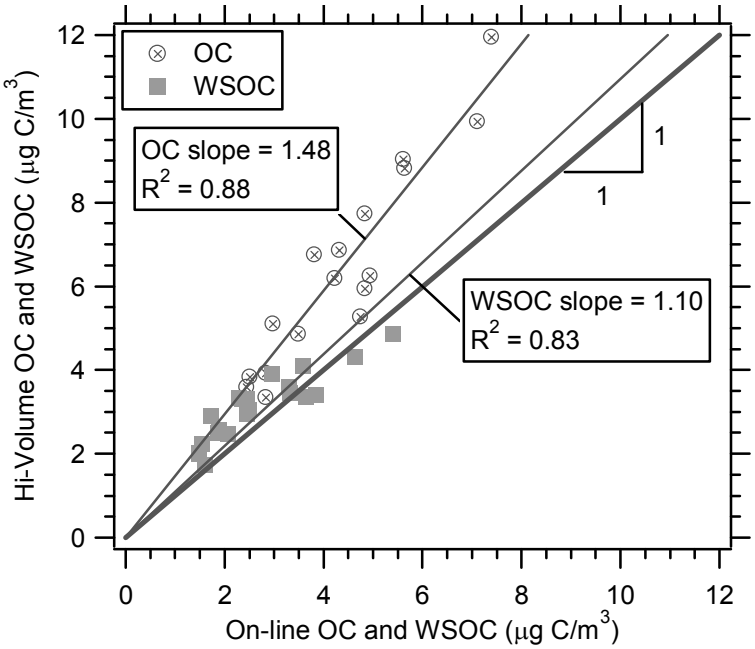

Figure 6.1. Comparison between the undenuded Hi-Volume 24 hour integrated filter measurement of OC and WSOC to denuded on-line systems using similar analysis and detection schemes. The 1 hour OC and 6 minute WSOC measurements were averaged over the Hi-Volume sampling period for the comparison. Only summertime data is plotted. Zero-intercept linear regression slopes are shown.

generally higher than the on-line measurements and largest discrepancies are for the OC. On-line measurements were not performed during the winter sampling and so no assessment can be made of possible sampling artifacts during this time. In this analysis, all comparisons between WSOC and its fractions with OC are made using the Hi-Volume measurements.

In addition to positive artifacts, semi-volatile organic compounds associated with aerosol particles may be lost from the Hi-Volume filter samples during the 24 hour integration period. These types of compounds are likely not measured efficiently with this method.

Possible interferences from blanks were assessed by measurement of pre-baked quartz filters set-aside during the sampling periods (i.e., field blanks). The blank OC measurements averaged 0.20 μg C/cm^2 for a filter punch, which translates to 0.05 μg C/m^3 ambient concentration. For the WSOC, filter background effects and background interferences from carbonaceous material in the purified water were insignificant compared to the concentrations of the aerosol analyzed and did not need to be considered.

6.1.2. Size-Exclusion Chromatography

SEC is traditionally used to measure the molecular size distribution of organic compounds and has recently been applied to organic aerosols [*Krivácsy et al.*, 2000; *Andracchio et al.*, 2002]. The approach is based on the use of a stationary phase consisting of porous particles. Molecules in the aqueous liquid sample that are smaller than the pore's size can enter the pores between particles and therefore have a longer path and transit time through the column than larger molecules that cannot enter the pores. In theory larger molecules are retained the least and will elute before smaller molecules, but in practice retention time also depends on hydrophobic and electrostatic interactions between the analytes and the stationary phase [*Krivácsy et al.*, 2000 and references within].

SEC is often employed to determine the molecular weight of humic substances in natural organic matter (NOM). In this application a solution of strong ionic strength is necessary to reduce interactions between the column and NOM [*Her et al.*, 2002b]. Direct application of this method to aerosol particle WSOC, however, was found to produce large dips in the SEC chromatograms, apparently from salting out effects from

the ionic strength adjustment. By not adjusting the solution ionic strength to minimize electrostatic interactions, it was found that the SEC provides a useful means of separating WSOC components by functional group. Previous studies have recognized that SEC does separate organic carbon functional groups [*Andracchio et al.*, 2002].

Low pressure SEC was performed with a 1 cm ID x 30 cm length glass column hand-packed with Superdex^{TM}-30 resin (Amersham Pharmacia Biotech, Stockholm, Sweden). This resin has a slightly cationic property. The eluent used was a phosphate buffer with pH 6.8. Phosphate buffer was chosen because it has been used by other groups [e.g., *Her et al.*, 2002a] who previously worked with this resin for analysis of NOM. Since this method worked with the TOC detector, due to the phosphate buffer being an inorganic eluent, and did not seem to cause artifacts, no other eluents were tested. However, it is noted that once phosphate is introduced into a sample it is very hard to remove.

A sample volume of 1 ml from the extracted Hi-Volume filter (i.e., for SEC on total WSOC) or XAD-8 isolated fractions was injected onto the column by the eluent at a flowrate of 1.3 ml/min. Each elution took approximately 1 hour to ensure the sample had passed through the entire column volume, however, as will be seen in the chromatograms only ~25 minutes are required for the separations. The TOC analyzer in Turbo mode, with a flowrate of 1.2 ml/min, was used as the detector to quantify the separated WSOC compounds on-line. It was found that a minimum analyte concentration of approximately 2 ppm C (2 μg C) was needed for this SEC analysis. The column was cleaned periodically with 0.1 M HCl, then 0.1 M NaOH, and lastly DI Water, each for 1 hour at a

flowrate of 1.3 ml/min to remove organics that were non-elutable in the phosphate eluent and had adsorbed to the resin.

The SEC column was calibrated using the same group of water-soluble organic compounds tested on the XAD-8 column (see section 5.1). SEC recovery efficiencies are given in Table 6.1. The results show that practically all compounds tested are recovered with ~85% efficiency within the column volume (50 minutes after injection). Syringaldehyde and catechol were not recovered within the column volume (eluted 54 and 64 minutes after the injection respectively), apparently because they do not ionize in the buffered aqueous sample. Saccharides are also non-ionizable, however, they have small octanol-water partitioning constants (log K_{ow}) unlike syringaldehyde and catechol. The larger the log K_{ow} value the less soluble in water the compound and the more likely the compound will have hydrophobic interactions with the SEC resin causing longer retention times. Other non-ionizable compounds with large log K_{ow} values may also not elute within the column volume for similar reasons.

Chromatographic separations of the various calibration compounds are shown in Figure 6.2. For the most part, individual chromatograms show compounds for a given functional group. These experiments indicate that SEC separates compounds by functional group, and that within most groups, higher molecular weight compounds elute first, due to size-exclusion processes within the column. For this application, the interest is in the SEC column's ability to isolate by functional groups the compounds within the hydrophilic and hydrophobic fractions recovered from the XAD-8 resin. For example, within the WSOCxp fraction, aliphatic mono-, di-, and oxocarboxylic acids eluted between 25 to approximately 32 minutes (WSOCxp_a, Figure 6.2a), then neutral

Table 6.1. SEC recovery efficiencies for various calibration water-soluble organic compounds listed by functional groups, where WSOCxp=hydrophilic, WSOCxrr=hydrophobic recovered, and WSOCxru=hydrophobic unrecovered. Mean and standard deviation are listed at the bottom of the table for these three classes.

Functional Group	Compound	[SEC calc] (ppb C)	[Measured] (ppb C)	% Recovery	Comment
Monocarboxylic acid	Formic acid	1659	1573	105	WSOCxp
	Acetic acid	1364	1467	93	WSOCxp
	Butyric acid	1488	1823	82	WSOCxru
	Caproic acid	1581	1750	90	WSOCxru
Dicarboxylic acid	Oxalic Acid	1803	2175	83	WSOCxp
	Malonic acid	1553	2030	77	WSOCxp
	Succinic acid	1308	1790	73	WSOCxp
	Glutaric acid	1770	1785	99	WSOCxru
	Azelaic acid	1356	1690	80	WSOCxru
Carbonyls	Glyoxal	1716	2183	79	WSOCxp
	Propanal	1227	1540	80	WSOCxp
	Butanal	1322	1520	87	WSOCxru
Oxocarboxylic acid	Glyoxylic acid	1495	2000	75	WSOCxp
Amines	Ethanolamine	1689	1620	104	WSOCxp
Saccharides	Levoglucosan	1512	1883	80	WSOCxp
	Inositol	1520	1810	84	WSOCxp
	Sucrose	1580	2030	78	WSOCxp
Phenols	Catechol*	1376	1930	71	WSOCxrr
	Salicylic Acid	1382	2000	69	WSOCxrr
	3-Hydroxybenzoic acid	1317	1670	79	WSOCxrr
Aromatic Acids	Benzoic Acid	1545	1970	78	WSOCxrr
	Phthalic acid	1670	1975	85	WSOCxrr
Cyclic Acids	Pinic Acid	1736	1955	89	WSOCxru
Organic Nitrates	Isopropyl nitrate	262	294	89	WSOCxru
		Mean ±	standard deviation	84 ± 11	WSOCxp
				78 ± 7	WSOCxrr
				88 ± 6	WSOCxru

*Catechol does not elute within the column volume.

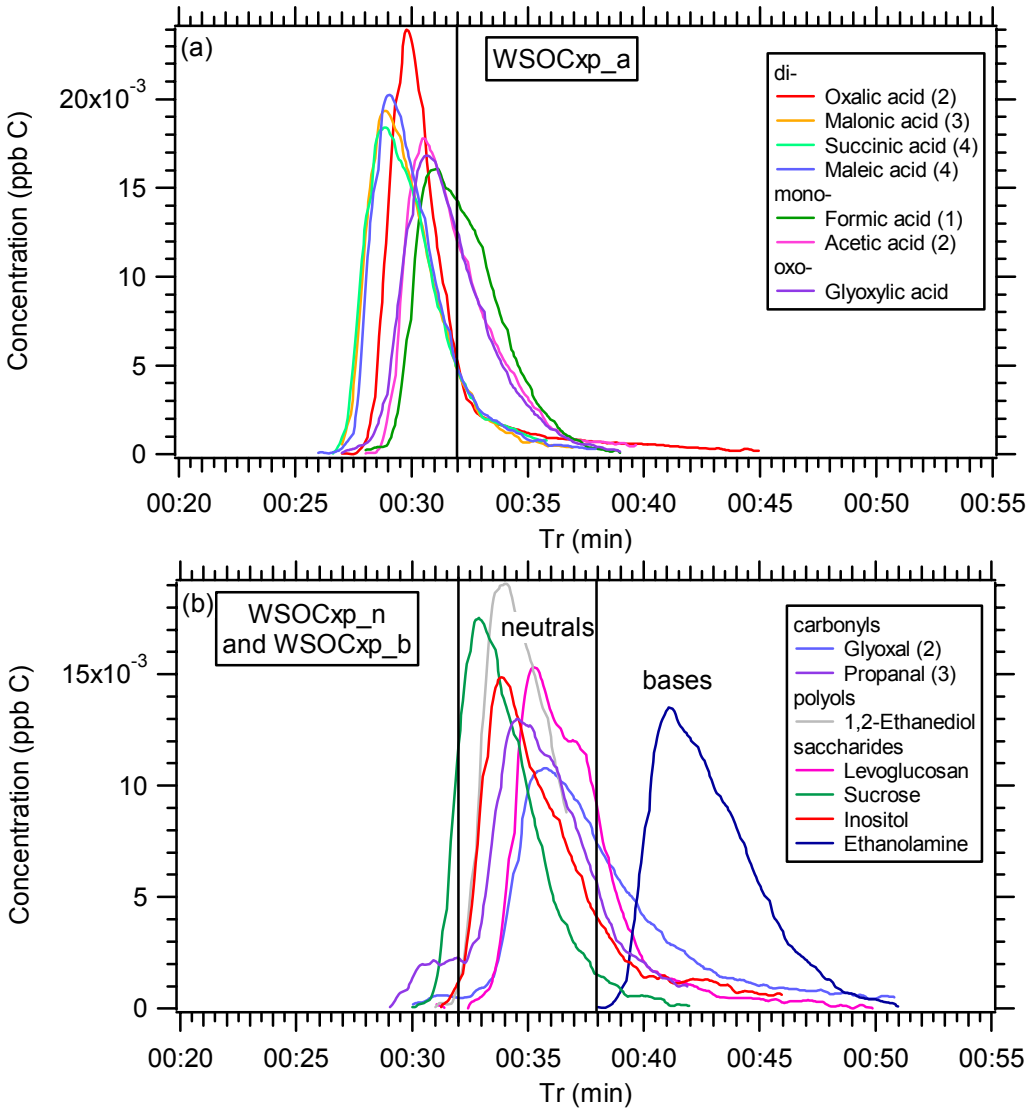

Figure 6.2. Normalized SEC chromatograms from calibrations with (a) hydrophilic acids (WSOCxp_a), (b) hydrophilic neutrals (WSOCxp_n) and bases (WSOCxp_b), (c) recovered hydrophobic acids (WSOCxrr_a), (d) recovered hydrophobic neutrals (WSOCxrr_n), and (e) unrecovered hydrophobic (WSOCxru) water-soluble organic compounds, where Tr is the retention time. Recoveries of these various compounds are given in Table 6.1. Listed in parenthesis is the number of carbon atoms per molecule for the series of mono- and dicarboxylic acids and carbonyls. The black lines represent the retention times before or after each group elutes.

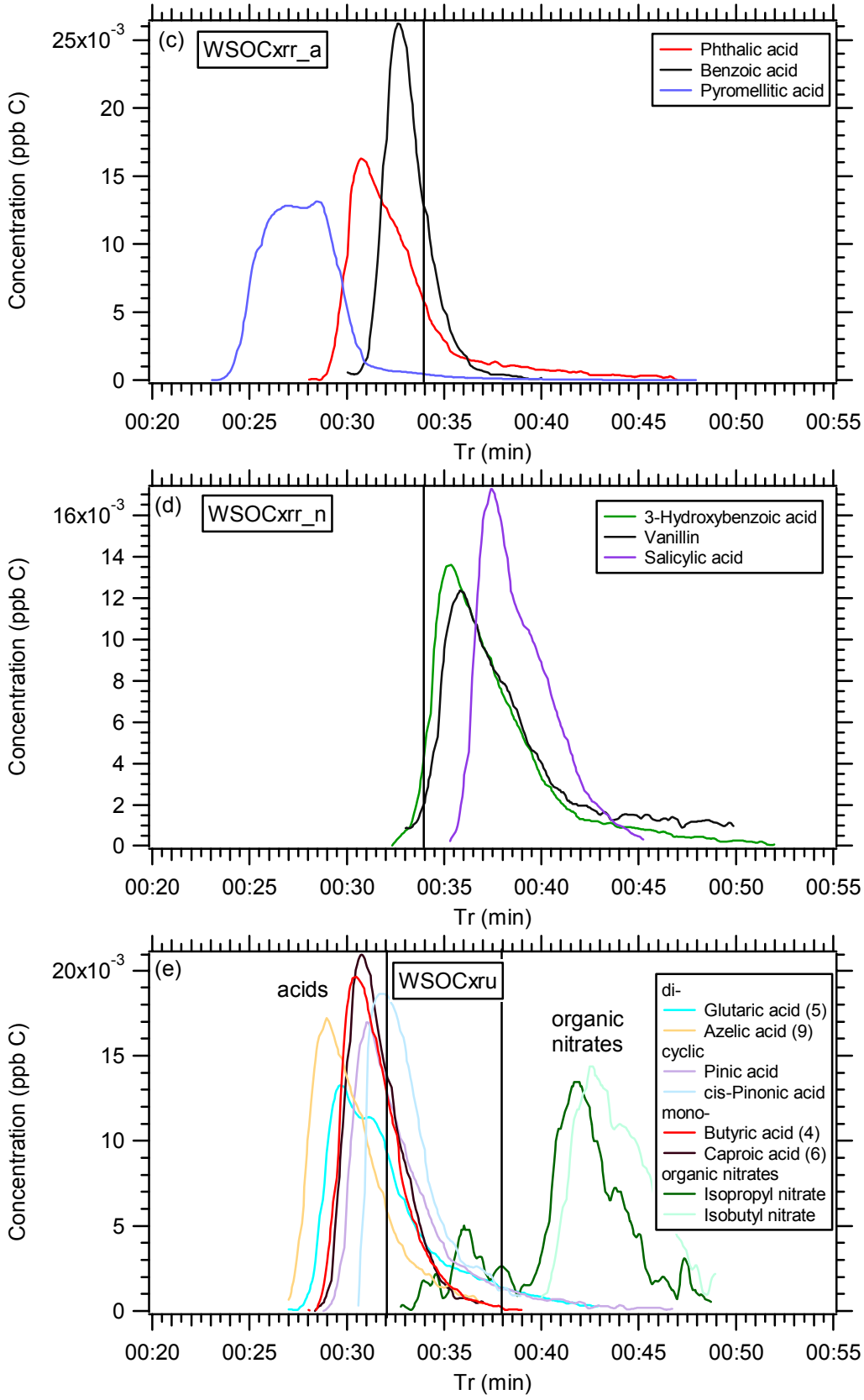

Figure 6.2. Continued.

compounds such as saccharides and carbonyls elute from 32 to approximately 38 minutes (WSOCxp_n, Figure 6.2b). Finally, between 38 to approximately 45 minutes the bases are eluted from the column (WSOCxp_b, Figure 6.2b). The WSOCxrr fraction tends to split into acids such as aromatic acids (WSOCxrr_a, Figure 6.2c), which eluted before about 34 minutes, and neutral compounds such as phenols that came out after 34 minutes (WSOCxrr_n, Figure 6.2d). For the WSOCxru fraction, compounds such as cyclic and mono- and dicarboxylic acids with greater than 3 or 4 carbons eluted before approximately 32 minutes (Figure 6.2e). Unrecovered XAD-8 organic nitrates eluted between 38 to about 45 minutes (Figure 6.2e). The separations are clearly not ideal since there is overlap between groups due to peak tailing. This is not unusual for a hand-packed column. Significant improvements might be expected with commercially available high pressure SEC columns. The hand-packed column, however, served the purpose for exploratory work to provide chemical insights into the WSOCxp and WSOCxrr fractions.

The general trend for all functional groups tested is that more acidic compounds elute from the column first, basic compounds elute last, and more neutral compounds elute somewhere between these extremes. This elution pattern can be largely explained by the sample buffering and charge interactions between the mobile and stationary phases. *Specht and Frimmel* [2000] showed that the retention times of various organic compounds on SEC columns are effected by how the sample is buffered. This method differs from traditional SEC methods in that the electrostatic interactions between the mobile and stationary phase are not suppressed. At pH 6.8 most carboxylic groups carry a negative charge and therefore are subject to ion-exclusion interactions that reduce

retention times. Molecules with several carboxylic acid groups enhance the ion-exclusion interactions and result in even shorter retention times. The calibrations show this trend for both the aliphatic and aromatic acids, where compounds with dicarboxylic acids come off the column before groups with monocarboxylic acid groups. Amino groups are, however, positively charged and can undergo ion exchange reactions with the stationary phase, which increases retention times. Neutral compounds in the mobile phase will not experience charge interactions with the stationary phase. Therefore, acids elute first, bases last, and neutrals in the middle. Hydroxyl groups are also known to increase the retention time and can enhance the attractive interactions of an aromatic ring [*Specht and Frimmel*, 2000], hence phenolic compounds elute after aromatic acids.

It should be pointed out that although the molecular weight of the organic compounds found in the aerosol is a subject of much debate, it is likely that the compounds are all within the 10,000 Dalton molecular weight cutoff for this resin. For example, *Kiss et al.* [2003] has provided experimental evidence that the molecular weight of HULIS, which is considered to be the high molecular weight component of organic aerosols, is between 200-300 Daltons. Since the groupings discussed above are based only on atmospherically relevant compounds that calibration standards are available for and as previously mentioned size-exclusion properties are observed, it is possible that larger molecular weight compounds from one group could be eluting in the previous group. However, there is confidence in these groupings since some of the largest molecular weight compounds in each group that have been observed in the atmosphere were tested.

A measure of the precision (reproducibility) for the SEC column was determined based on the standard deviation of the peak areas for multiple injections of the same ambient sample. Repeating for each XAD-8 fraction, the standard deviations were ±2.5%, ±5.8%, and ±8.1% for WSOC, WSOCxp, and WSOCxrr respectively. During these injections, no shifts in the retention time were noted.

6.1.3. Measurement Approach

A total of 21 summer, 10 winter, and 2 biomass burning integrated filter samples were analyzed. A portion of each filter was extracted for the WSOC component. A series of measurements were then performed on each aqueous sample. In all cases, the WSOC content was measured directly by the TOC analyzer. Following the method described in section 5.1, a XAD-8 resin column was used to isolate the WSOCxp (hydrophilic) and WSOCxrr (recovered hydrophobic) fractions. The WSOCxru (unrecovered hydrophobic) fraction was determined by difference (= WSOC - WSOCxp - WSOCxrr). The three samples, WSOC, WSOCxp, and WSOCxrr, were then each further analyzed by SEC with TOC detection. The equations used to calculate these various concentrations can be found in section A.2 of Appendix A. To help clarify the various functional groups delineated by the XAD-8 and then by SEC, Figure 6.3 shows a schematic of the break down of the various groups.

6.1.4. Measurements of OC, EC, and Light Organic Acids

OC and EC concentrations for each Hi-Volume sample were determined on a 1.4 cm^2 filter punch using the bench top model of the Sunset Labs ECOC analyzer described

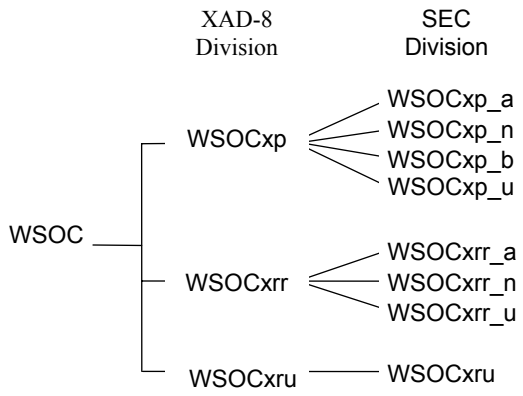

Figure 6.3. Schematic diagram of the WSOC fractions isolated first by XAD-8 and then by SEC. In the first step the XAD-8 is used to isolate WSOCxp from WSOCxr. Only a fraction of the WSOCxr compounds retained on the XAD-8 column can be recovered, and these are referred to as WSOCxrr. Those not recovered are WSOCxru. Tables 5.1 and 6.1 summarize the types of compounds in WSOCxp, WSOCxrr, and WSOCxru based on single compound calibrations. Fractions WSOCxp and WSOCxrr are then divided into functional groups by the SEC method. Abbreviation definitions are listed in the List of Abbreviations.

in section 3.1. The instrument was operated following NIOSH Method 5040 [*Eller and Cassinelli*, 1996].

Concentrations of oxalate, formate, and acetate were also measured in the WSOCxp liquid extracts using a dual-channel Dionex DX-500 ion chromatograph with EG40 potassium hydroxide eluent generator and AG11-HC IonPac analytical column (2 mm microbore ID). The ion chromatograph operates with a self-regenerating SRS-ULTRA suppressor in external DI Water mode, a CD20 conductivity detector, and a GP50 gradient pump.

6.2. Ambient Results

6.2.1. Analysis of OC, WSOC, and XAD-8 fractions WSOCxp and WSOCxrr

For the data used in the following SEC analysis, Figure 6.4 shows results of linear regressions between WSOC and OC, and between the hydrophilic and hydrophobic fractions and WSOC, for data segregated into summer and winter periods. In both seasons the WSOC and OC are highly correlated, as are the WSOCxp, WSOCxr, and WSOCxrr fractions of WSOC. The WSOC to OC ratio was higher in the summer (slope = 0.47) than in the winter (slope = 0.42), which was similar to observations for the on-line data discussed in section 5.2. In other studies [e.g., *Zappoli et al.*, 1999] the difference in summer and winter WSOC to OC ratios are typically much larger than what was observed here. Lower WSOC to OC ratios may be related to the unusually wet and clean conditions during the summer of 2004, which resulted in Atlanta having the fewest poor air quality days since 1998. Also, as a southern city, winter/summer seasonal differences are likely to be less dramatic than urban areas located at higher latitudes.

Along with the somewhat higher summer WSOC/OC, the summer hydrophilic (WSOCxp) fraction was greater than the hydrophobic fractions, whereas the opposite is observed in the winter. The analysis of the hydrophobic compounds has been extended beyond that discussed in section 5.2 in that the WSOCxrr fraction is now included. By comparing zero-intercept slopes, the average fractions of WSOCxp, WSOCxrr, and WSOCxru of the WSOC can be determined for summer and winter. In summer these fractions of WSOC are: WSOCxp 61%, WSOCxrr 23%, and WSOCxru 16%. For winter the fractions are: WSOCxp 46%, WSOCxrr 29%, and WSOCxru 25%. The data are consistent with greater summertime oxidation processes leading to larger fractions of

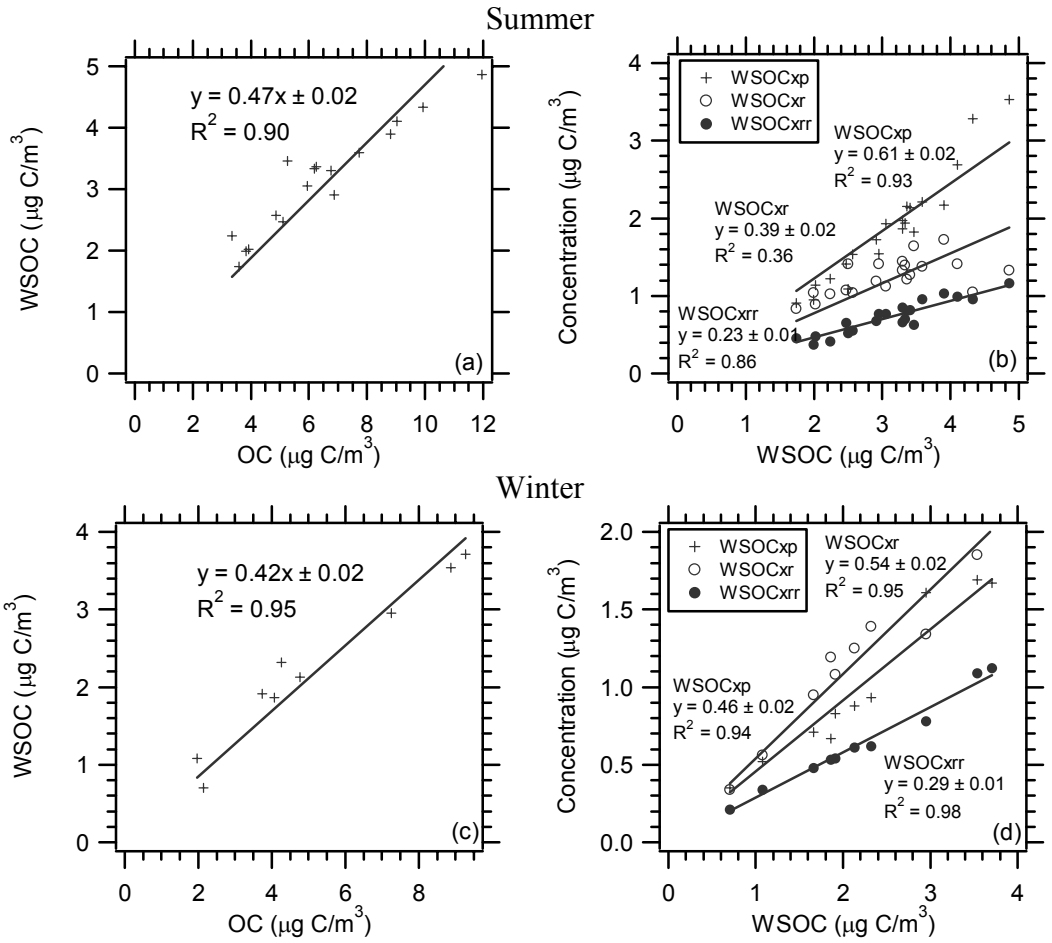

Figure 6.4. Correlations based on linear regressions forced through zero of WSOC versus OC for (a) summer and (c) winter, and WSOCxp, WSOCxr, and WSOCxrr versus WSOC for (b) summer and (d) winter. All are based on 24 hour integrated filter measurements. The slope uncertainty is one standard deviation.

WSOC. The fact that WSOCxp increases in the summer suggests that more oxidation occurs. All these fractions are based on 24 hour integrated filter measurements, which will tend to suppress larger variations due to any day/night differences. Moreover, these are average conditions for the summer and winter periods investigated. Differences in these ratios are much more dramatic under PM events (see section 5.2). SEC is now applied to the WSOCxp and WSOCxrr fractions to investigate changes in functional group concentrations from winter to summer.

6.2.2. SEC of WSOC, WSOCxp, and WSOCxrr

6.2.2.1 SEC Chromatograms of Ambient Samples

SEC was performed on the XAD-8 fractions obtained from the Hi-Volume samples. Figure 6.5 shows an example of the SEC data from a summer, winter, and a biomass burning filter sample. The summer and winter WSOCxp chromatograms display three modes, whereas the WSOCxrr chromatograms have two modes. Based on retention times of the ambient samples compared to calibration compounds shown in Figure 6.2, the modes that appear in the chromatograms can be related to various functional groups.

Based on our limited calibrations, acids are found mainly to the left of the 32 minute line, more neutral compounds to the right of 32 minutes, and basic compounds come out last. Peaks for the acid and neutral compounds can be seen in each of the total WSOC chromatograms. The calibrations suggest that for the WSOCxp fraction the peaks in order of increasing retention time are: short-chain aliphatic acids, neutrals (such as saccharides, short-chain carbonyls, and polyols), and finally a small peak from organic

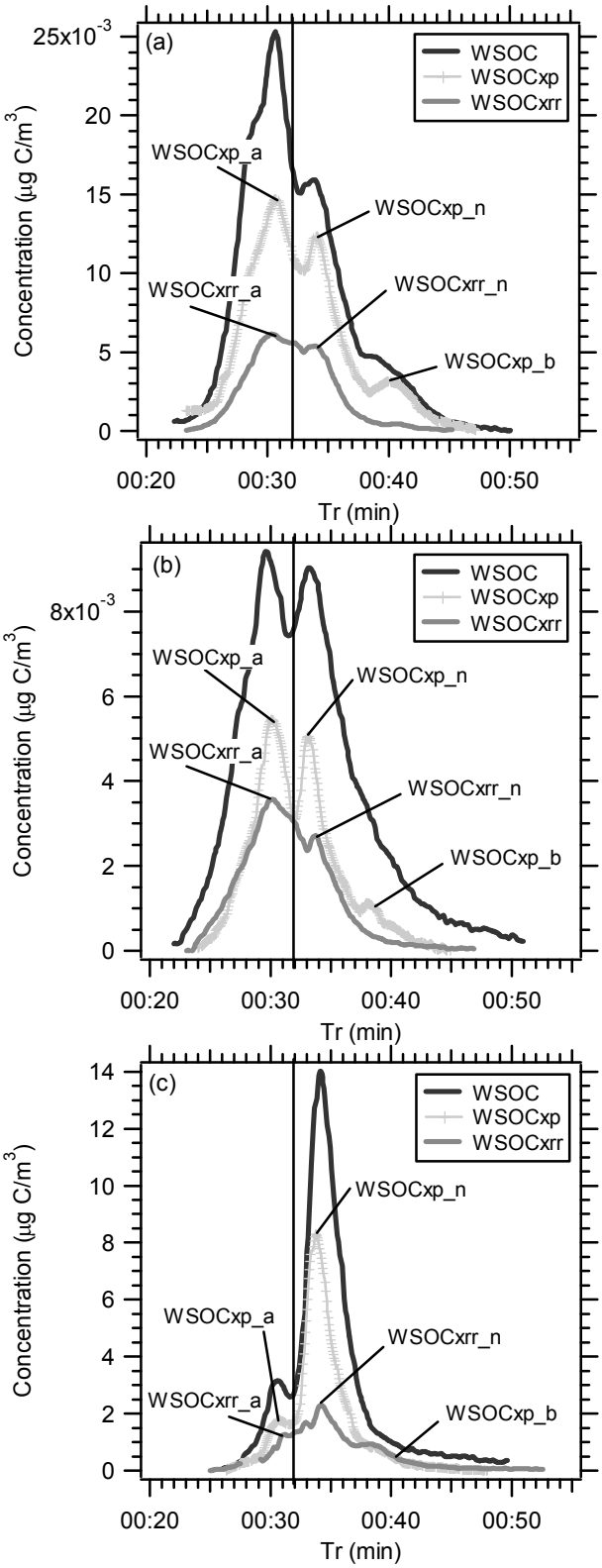

Figure 6.5. Examples of typical SEC chromatograms from a (a) summer (Atlanta August 29, 2004), (b) winter (Atlanta December 19, 2004), and (c) biomass burning sample (Fort Benning, Columbus, GA April 29, 2004).

bases. In the WSOCxrr chromatogram the two peaks are not as well resolved. The first peak is likely associated with acids and the second peak neutral compounds.

It cannot be precluded that other unknown compounds are also associated with these various peaks since the ambient organic aerosol is highly chemically complex and calibrations were performed with only a limited number of compounds that must be viewed as at best, only representative of true ambient compounds. However, the summer, winter, and biomass burning chromatograms are consistent with current views on aerosol sources. Oxidation processes, either in the gas or aerosol phase, leads to formation of acidic aerosol particle compounds [*Grosjean and Friedlander*, 1980; *Hatakeyama et al.*, 1985, 1987], and Figure 6.5 shows that WSOC acidic compounds (WSOC peak to the left of the 32 minute line) dominant in the summer sample compared to the winter sample (i.e., compare WSOC in Figures 6.5a and 6.5b). In contrast, single component analysis has shown that biomass aerosol particles contain saccharides (WSOCxp_n) and phenolic compounds (WSOCxrr_n) and in Figure 6.5c the second WSOC peak (to the right of the 32 minute line) dominates, the region where these types of compounds elute. The winter sample could be viewed as a combination of the summer and biomass in that the WSOC chromatogram's two peaks were typically near the same height, possibly suggesting a larger contribution from more biomass-like components in the winter, but still contributions from sources (oxidation processes) that produce acidic compounds. Note that for these data the winter concentrations are much lower than the summer values.

6.2.2.2. Quantitative Determination of Functional Groups

To calculate the carbon mass concentrations for the various organic functional groups isolated by SEC, chromatographic peaks that eluted first were fit with a Gaussian function using data from the leading edge to slightly following its maximum value. The second peak was then taken as the difference in the ambient chromatogram and the Gaussian function. Bases, if they existed, were subtracted from the second peak by fitting with a linear baseline. Figures 6.6a and 6.6b show an example of this fitting for the WSOCxp and WSOCxrr fractions respectively.

The calibration data show that for single components the chromatograms are not symmetrical but are skewed to higher retention times and known as a tailing Gaussian. Fitting with lognormal, Weibull, or inverse-normal distributions to better capture this asymmetry did not significantly improve the overall fit to the ambient chromatograms and were not employed for the sake of simplicity. Algorithms, such as PEAKFIT (Jandel Scientific) can be used to deconvolute overlapped chromatographic peaks, but again were not employed for this initial analysis.

It is noted that this approach will lead to a minor under estimation of compounds associated with the first peak (WSOCxp_a and WSOCxrr_a) and over estimation of compounds associated with the second peak (WSOCxp_n and WSOCxrr_n) due to the Gaussian fit to the asymmetrical actual tailing chromatograms. Thus, these results should be treated as first order estimates.

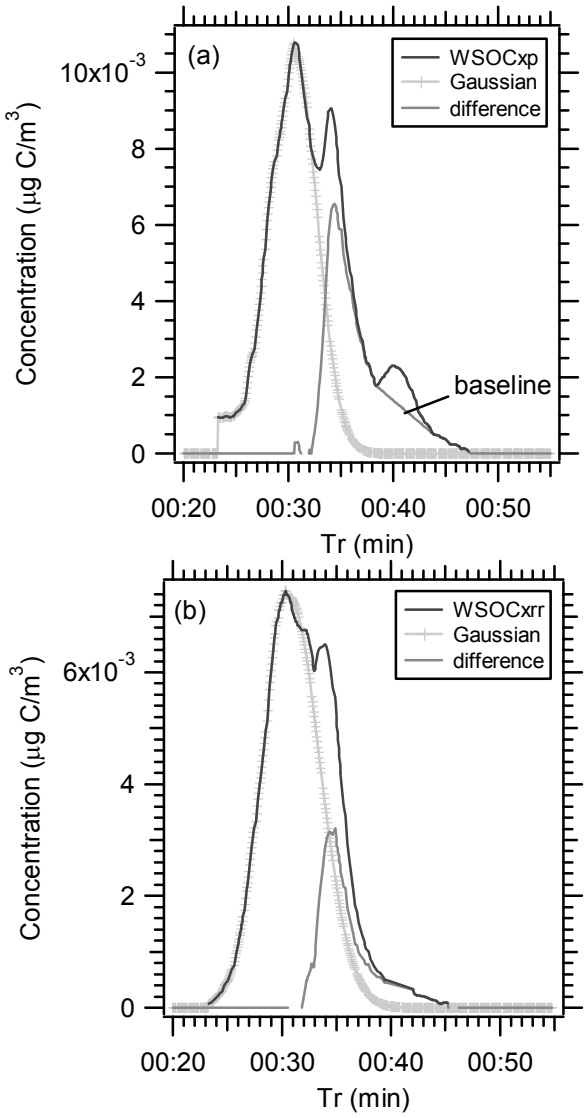

Figure 6.6. Example of fitting of (a) WSOCxp and (b) WSOCxrr, for the summer sample shown in Figure 6.5a, to obtain concentrations for the various functional groups. WSOCxp_a and WSOCxrr_a in (a) and (b), respectively, are the Gaussian fits to the first peak. The peak resulting from subtracting the Gaussian fit from the original chromatogram is also plotted. The baseline for determining hydrophilic bases is also shown in (a).

6.2.2.3. SEC Recoveries of Ambient Samples

Ambient concentrations of WSOC and isolated fractions for the integrated filters analyzed are summarized in Table 6.2. Also included in this table are the recoveries from the SEC analysis of ambient samples of WSOC, WSOCxp, and WSOCxrr. (Note, the WSOCxrr data in Table 6.2 are corrected for an eluent artifact, which will be discussed in more detail below.) Recoveries are calculated through a carbon mass balance by comparing the carbon mass concentration from the integral over the SEC chromatogram to the carbon mass concentration measured in the liquid sample applied to the SEC column. Once corrected for an artifact, with the exception of the biomass burning and winter WSOCxrr samples, the WSOC, WSOCxp, and WSOCxrr fractions all had recoveries better than about 75%, similar to the results with the calibration standards (see Table 6.1). The lower recovery for the biomass burning and winter WSOCxrr is likely due to significant concentrations of non-ionizable compounds, possibly all associated with biomass burning smoke. For example, the calibrations showed compounds such as catechol, a known biomass burning product [*Simoneit*, 2002], did not elute in the column volume.

6.2.2.4. Eluent Artifacts

Unlike the laboratory test with calibration compounds, the ambient WSOCxrr samples contained NaOH, the eluent used to recover hydrophobic compounds from the XAD-8 column. For most of the ambient WSOCxrr samples, the SEC recovery was over 100%. For example, for WSOCxrr compounds the mean ± standard deviations for recoveries for summer, winter, and biomass burning samples were 131 ± 32%, 100 ±

Table 6.2. SEC recovery efficiencies for the WSOC, WSOCxp, and WSOCxrr for all summer, winter, and biomass burning samples. Upstream = concentration applied to the SEC column, SEC Integral = concentration determined from the integral over the chromatogram, Recovery = (SEC Integral)/Upstream

Filter #	WSOC Upstream (μg C/m^3)	WSOCxp Upstream (μg C/m^3)	WSOCxrr Upstream (μg C/m^3)	WSOC SEC Integral (μg C/m^3)	WSOCxp SEC Integral (μg C/m^3)	WSOCxrr SEC Integral (μg C/m^3)	% WSOC recovery	% WSOCxp recovery	% WSOCxrr recovery
Summer									
F2 (6/11)	4.33	3.28	0.96	4.17	2.48	0.80	98	76	83
F3 (6/13)	3.30	1.86	0.66	2.63	1.57	0.59	80	84	89
F5 (6/17)	2.50	1.09	0.52	1.65	1.10	0.43	66	101	82
F6 (6/19)	3.33	1.94	0.70	1.69	0.93	0.44	51	48	63
F7 (6/21)	3.46	1.82	0.63	1.75	1.14	0.48	51	63	76
F8 (6/23)	1.99	0.95	0.37	1.07	0.55	0.29	54	58	79
F10 (6/27)	2.24	1.22	0.41	1.67	0.87	0.46	75	71	113
F2B (8/8)	3.30	1.97	0.85	1.87	0.89	0.46	57	45	54
F3B (8/10)	4.10	2.69	0.99	4.58	1.59	0.76	112	59	77
F4B (8/12)	1.74	0.91	0.45	1.48	0.99	0.77	89	109	170
F5B (8/14)	2.95	1.54	0.77	2.82	0.87	0.62	96	56	81
F6A (8/15)	2.57	1.53	0.55	2.53	1.30	0.62	98	85	113
F7B (8/16)	2.47	1.41	0.65	1.61	1.05	0.43	65	74	66
F8B (8/17)	3.59	2.21	0.96	3.97	2.04	1.13	111	92	118
F9B (8/19)	4.86	3.53	1.16	5.01	2.71	1.21	103	77	104
F12B (8/23)	3.41	2.14	0.82	3.23	1.84	0.78	95	86	95
F13B (8/25)	3.36	2.15	0.81	3.11	1.99	0.75	93	93	94
F14B (8/27)	3.90	2.17	1.03	2.54	1.27	0.74	65	59	72
F15B (8/29)	3.05	1.93	0.77	2.52	1.42	0.61	83	74	80
F16B (8/31)	2.91	1.72	0.68	3.13	1.31	0.75	108	76	110
F17B (9/2)	2.02	1.14	0.48	1.92	0.71	0.40	95	62	82
					mean ± standard deviation		80±20	76±17	91±25

Table 6.2. Continued.

Winter									
F1BB (12/11)	0.70	0.35	0.25	0.73	0.31	0.15	104	89	59
F2BB (12/19)	2.13	0.88	0.61	1.55	0.77	0.44	73	88	72
F3BB (1/11)	2.95	1.61	0.78	2.52	1.47	0.91	85	91	117
F4BB (1/13)	2.32	0.93	0.62	1.70	0.77	0.46	73	83	74
F5BB (1/18)	1.86	0.67	0.53	1.01	0.50	0.31	54	75	58
F6BB (1/20)	3.54	1.69	1.09	2.76	1.20	0.70	78	71	64
F7BB (1/23)	1.08	0.52	0.34	1.14	0.39	0.20	106	75	58
F8BB (1/25)	3.71	1.67	1.12	2.80	1.31	0.73	75	78	66
F9BB (1/28)	1.67	0.71	0.48	1.31	0.54	0.32	78	76	67
F10BB (2/2)	1.91	0.83	0.81	1.39	0.63	0.37	73	76	46
					mean ± standard deviation		80±15	80±7	68±19
Biomass	**Burning**								
GT14 (4/16)	1236	607	303	797	459	218	64	76	72
GT46 (4/29)	938	471	248	593	426	152	63	90	61
					mean ± standard deviation		64±1	83±10	67±6

23%, and 83 ± 6% respectively. Subsequent experiments showed that the SEC recoveries higher than 100% were due to interference from the NaOH from the XAD-8 extraction procedure. To correct for this artifact, experiments were performed in which single synthetic compounds were run through the complete extraction procedure (XAD-8 plus SEC). Two recovered hydrophobic acids (benzoic and phthalic acid) and neutrals (3-hydroxybenzoic and salicylic acid) were passed over the XAD-8 at various concentrations, recovered in NaOH eluent, and then injected onto the SEC column and the resulting chromatograms integrated. The slopes of actual concentrations versus integrated SEC concentrations were 0.59, 0.76, 0.95, and 1.08 for phthalic, benzoic, salicylic, and 3-hydroxybenzoic acids, respectively, with all R^2 values greater than 0.99. In this experimental data (as was also observed in the ambient data), the NaOH interference mainly affects the WSOCxrr_a region of the SEC chromatogram. Based on these results, the integrated concentrations for WSOCxrr_a were multiplied by 0.59 and for the WSOCxrr_n by 0.95 (the lower of the two slopes from each group). Clearly this eluent interference leads to most uncertainty in the WSOCxrr_a concentrations; estimated to be on the order of ± 20%. However, these corrections seem valid since, as shown in Table 6.2, after the correction is applied the recoveries for summer samples of WSOC, WSOCxp, and WSOCxrr all are within similar values (WSOC 80%, WSOCxp 76%, and WSOCxrr 91%) and comparable to calibration results performed with no NaOH eluent (Table 6.1).

6.2.3. Ancillary Measurements: Comparison of SEC and ^{13}C-NMR

Interpretation of the ambient SEC chromatograms based solely on the synthetic calibration standards could be misleading since actual compounds in the ambient WSOC aerosol remain largely unknown and the standards may not represent the real aerosol. However, ancillary measurements seem to support the calibrations.

The WSOCxrr fraction was found to absorb visible light. This indicates the presence of conjugated bonds (e.g., aromatic compounds). Straight-chain compounds can also contain conjugated bonds, but would require there to be at least four carbons in the chain. Based on the XAD-8 calibrations, both of these types of compounds were found to be hydrophobic.

Tensiometer measurements, which determine the reduction of droplet surface tension as a function of solution carbon mass, showed that the recovered hydrophobic (WSOCxrr) fraction also exhibited surfactant properties. In contrast, the hydrophilic (WSOCxp) fraction did not demonstrate either of these properties. It has been shown that long-chain (> C_5), nonpolar groups attached to polar tails (e.g. carboxylic acids and carbonyls) can have surfactant properties and form a surface film on droplets by lining up with the polar ends in the water and nonpolar, hydrophobic ends projecting into the air [*Gill et al.*, 1983]. Interestingly, as mentioned in chapter 5, the XAD-8 calibration results showed that for the series of mono- and dicarboxylic acids and carbonyls, the transition from hydrophilic to hydrophobic occurred for compounds with approximately 4 to 5 carbons in the chain.

Additionally, as a means to further identify compounds in WSOC, and to compare with our isolated fractions, solid-state ^{13}C-NMR was performed on WSOC, WSOCxp,

and WSOCxrr samples separated by XAD-8 resin. ^{13}C-NMR was performed on samples from two sources: a sample of pooled summer filters and a biomass burning sample.

Liquid samples for each of the three fractions were vacuum freeze dried and the resulting solids collected. For the summer sample, eight individual $PM_{2.5}$ Hi-Volume integrated filters from June and August were extracted separately, freeze dried, and then combined to obtain sufficient mass for the analysis (minimum of 3 mg C is required). Following the ^{13}C-NMR analysis, the freeze dried solid from the total WSOC sample was reconstituted in 125 ml deionized water and then separated through the XAD-8 column to collect WSOCxp and WSOCxrr fractions for subsequent SEC analysis. The ^{13}C-NMR biomass burning sample was easier to prepare due to the much higher filter loadings than the urban samples. This sample was prepared by extracting a quarter of 4 different Hi-Volume integrated filters together and freeze drying a portion of the liquid extract. Therefore, in this case, liquid extracts were available for SEC analysis of WSOC, WSOCxp, and WSOCxrr, and no reconstitution of solid samples was required. A more detailed description of the ^{13}C-NMR sample preparation, method, and results can be found in *Sannigrahi et al.* [2006].

The SEC chromatograms for the ^{13}C-NMR summer and biomass burning samples are shown in Figures 6.7a and 6.7b respectively. Concentrations of the various functional groups were determined from the chromatograms and shown as pie charts in Figures 6.7a and 6.7b. The most prominent ^{13}C-NMR spectral peaks for the WSOCxp and WSOCxrr fractions of the summer and biomass sample are shown in Table 6.3. This table gives the percentage of peak area for the top four out of seven ^{13}C-NMR spectral peak regions. Integration of ^{13}C-NMR spectra has been shown to provide quantitative information on

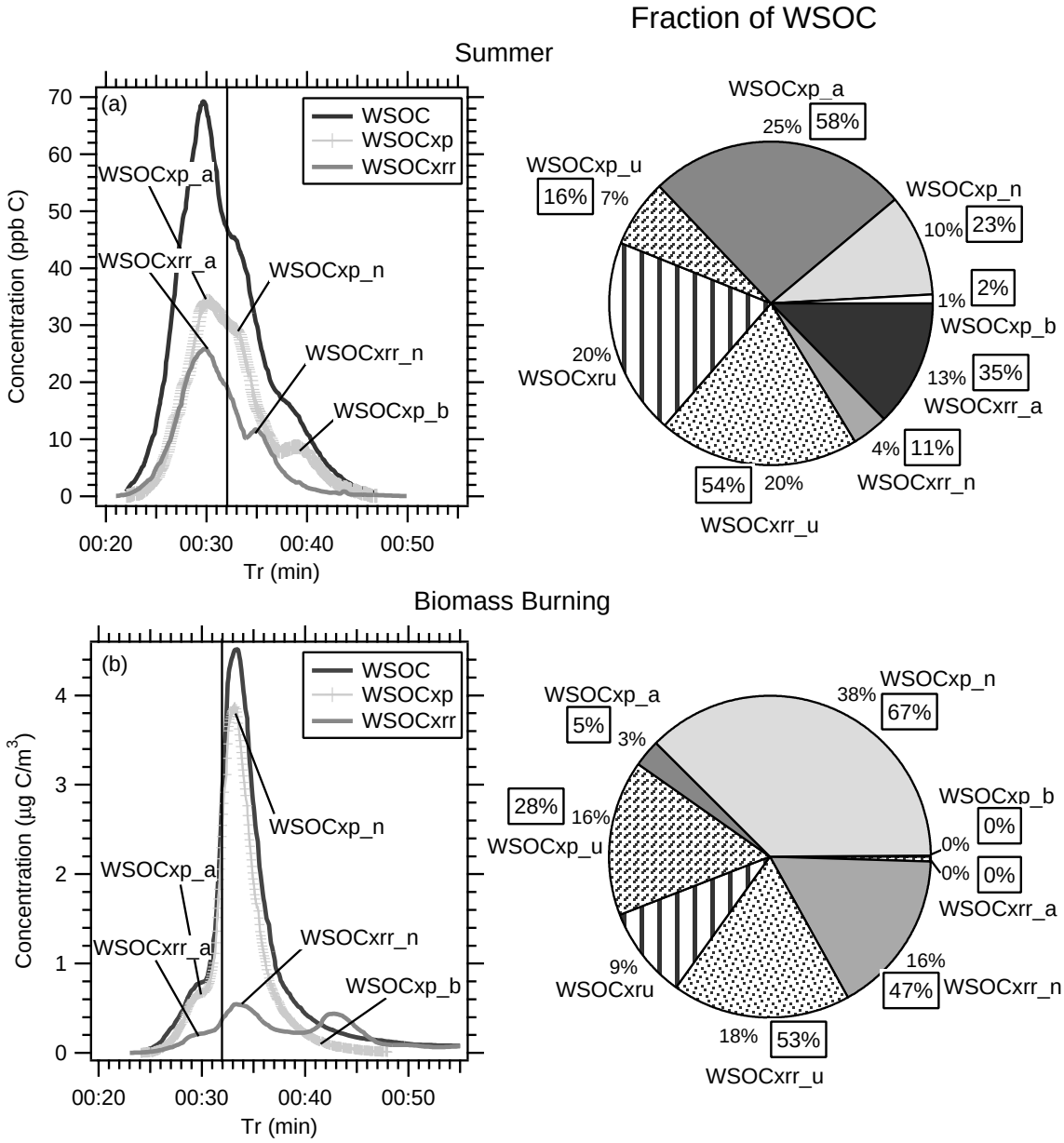

Figure 6.7. SEC chromatograms and percentage each functional group contributes to the total WSOC for the ^{13}C-NMR (a) summer and (b) biomass burning samples. Note in (a) and (b), due to the differences in sample preparation, the summer SEC chromatogram is presented in liquid concentration and the biomass burning sample in air concentrations. For comparison with ^{13}C-NMR results in Table 6.3, the boxed percentages show each fraction relative to their respective groups (WSOCxp or WSOCxrr) instead of as a fraction of WSOC.

Table 6.3. Comparison of SEC and ^{13}C-NMR for WSOCxp and WSOCxrr fractions of summer and biomass burning samples. Both the SEC and ^{13}C-NMR functional group results are given as a percent of the total WSOCxp and WSOCxrr fractions. For the ^{13}C-NMR, only the top 4 spectral regions for each measurement are shown. A more complete table on the ^{13}C-NMR results can be found in *Sannigrahi et al.* [2006].

	Summer		Biomass Burning	
	SEC	^{13}C-NMR	SEC	^{13}C- NMR
WSOCxp	58% WSOCxp_a 23% WSOCxp_n 16% WSOCxp_u 2% WSOCxp_b	60% C-alkyl 24% O-alkyl 10% carboxylic 7% N-alkyl	67% WSOCxp_n 28% WSOCxp_u 5% WSOCxp_a 0% WSOCxp_b	76 % O-alkyl 24% N-alkyl All others 0
WSOCxrr	54% WSOCxrr_u 34% WSOCxrr_a 11% WSOCxrr_n -	60% C-alkyl 18% O-alkyl 9% carboxylic 8% alkyl aromatic	53% WSOCxrr_u 47% WSOCxrr_n 0% WSOCxrr_a -	36% C-alkyl 22% alkyl aromatic 12% anomeric/acetal C 9% N/O aromatic, O-alkyl*

*9% N/O aromatic and 9% O-alkyl

the fraction, in terms of carbon mass, of the bonds between carbon and various functional groups, for all molecules in the sample [*Wilson*, 1987; *Hedges et al.*, 2002; *Sannigrahi et al.*, 2005]. Thus, unlike the XAD-8 and SEC, which isolates compounds based on composition of individual molecules, in ^{13}C-NMR one molecule can contribute to many spectral regions.

An overall result from the ^{13}C-NMR is that for both the summer WSOCxp and WSOCxrr fractions, the C-alkyl group is by far the most common (~60%), followed by O-alkyl (~20%), and then carboxylic acids (~15%). Table 6.3 compares the ^{13}C-NMR results on the two XAD-8 isolated fractions of WSOC to the various functional groups isolated by SEC performed on the same XAD-8 fractions. The WSOCxp fraction is compared first, then the WSOCxrr fraction.

6.2.3.1. Comparisons Between WSOCxp Compounds

For the most part, the SEC and ^{13}C-NMR for the summer and biomass WSOCxp samples qualitatively agree. Table 6.3 shows that the WSOCxp fraction from the summer sample is mainly WSOCxp_a with a smaller amount of WSOCxp_n. The ^{13}C-NMR results show that the carbonaceous material in the sample is composed of molecules with mostly C-alkyl bonds, followed by O-alkyl, then carboxylic acids. C-alkyls are expected in both the WSOCxp_a and WSOCxp_n since these groups can be composed of aliphatic acids and carbonyls. Thus a high C-alkyl fraction is expected. O-alkyls could be mostly associated with the WSOCxp_n since carbonyls, saccharides, and polyols contain larger fractions of oxygenated aliphatic carbons. Although not shown in Table 6.3, no aromatic peaks were found in the WSOCxp ^{13}C-NMR spectra; alkyl-

substituted aromatics and N/O substituted aromatics were both zero. This agrees with the XAD-8 calibration results that aromatic compounds are only separated into the WSOCxrr fraction.

For the biomass burning sample, the SEC result shows the WSOCxp fraction is composed mainly of WSOCxp_n compounds and the ^{13}C-NMR gives mainly O-alkyl bonds. These observations seem to be in agreement since biomass burning is known to be composed of saccharides. WSOCxp_a makes only a minor contribution and ^{13}C-NMR detects no carboxylic acids (at this sensitivity). N-alkyls, which make up 24% of the WSOCxp group, may be associated with aliphatic amines [*Graham et al.*, 2002]. Again, the calibrations suggest no aromatic compounds are associated with hydrophilic species and none are found in the WSOCxp ^{13}C-NMR results. Overall, similar functional groups have been observed using H-NMR on biomass burning aerosols in Amazonia [*Graham et al.*, 2002].

6.2.3.2. Comparisons Between WSOCxrr Compounds

Calibrations with synthetic samples have indicated that only compounds with aromatic groups that are retained on the XAD-8 column are recovered (WSOCxrr). Hence a large fraction of the ^{13}C-NMR spectra for the WSOCxrr class would be expected to contain aromatic groups, however, this is not the case. Considering first the summer WSOCxrr sample, SEC shows that the largest fraction is unrecovered hydrophobic (WSOCxrr_u) compounds. That is, compounds recovered from the XAD-8 (i.e., possibly aromatic), but not recovered by the SEC (non-ionizable). The next largest fraction from the SEC is WSOCxrr_a, and then WSOCxrr_n. (Note that this sample is unusual and

could be a result of having to reconstitute the sample following ^{13}C-NMR analysis. For the summer average, WSOCxrr_a = 52%, WSOCxrr_n = 39%, and WSOCxrr_u = 9% of the WSOCxrr.) ^{13}C-NMR shows that the C-alkyl group is by far the largest fraction, and then to lesser extents O-alkyls, carboxylic acids, and alkyl-substituted aromatics at only 8%. Thus, there are significant differences between the SEC and ^{13}C-NMR; a high fraction of aromatic groups are expected, but instead C-alkyl groups dominate. SEC and ^{13}C-NMR both agree that there were few phenol-like compounds; SEC puts WSOCxrr_n last and no peak was observed in the ^{13}C-NMR for the N/O substituted aromatics.

For the WSOCxrr biomass sample, SEC shows that the largest fractions are WSOCxrr_u and the WSOCxrr_n. WSOCxrr_a is near zero. However, again the largest ^{13}C-NMR peak area for this group is associated with the C-alkyl region and the ^{13}C-NMR shows that N/O substituted aromatics (includes phenolic compounds) at 9% are a smaller fraction than the alkyl-substituted aromatics (includes aromatic acids) at 22%. Thus, there are two discrepancies here when comparing the ^{13}C-NMR to SEC biomass burning results. First, like the summer sample, there are high levels of C-alkyls in the ^{13}C-NMR when SEC suggests mainly aromatics. Secondly, the SEC gives a high fraction of WSOCxrr_n and no WSOCxrr_a, whereas ^{13}C-NMR has higher levels of aromatic acids (alkyl-substituted aromatics).

The first discrepancy could be explained by the fact that the calibrations do not prove that the WSOCxrr fraction is exclusively associated with molecules that contain aromatics. The calibration data show that aromatics are found only in the WSOCxrr fraction, but it cannot be proved that the WSOCxrr fraction for ambient aerosol particles is exclusively composed of molecules containing at least one aromatic ring. It is well

known that readily available calibration compounds are likely not representative of ambient particulate organic constituents. Thus, as-of-yet unknown compounds may also be in this fraction and contribute to the large fraction of observed C-alkyl bonds. Another possibility is that the WSOCxrr fraction contains aromatic compounds that have a high degree of substitution by other functional groups. Other investigators [e.g., *Krivácsy et al.*, 2001] have found evidence for highly polyconjugated weak polyacids (humic-like substances) and these types of compounds are expected in the WSOCxrr fraction. (Recall, XAD-8 has been used extensively to isolate humic material from natural waters [*Thurman and Malcolm*, 1981].) Similar reasoning applies to the summer WSOCxrr, where C-alkyls dominate over aromatic groups. Additional chemical analysis is required to further investigate this.

The second discrepancy is more easily explained. Based on the SEC calibration with synthetic compounds (see Figures 6.2c and 6.2d), if an O-H group is present on an aromatic ring the retention time of that compound will be shifted to longer times (e.g. benzoic acid with zero O-H groups has a retention time of 32 minutes, salicylic acid with one ortho position O-H group has a retention time of 38 minutes). Thus, any aromatic with an O-H group is called WSOCxrr_n, despite the presence of additional functional groups including carboxylic acids. Aromatics with no O-H group, but some carboxylic acid groups, are found only in the WSOCxrr_a fraction. A reason why SEC has more WSOCxrr_n than WSOCxrr_a, whereas the ^{13}C-NMR displays it the opposite, could be because ^{13}C-NMR spectra quantify the fraction of various bonds, whereas SEC appears to separate compounds by the presence of specific functional groups associated with single molecules. A scenario consistent with the observations is that most of the aromatic

molecules in this biomass burning sample display at least one O-H functional group (the SEC result of high WSOCxrr_n and no WSOCxrr_a), but also many additional aromatic carboxylic acid functional groups (the ^{13}C-NMR results). Within the actual ^{13}C-NMR spectra a number of unresolved peaks were observed in the C-alkyl region, indicating the presence of different forms of aliphatic carbon that could be associated with a variety of aliphatic as well as aromatic compounds. These arguments are also consistent with highly substituted aromatic compounds as discussed above.

The comparisons are also complicated by influences from WSOCxru compounds from the XAD-8 separation. Recall that the WSOCxru compounds include acids and carbonyls with greater than 3 or 4 carbons, cyclic acids, and organic nitrates (see Table 6.1). These calibrations show that up to approximately 20% of these WSOCxru compounds are included in the WSOCxrr (see Table 5.1) and will be analyzed by the ^{13}C-NMR in the WSOCxrr fraction. Many of these compounds are likely to be aliphatic and would contribute to the observed hydrophobic C-alkyl peaks. However, this is not likely to explain all of the C-alkyl dominance since from the summer SEC results, WSOCxru is only 20% of the WSOC, thus its maximum influence on the WSOCxrr would be ~ 4% of the WSOC (20% of 20%) or for comparison to Table 6.3, ~ 10% as a fraction of the WSOCxrr. This effect would be even less significant for the biomass sample, since WSOCxru is only 9% of WSOC in this case (20% of 9% = 2%), and ~ 5% of the WSOCxrr.

6.2.4. Speciation of the WSOC in Summer, Winter, and Biomass Burning Samples: Overall Results

Group speciation of the WSOC aerosol with XAD-8 and SEC identifies a large fraction of the chemical components of ambient particles. As shown in section 5.2, this is especially true in periods when the WSOC is a large fraction of OC, often the case in Atlanta summer during PM events when apparently significant aerosol production by oxidation processes lead to greater fractions of WSOC. Table 6.4 gives the concentrations of various groups of WSOC isolated by XAD-8/SEC for all the filter samples previously mentioned. The mean percentage that each of these functional group contributes to the WSOC and total OC is shown as pie charts in Figures 6.8a for summer, 6.8b for winter, and 6.8c for biomass burning samples.

Different isolated fractions of WSOC dominated in each group of samples. In the summer the dominant WSOC group was WSOCxp_a, in winter WSOCxru, and in biomass smoke WSOCxp_n. In the summer when gas phase and heterogeneous oxidation processes are expected to contribute larger fractions to the ambient WSOC (i.e., SOA formation), the WSOCxp_a and WSOCxrr_a dominate their respective groups. This is especially true for the WSOCxp_a, which accounts for 14% of the summer OC and combined these two acid groups account for 20% of the OC. In contrast, in winter these two acid groups make up 14% of OC. The larger summertime organic acid fractions are consistent with smog chamber studies, which show that SOA formation often leads to generation of carboxylic acids [*Grosjean and Friedlander*, 1980; *Hatakeyama et al.*, 1985, 1987].

In contrast to the summer, the WSOCxp fraction of the biomass burning sample is

Table 6.4. Concentrations of OC, EC, and the various functional groups for all summer, winter, and biomass burning samples. Table 6.2 shows the WSOC concentrations that can be used with this data to calculate the concentrations of WSOCxp_u and WSOCxrr_u. NA = not applicable, ND = not detected

Filter # (month/day)	OC (μg C/m^3)	EC (μg C/m^3)	WSOCxp_a (μg C/m^3)	WSOCxp_n (μg C/m^3)	WSOCxp_b (μg C/m^3)	WSOCxrr_a (μg C/m^3)	WSOCxrr_n (μg C/m^3)	WSOCxru (μg C/m^3)
Summer								
F2 (6/11)	9.94	1.03	1.63	0.80	0.04	0.46	0.36	0.09
F3 (6/13)	NA	NA	0.87	0.69	0.02	0.35	0.24	0.79
F5 (6/17)	NA	NA	0.56	0.49	0.05	0.21	0.22	0.89
F6 (6/19)	6.20	0.41	0.76	0.16	0.02	0.33	0.11	0.69
F7 (6/21)	5.27	0.46	0.76	0.36	0.02	0.34	0.13	1.00
F8 (6/23)	3.84	0.39	0.37	0.16	0.02	0.19	0.11	0.67
F10 (6/27)	3.35	0.16	0.46	0.39	0.02	0.18	0.29	0.61
F2B (8/8)	6.76	0.29	0.72	0.16	0.01	0.35	0.11	0.48
F3B (8/10)	9.04	0.80	1.07	0.50	0.02	0.49	0.27	0.42
F4B (8/12)	3.59	0.44	0.58	0.40	0.01	0.35	0.41	0.39
F5B (8/14)	NA	NA	0.66	0.20	0.01	0.12	0.50	0.64
F6A (8/15)	4.86	0.19	0.83	0.45	0.02	0.35	0.27	0.49
F7B (8/16)	5.10	0.25	0.89	0.16	ND	0.33	0.10	0.41
F8B (8/17)	7.73	1.06	1.27	0.74	0.03	0.68	0.45	0.42
F9B (8/19)	11.96	1.01	1.72	0.97	0.02	0.80	0.41	0.17
F12B (8/23)	NA	NA	1.15	0.67	0.03	0.48	0.30	0.44
F13B (8/25)	6.26	0.65	1.27	0.70	0.03	0.49	0.27	0.40
F14B (8/27)	8.81	0.60	0.98	0.30	ND	0.48	0.26	0.69
F15B (8/29)	5.95	0.41	0.92	0.45	0.04	0.43	0.18	0.35
F16B (8/31)	6.86	0.87	0.88	0.39	0.03	0.43	0.32	0.52
F17B (9/2)	3.93	0.36	0.41	0.29	0.01	0.26	0.14	0.41
mean ± standard deviation	6.44±2.42	0.55±0.30	0.89±0.36	0.45±0.23	0.02±0.01	0.39±0.16	0.26±0.12	0.53±0.22

Table 6.4. Continued.

Winter								
F1BB (12/11)	2.14	0.30	0.14	0.17	ND	0.07	0.08	0.14
F2BB (12/19)	4.77	0.40	0.45	0.32	0.01	0.32	0.12	0.63
F3BB (1/11)	7.25	0.93	0.82	0.64	0.01	0.37	0.55	0.56
F4BB (1/13)	4.26	0.52	0.43	0.32	0.02	0.26	0.20	0.77
F5BB (1/18)	4.07	0.55	0.29	0.20	0.02	0.19	0.11	0.66
F6BB (1/20)	8.87	1.03	0.66	0.53	0.01	0.40	0.30	0.76
F7BB (1/23)	1.96	0.12	0.19	0.21	ND	0.08	0.11	0.22
F8BB (1/25)	9.28	1.06	0.73	0.57	0.01	0.39	0.34	0.91
F9BB (1/28)	NA	NA	0.27	0.28	ND	0.21	0.11	0.47
F10BB (2/2)	3.74	0.27	0.34	0.29	ND	0.19	0.18	0.54
mean ± standard deviation	5.15±2.71	0.58±0.35	0.43±0.23	0.35±0.17	0.01±0.01	0.25±0.12	0.21±0.15	0.57±0.24
Biomass	**Burning**							
GT14 (4/16)	1367	23.47	80.11	379	12.81	52.87	165	326
GT46 (4/29)	1309	108	62.33	363	0.86	13.96	139	219
mean ± standard deviation	1338±41	66±60	71.22±12.57	371±11	6.34±7.74	33.41±27.52	152±19	273±76

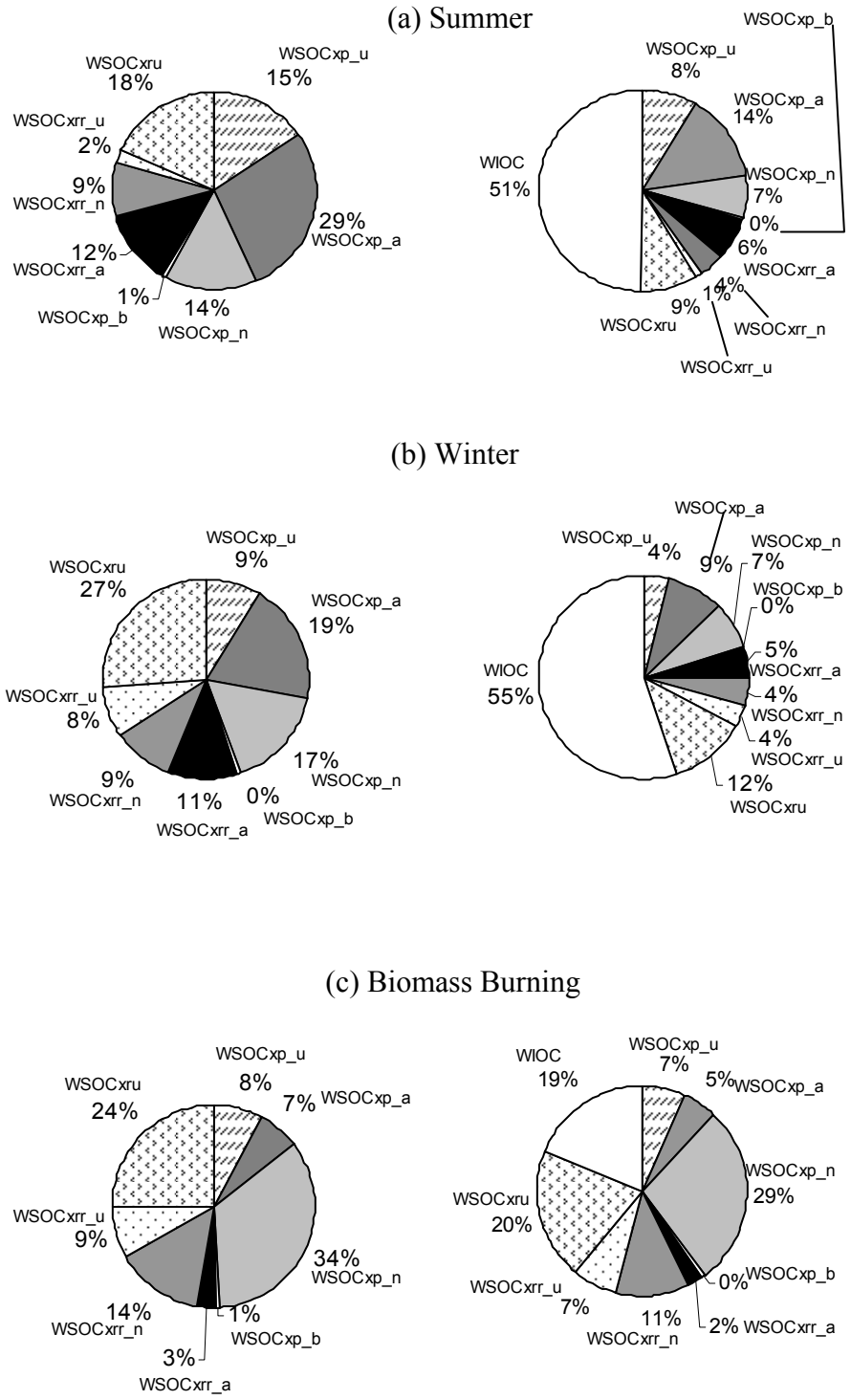

Figure 6.8. Pie charts showing the carbon mass percentage that each functional group contributes to the WSOC and total OC based on the average of all (a) summer, (b) winter, and (c) biomass burning samples.

predominately WSOCxp_n and the WSOCxrr fraction is WSOCxrr_n. The average of the winter samples is somewhere between the summer and biomass burning samples. This seems likely since although oxidation processes can still occur in the winter they are not as strong, but there is generally an increase in burning possibly due to heating of homes for the winter.

6.2.5. Correlations Between Functional Groups and Possible Sources of WSOC

Correlations between the various isolated functional groups and other relevant atmospheric parameters is undertaken to investigate their possible sources. It is recognized, however, that the use of 24 hour integrated data restricts this type of analysis compared to what is possible with time-resolved measurements, and thus the following only provides rough linkages between various components.

Correlations between the isolated WSOC functional groups and total WSOC show that in the summer most of the 24 hour averaged variability in WSOC concentration was due to WSOCxp_a and WSOCxrr_a with R^2 values of 0.74 and 0.55, respectively, the highest for each group. Similarly, compared to OC, the R^2 values for the WSOCxp_a and WSOCxrr_a were 0.78 and 0.71 respectively. In the winter, correlations of the SEC isolated functional groups to WSOC and OC were actually higher than in summer. The R^2 values for the various functional groups versus WSOC were 0.86 for WSOCxp_a, 0.82 for WSOCxp_n, 0.92 for WSOCxrr_a, and 0.57 for WSOCxrr_n, and versus OC were 0.86 (WSOCxp_a), 0.84 (WSOCxp_n), 0.88 (WSOCxrr_a), and 0.57 (WSOCxrr_n). It may be that a combination of both oxidation and biomass burning

sources combined with limited dispersion accounts for high correlations amongst all wintertime WSOC fractions.

Scatter plots that include zero-intercept slopes and R^2 values amongst the various isolated WSOC functional groups in summer and winter are shown in Figures 6.9a and 6.9b. WSOCxp_b is not included in the correlations because it was only periodically observed and comprised a very minor fraction of the WSOC and total OC. Unrecovered fractions are not included since they were not measured directly but instead determined by difference. In summer, the acids WSOCxp_a and WSOCxrr_a are the most highly correlated fractions ($R^2 = 0.74$). WSOCxp_n is moderately correlated with WSOCxp_a ($R^2 = 0.61$) and WSOCxrr_a ($R^2 = 0.52$). WSOCxrr_n is not well correlated with any of the other species suggesting a different source.

The correlations amongst the WSOCxp_a, WSOCxrr_a, and WSOCxp_n could at least in part be explained by current understanding of sources for these compounds. Many of the functional groups identified by the SEC have primary emissions (see Table 13.8 in *Seinfeld and Pandis* [1998] for a summary). However, and likely more importantly, secondary processes can also generate these compounds. (Note, recent experiments in Atlanta, which will be discussed in more detail in chapter 7, suggest that in the absence of biomass burning influences, WSOC is mainly secondary.) Short-chain aliphatic acids can be produced by SOA of cyclic olefins and aromatic hydrocarbons [*Kawamura and Ikushima*, 1993]. Oxidation of polycyclic aromatic hydrocarbons can produce aromatic acids [*Jang and McDow*, 1997; *Fraser et al.*, 2003]. Moreover, some aromatic compounds (e.g., toluene) when oxidized can produce both aromatic acids and

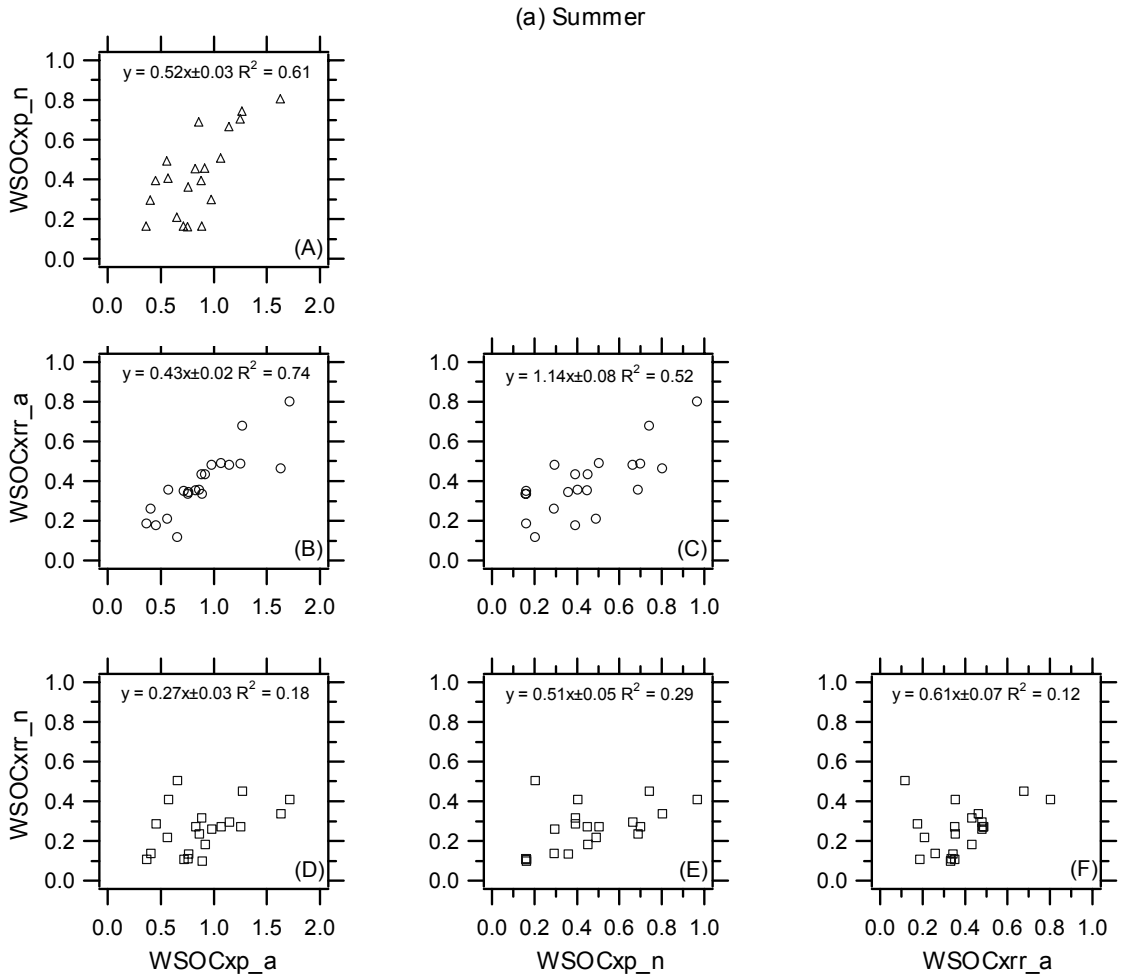

Figure 6.9. Linear regressions forced through zero and correlations of the various SEC functional groups for the (a) summer and (b) winter samples. Indicated across the bottom is the x-axis and along the side the y-axis labels. The slope uncertainty is one standard deviation.

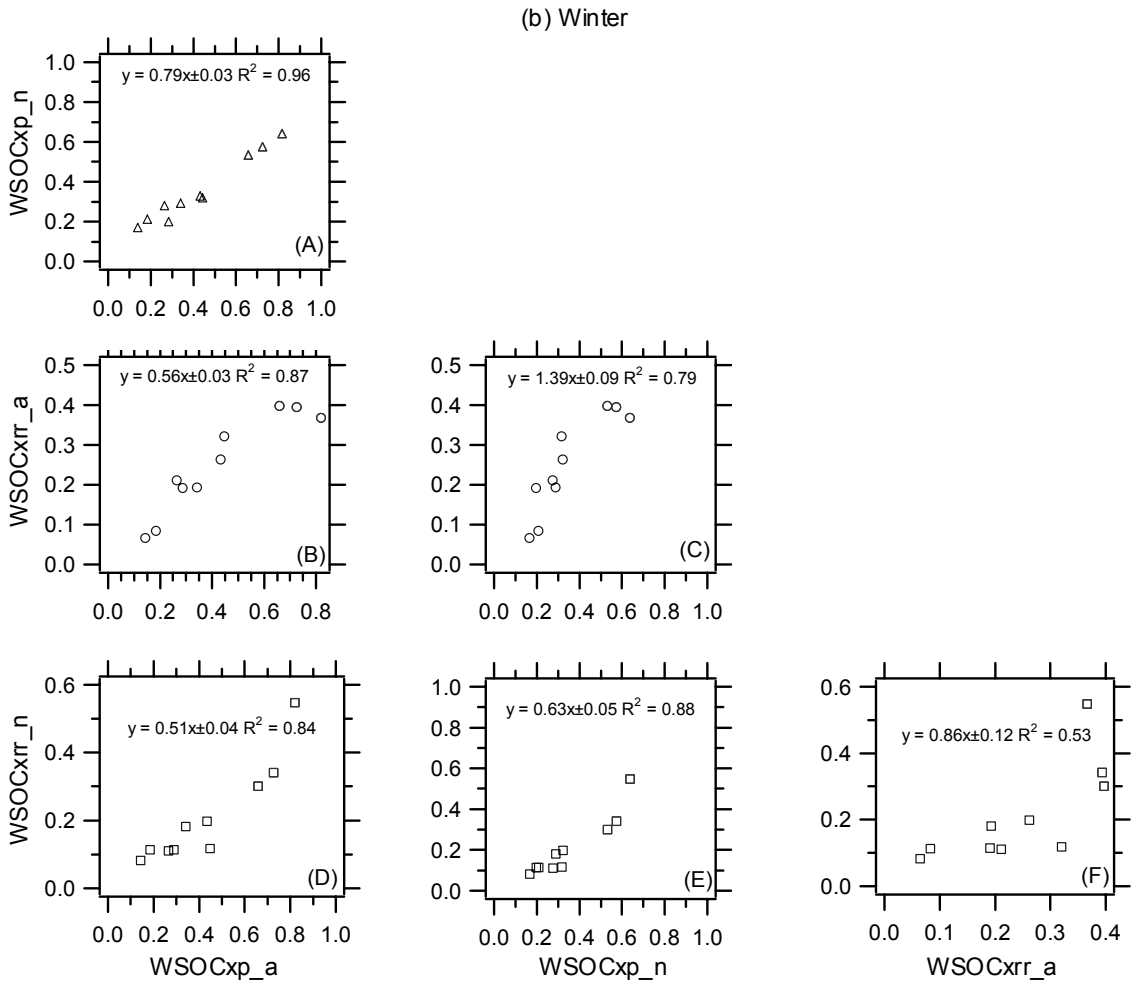

Figure 6.9. Continued.

short-chain aliphatic acids (e.g., oxocarboxylic acids) [*Jang and Kamens*, 2001]. These types of SOA mechanisms could in part account for the observed correlations between WSOCxp_a and WSOCxrr_a. In addition, these SOA reactions also produce significant amounts of carbonyls (i.e., WSOCxp_n), consistent with observed correlations between WSOCxp_n and both WSOCxp_a and WSOCxrr_a.

Given the expected large influence of light-duty vehicle emissions at this sampling site, these compounds could be mainly from SOA of mobile source emissions. There is evidence for a link between the major fractions of WSOC and mobile sources. WSOCxp_a and WSOCxrr_a were both correlated with elemental carbon (R^2 = 0.64 to 0.66) and daily maximum CO (R^2 = 0.65 to 0.73). The acid WSOC groups, WSOCxp_a and WSOCxrr_a, were also correlated with a number of VOCs measured at the Georgia EPA PAMS (Photochemical Assessment Monitoring Stations) site allocated at South DeKalb in Atlanta, approximately 20 km southeast of the aerosol measurements. WSOCxp_a and WSOCxrr_a were correlated with various pentanes (e.g., isopentane R^2 = 0.67 and 0.68 respectively) and acetylene (R^2 = 0.61 and 0.56); compounds found in gasoline emissions [*Harley et al.*, 1992].

WSOCxp_a is the largest summertime fraction of WSOC. Some of the compounds that could be expected in this group can be readily measured with ion chromatography. All samples of the WSOCxp were analyzed for acetate, formate, and oxalate. Even though there was significantly higher summertime WSOCxp_a concentrations no noticeable difference was observed between summer and winter samples. Acetate and formate were not detected in any sample. Oxalate was detected in all samples, but only accounted for ~3% of the WSOCxp_a fraction and so cannot

explain the observed levels of WSOCxp_a. The low concentrations of oxalate are similar to measurements made during the August 1999 Atlanta Supersite, where oxalate was generally close to or just above its detection limit of 0.02 ppbv (0.07 $\mu g/m^3$) during non-PM events [*Baumann et al.*, 2003]. Malonic or succinic acids, compounds that could also comprise the WSOCxp_a (see Table 6.1), were not tested for. Other urban studies have shown that these species are often at lower concentrations than oxalate [e.g., *Kawamura and Ikushima*, 1993]. It is possible that the WSOCxp_a is instead composed of more substituted short-chain acids, such as oxocarboxylic acids. *Jang and Kamens* [2001] found these types of acids in the ring-opening products from photooxidation of toluene. Finally, no correlation was found between temperature and any of the summertime WSOC functional groups despite a daily average variability in temperature of 27 to 39^oC for this data.

For winter, all isolated fractions were highly correlated with each other (Figure 6.9b), except for WSOCxrr_n versus WSOCxrr_a. In Atlanta during the winter, SOA formation may still occur, albeit at a lower rate than summer. Biomass burning contributions, however, are likely to be significantly higher in winter than summer. Since SOA and biomass emissions can produce WSOC compounds that contribute to the same SEC isolated groups, co-variability between many functional groups may be expected when neither source dominates. Thus, as in summer, SOA of wintertime mobile source emissions can lead to correlations between WSOCxp_a, WSOCxrr_a, and WSOCxp_n (e.g., carbonyls). Biomass burning emissions could account for correlations between the WSOCxrr_n (known biomass burning markers [*Simoneit*, 2002]), WSOCxp_a (which can be produced from vegetation and biomass combustion of domestic and industrial heating

[*Khwaja*, 1995]), and the WSOCxp_n (which can include saccharides, i.e., levoglucosan). The least correlated compounds are the WSOCxrr_a and WSOCxrr_n ($R^2 = 0.53$), which appear to come mainly directly or indirectly from different sources (WSOCxrr_a from refined fossil fuel hydrocarbons and WSOCxrr_n from biomass burning).

6.2.6. Unrecovered Compounds

In the previous sections the focus was on the recovered fractions of the WSOC, here possible sources for the various unrecovered fractions are discussed. These are divided into two groups: the unrecovered portions from the SEC analysis of hydrophilic (WSOCxp_u) and recovered hydrophobic (WSOCxrr_u) compounds and the group of compounds that could not be recovered from the XAD-8 (WSOCxru).

6.2.6.1. WSOCxp_u and WSOCxrr_u

The WSOCxp_u and WSOCxrr_u fractions are both calculated assuming a carbon mass balance by taking the difference in the measured WSOCxp or WSOCxrr fractions and the corresponding integrated SEC chromatograms. It should be noted these fractions are more uncertain since they are determined by the difference of two large numbers. Based on calibration compounds, generally only 80 to 90% of all species tested were recovered by the SEC (see Table 6.1). The remaining 10 to 20% will be included in WSOCxp_u and WSOCxrr_u. It can roughly be tested if these unrecovered fractions are due to this ~80% efficiency. For example, if the percentage of unrecovered SEC compounds of the total WSOCxp and WSOCxrr fractions (i.e. WSOCxp_u of WSOCxp and WSOCxrr_u of WSOCxrr in Figure 6.8) is on the order of 10 to 20%, then most of

this unrecovered fraction is just due to SEC recovery inefficiencies and not some unique compound. For the summer average, WSOCxp_u is ~ 30% of WSOCxp (WSOCxp_u/WSOCxp) and WSOCxrr_u is ~ 9% of WSOCxrr (WSOCxrr_u/WSOCxrr). For the winter average WSOCxp_u/WSOC is 20% and WSOCxrr_u/WSOCxrr is 29%, for the biomass sample WSOCxp_u/WSOCxp is 16% and WSOCxrr_u/WSOCxrr is 34%. Consequently, for the summer WSOCxrr and biomass WSOCxp, much of the unrecovered SEC fractions could be attributed to less than 100% efficiency of the SEC for all compounds, and not due to some other compounds that penetrate the SEC column with very low efficiency. Although it is also possible it could be due to analytical error in the integration method used for the SEC peak analysis. In contrast, for summer WSOCxp, winter WSOCxrr, and biomass WSOCxrr, it appears likely that some compounds were present in the WSOC that had low SEC penetration efficiencies. (Note that these compounds with low SEC penetrations are not large fractions of the WSOC, likely accounting for at most 10 to 15% of each of WSOCxp or WSOCxrr.) Non-ionizable compounds produced in biomass burning could explain much of the WSOCxrr_u (e.g., catechol). For WSOCxp_u, no hydrophilic compounds have yet been identified that penetrate the SEC with low efficiency.

6.2.6.2. WSOCxru: Biogenic versus Anthropogenic WSOC

Experiments show compounds in the WSOCxru fraction can include organic nitrates, cyclic acids, and long-chain (carbons > 3 or 4) aliphatic acids and carbonyls. As a percentage of OC, this group is actually lowest in the Atlanta summer (9%), higher in Atlanta winter (12%), and highest in the biomass burning sample (20%). The trend may

partly be explained by the contributions of organic nitrates, which are high in winter [*Zhang et al.*, 2002] and maybe high in biomass burning smoke.

An interesting aspect of this classification is that biogenic emissions leading to SOA are thought to produce compounds that would mainly be in this group. *Kawamura and Sakaguchi* [1999] and *Mochida et al.* [2003] have both suggested that longer chain carboxylic acids could be due to oxidation of fatty acids, which are emitted from plants, soils, and marine sources. Cyclic acids and long-chain aldehydes can be SOA products from biogenic emissions. Smog chambers show that pinonic and pinic acids are produced from oxidation of pinene, which is emitted from conifers [*Glasius et al.*, 2000]. Organonitrate functional groups have also been detected in smog chamber photooxidation experiments of isoprene and ß-pinene, both biogenic hydrocarbons [*Palen et al.*, 1992]. As of yet, no references have been found that show short-chain aliphatics can be produced via biogenic SOA formation. Under the assumption that biogenics produce compounds that would appear exclusively in the WSOCxru, the data suggest that for this site during the summer of 2004, biogenic emissions contribute at most 20% to the WSOC and 9% to the OC. For comparison, the WSOCxp_a and WSOCxrr_a, which may be linked through SOA formation of mobile source emissions, accounted for on average ~20% of the OC. Thus, not even considering the WSOCxp_n, which some fraction may also be linked to mobile sources (recall WSOCxp_n is also correlated to WSOCxp_a and WSOCxrr_a), by this analysis SOA from mobile source emissions are about a factor of 2 greater than biogenic sources.

Overall, these results are qualitatively consistent with a study previously mentioned in chapter 4, which investigated the carbon budget in polluted air masses

advecting from New England [*de Gouw et al.*, 2005]. These authors report SOA mainly from anthropogenic sources and suggest that short-chain alkanes and alkenes may play a significant role. In contrast, modeling and carbon isotope analysis have suggested biogenic emissions often dominate over anthropogenic. For example, a modeling study on SOA formation in Houston, TX and surrounding regions show that biogenic SOA, mainly from pinenes, dominate over anthropogenic SOA, mainly from aromatics [*Russell and Allen*, 2005]. Carbon isotope analysis tends to support the conclusions of this study [*Lemire et al.*, 2002]. One way to reconcile the discrepancy between the XAD-8/SEC observations versus modeling and radiocarbon analysis is that a significant fraction of the isolated functional groups that are attributed to anthropogenic sources have a biogenic source. Possibly, functional groups with biogenic SOA products are the WSOCxp_u group, or possibly some fraction of WSOCxp_a. Extending these measurements to regions where biogenic emissions are known to dominate over anthropogenic emissions could provide further insight into the validity of the assumption of estimating the relative contributions of secondary anthropogenic and biogenic sources.

6.3. Summary

Based on calibrations with synthetic single component compounds, SEC separates the WSOCxp into short-chain acids, neutrals, and bases, and the WSOCxrr compounds into recoverable hydrophobic acids and neutrals. All recoveries are typically 80% or better. It is noted that the calibrations, and thus the labels for the groups, serve only as a guide to the types of ambient aerosol compounds that are actually isolated by this method.

WSOC was extracted from 24 hour integrated filter samples collected with a Hi-Volume sampler at an urban Atlanta site during the summer and winter. Samples collected within the midst of a prescribed burn are also used to contrast concentrations of various WSOC functional groups between urban and biomass burning aerosol particles. Comparisons of SEC and ^{13}C-NMR for urban summer and a biomass burning sample are consistent with both expectations and the calibration results. There is evidence, however, that the summer WSOCxrr_a and winter and biomass WSOCxrr_n are much more highly substituted than the simple calibration standards.

Average WSOC to OC summertime ratios were near 50% (the year 2004 was unusually clean with the fewest poor air quality days since 1998). The predominant summertime WSOC component was WSOCxp_a (short-chain aliphatic acids with less than approximately 4 or 5 carbons), comprising 29% ± 6% μg C/μg C (mean ± standard deviation) of WSOC. Formate, acetate, and oxalate were small fractions of WSOC (<1%). In the biomass burning sample, the WSOCxp_n (e.g., likely saccharides) dominated at 34% ± 6% μg C/μg C of WSOC. The urban Atlanta winter samples could be described as a mixture of the summer and biomass results where a more equal distribution of these WSOC fractions was observed.

Summer results are particularly interesting because more vigorous oxidation processes should lead to higher WSOC through SOA production. Combined, on average, the acids WSOCxp_a and WSOCxrr_a accounted for ~20% μg C/μg C of the Atlanta summertime OC. This data does not include any particularly strong PM events. However, as shown in chapter 5, it has been observed at the same site that WSOC can reach 75% μg C/μg C of OC under a stagnation-driven PM episode, and similar to this

data, WSOCxp was the dominant WSOC component (~60% μg C/μg C). Thus, it is reasonable to expect that WSOCxp_a and WSOCxrr_a comprise substantially more than 20% of the OC during Atlanta summer PM events, and that the short-chain aliphatic acids (WSOCxp_a) would dominate. The acids, WSOCxp_a and WSOCxrr_a, were the most highly correlated of the WSOC isolated groups ($R^2 = 0.74$). They were also reasonably correlated (R^2 values typically 0.5 to 0.7) with compounds expected from mobile sources, such as CO, EC, and various VOCs, including acetylene a tracer for mobile sources. Because these correlations are based on 24 hour integrated averages, they likely do not indicate WSOC from primary emissions, but instead point to possible linkages between the observed WSOC fractions and emissions from mobile sources that can form SOA. Well-known SOA products of biogenic precursors, such as long-chain aliphatic (carbons greater than 3 or 4) and cyclic acids contributed at most 18% μg C/μg C to the summertime WSOC and 9% μg C/μg C to the OC. Overall the data imply that SOA production from mobile sources led to at least twice the aerosol carbon mass than SOA formation from biogenic compounds. Biogenic SOA products that appear in functional groups in addition to the WSOCxru group would increase the estimate of biogenic contributions and be in better agreement with model predicted SOA production and carbon isotope analysis performed by other investigators.

In the next chapter the roles of biogenic versus anthropogenic sources on the formation of WSOC in the Atlanta metropolitan region is further explored based on a combination of airborne and ground-based measurements. The airborne data includes highly time-resolved measurements of both WSOC and VOCs.

CHAPTER 7
SOURCES OF WSOC IN ATLANTA, GA

7.1. Motivation

The Atlanta, GA metropolitan region, smaller cities in the state (e.g. Macon, Augusta, Columbus), and many other locations in the southeastern U.S. have sufficiently high concentrations of fine particles to jeopardize compliance with standards set by the U.S. EPA. Consistently non-compliant communities must develop mitigation plans, which to be effective, requires reasonably accurate knowledge of aerosol particle sources. Measurements of fine particle composition in the southeast show that there are two major components to the ambient aerosol: sulfate and carbonaceous compounds. It is well established that sulfate arises mainly from the oxidation of sulfur dioxide [*Berresheim et al.*, 1995], which in the eastern U.S. is emitted largely by stationary power generation [*EPA*, 2004]. In urban areas like Atlanta, this sulfate can come from distance sources, or from relatively nearby coal-fired power plants [*Brock et al.*, 2002], the latter readily identified by large localized enhancements in fine particle mass [*Weber et al.*, 2003].

Unlike sulfate, the sources for the carbonaceous fraction are not well established. Carbonaceous aerosol is composed of EC and OC, with OC comprising about 80 to 90% of the total on a carbon mass basis [*Lim and Turpin*, 2002]. Since the OC fraction is composed of a myriad of compounds it has never been comprehensively characterized on an individual compound basis and its sources are not well known. It is, however, known that OC is composed of directly emitted particles (primary), and those formed in the atmosphere (secondary) by gas-phase oxidation reactions that lead to products of lower volatility, which may condense and form organic particles. Reactions in the condensed

phase may also influence the carbonaceous aerosol chemistry, however, this is not viewed as SOA formation and has not been as widely investigated. Based on EC as a tracer for primary emissions, analysis of Atlanta OC and EC during summer suggests that about 50% of the OC is secondary and this can reach near 90% on short time scales [*Lim and Turpin*, 2002].

As previously discussed in chapter 1, SOA can have anthropogenic and biogenic sources. Of the anthropogenic VOCs it is currently viewed that mobile emissions of aromatic compounds lead to the majority of anthropogenic SOA in urban centers [*Odum et al.*, 1997; *Seinfeld and Pandis*, 1998]. Chamber studies also show that biogenic emissions, especially monoterpenes from conifers, are readily oxidized by ozone, and the hydroxyl radicals, to produce biogenic secondary organic aerosol [*Hoffman et al.*, 1997; *Griffin et al.*, 1999]. Particulate OC compounds observed in remote forested regions include various carboxylic acids, such as pinic (C_9), pinonic (C_{10}), and others of similar structure with high carbon number, and C_9 and higher aliphatic dicarboxylic acids [*Glasius et al.*, 2000; *Sheesley et al.*, 2004; *Anttila et al.*, 2005].

Interestingly, many urban centers and their surrounding regions in the south and southeast are densely forested with coniferous trees leading to speculation that biogenic precursors, like terpenes, are a major contributor to their SOA. As mentioned in section 6.2.6.2, a modeling study of SOA formation in Houston, TX, which like Atlanta, GA, has a combination of large anthropogenic and biogenic VOC emissions, indicated that most of the regional SOA is from biogenic sources. Despite continued progress, it is still largely unclear as to what extent the organic aerosol in the urban southeast is from SOA formation, and what fraction of the SOA is from anthropogenic versus biogenic sources.

In this chapter further evidence is provided showing that WSOC is not directly emitted by cars but is closely linked to vehicle emissions.

7.2. Methods

Comprehensive methods for chemically characterizing the products of SOA may provide new insights into its source; insights that have not been achieved so far by identifying relatively few single components. Because the process of SOA formation leads to oxygenated compounds, many are expected to be soluble in water. This implies that the methods previously discussed for separation and analysis of organic compounds in aqueous solutions can be applied to investigate products of SOA in the ambient aerosol. For this analysis, this includes airborne WSOC measurements (chapter 4) and the two-step XAD-8/SEC speciation method (chapters 5 and 6) performed on 12 or 24 hour integrated Hi-Volume filter samples.

OC and EC were determined from the Hi-Volume filters using the method discussed in section 6.1.4. A host of biogenic and anthropogenic VOCs were measured on- and off-line. On-line measurements were made using a PTR-MS (as discussed in section 4.1). Off-line measurements were made from whole air samples using gas chromatography with a variety of detection methods.

7.3. Ambient Results

7.3.1. Airborne Measurements

7.3.1.1. Measurements Over Atlanta

On 15 August 2004, at the conclusion of the NEAQS/ITCT 2004 experiment, discussed in chapter 4, a series of low altitude over-flights of metro Atlanta and the surrounding regions were conducted. At the time of the over-flight surface measurements in Atlanta indicated air quality was moderate with $PM_{2.5}$ mass concentrations of 17.2 $\mu g/m^3$, typical for the relatively clean summer of 2004. These airborne measurements show a distinct and well-defined region of enhanced WSOC and CO concentrations as the aircraft entered the boundary layer. A map and flight track colored by CO concentrations, and the time series of altitude and CO, acetylene, and WSOC concentrations are shown in Figures 7.1 and 7.2, respectively. In regions where measured wind directions indicate air masses were from more rural sectors (e.g. regions to the south-east of the city, between points labeled A and B, and on the northbound leg labeled D in Figures 7.1 and 7.2), both CO and WSOC were lower, whereas in air masses residing over, or advecting from, more densely populated regions (e.g., the legs that include labels C and E) the CO and WSOC concentrations were significantly higher. Variability in WSOC and CO throughout these passes is likely not due to variations in concentration with altitude since the aircraft maintained a fairly constant altitude of near or below l km. This region of high WSOC and CO mapped out by the aircraft covered a large section of northern Georgia, encompassing an area of approximately 15,000 km^2. Superimposed on what appears to be the more regional CO are smaller areas of

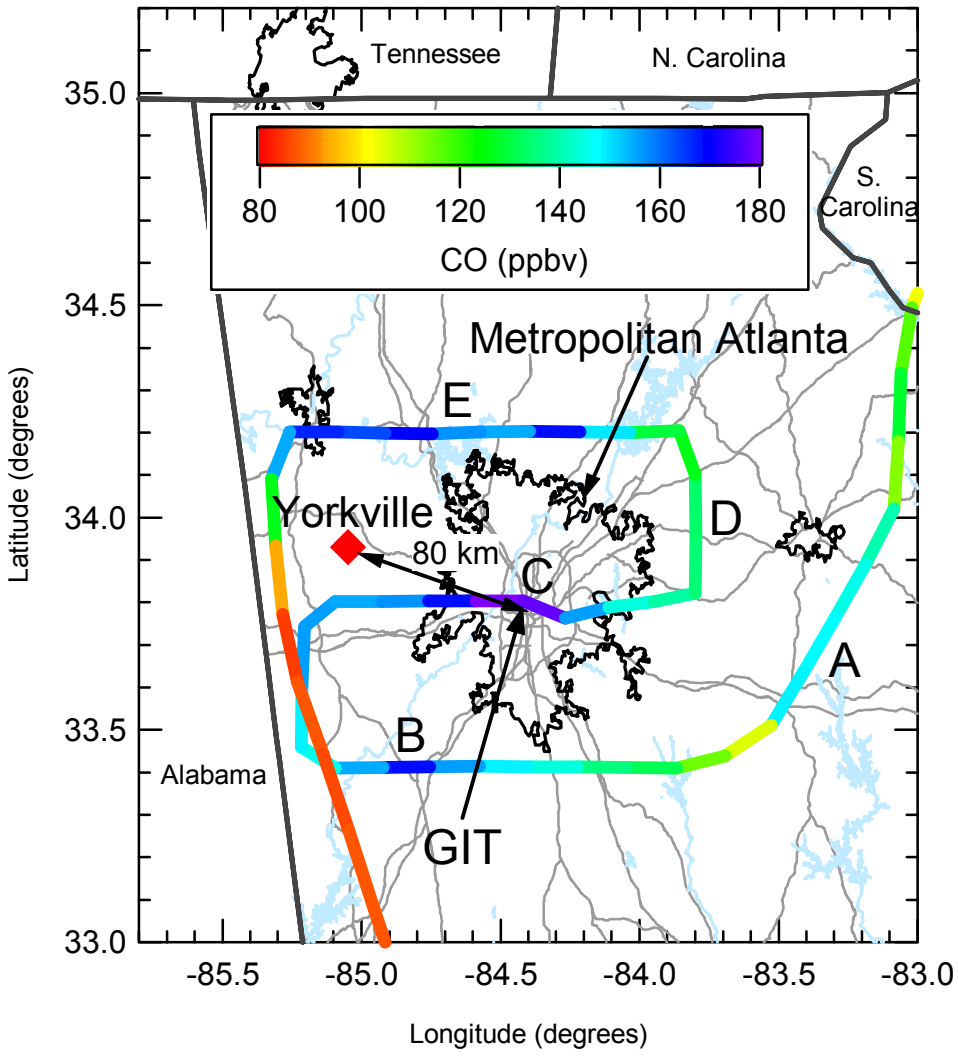

Figure 7.1. Map of aircraft flight path over Atlanta and the surrounding region colored by CO concentrations. GIT, which is located near the Atlanta urban center, and the rural Yorkville site are identified. CO and fine WSOC concentrations along the flight path are shown in Figure 7.2, along with the locations identified as A, B, C, D, and E.

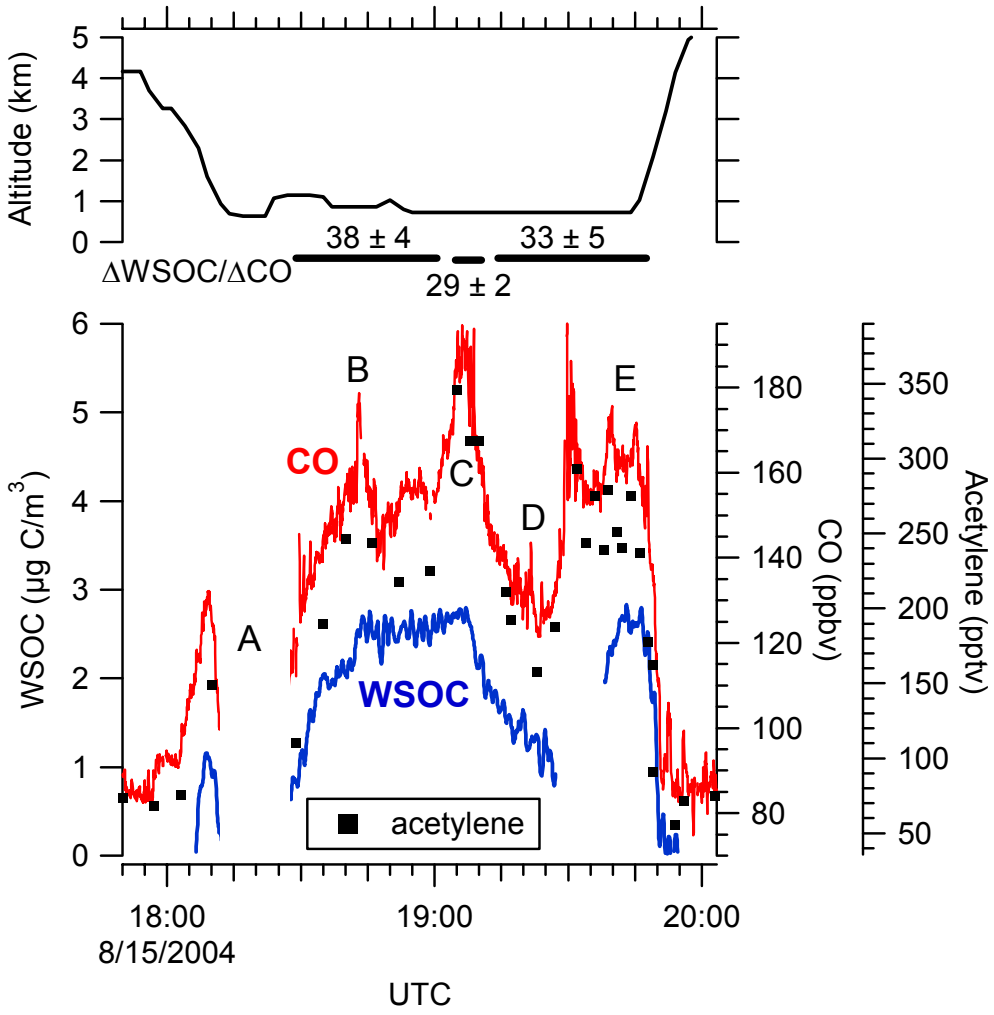

Figure 7.2. Airborne measurements of fine particle WSOC, gases CO and acetylene, and altitude recorded over Atlanta and the surrounding region. Letters A, B, C, D, and E correspond to measurement locations shown in Figure 7.1. Data during in-cloud sampling are excluded (region A). Missing WSOC data at approximately 19:30 UTC is due to an automatic sample blank measurement. CO was measured at 1 s, WSOC is a 3 s integrated measurement, and acetylene was measured following the mission from a whole air sampling system. Horizontal bars indicate the interval over which average and ± standard deviation of ΔWSOC to ΔCO ratios (µg C/m^3/ppmv) are calculated. Local time is EDT = UTC – 4 hours.

significantly higher CO concentrations. The most striking of these areas is identified as point C in Figures 7.1 and 7.2, which was recorded when the aircraft sampled directly over urban Atlanta. Although WSOC is correlated with the more regional CO trends (R^2 = 0.80, for all data in Figure 7.2), it does not track CO in what are likely fresher plumes; the correlation (R^2) between WSOC and CO is higher at 0.86 when the fresh CO plumes are not included. Biomass burning was also not a significant contributor to the observed CO and WSOC since acetonitrile, a known biomass burning tracer, was near background levels with an average concentration of 127 pptv.

7.3.1.2. Comparison of Atlanta to Northeastern Cities

The airborne data collected over Atlanta are similar to those recorded in plumes from northeastern cities in that WSOC was correlated with CO (see Figure 4.4 and section 4.3.1). However, due to differences in vegetation, Atlanta is expected to have much higher emissions of biogenic VOCs, and thus should have higher biogenic SOA.

In this analysis the concentrations of acetylene, iso-propyl nitrate, α-pinene, β-pinene, isoprene, methyl vinyl ketone (MVK), and methacrolein (MACR) are examined. Acetylene and iso-propyl nitrate are mainly from anthropogenic sources whereas the others are from biogenic sources [*de Gouw et al.*, 2005]. Acetylene is a relatively inert VOC and comes mostly from automobile emissions. Iso-propyl nitrate has no direct emission sources and is formed in the atmosphere from the oxidation of propane and other anthropogenic VOCs. MVK and MACR are mainly formed as oxidation products of isoprene.

Comparisons between the Atlanta and northeastern plumes (discussed in detail throughout section 4.3) show much higher biogenic VOC concentrations for Atlanta but no clear evidence for higher WSOC concentrations. This is demonstrated in Table 7.1, which shows the ratios of WSOC, CO, and anthropogenic and biogenic VOCs recorded over Atlanta to concentrations measured in urban plumes advecting from urban regions in the northeastern U.S.

From Table 7.1, it is noteworthy that all anthropogenic species (CO, acetylene, iso-propyl nitrate) were higher in the northeastern U.S. plumes by factors just larger than

Table 7.1. Ratios of median concentrations recorded over Atlanta to the median of the concentrations in 9 plumes advecting from urban centers in the northeastern U.S. VOC data are all from whole air samples.

	Atlanta/Northeastern U.S.
WSOC	0.55
CO	0.61
Acetylene	0.84
Iso-propyl nitrate	0.57
α-pinene	29
β-pinene	7.4
Isoprene	100
MVK	14
MACR	11

1 to ~2. In contrast biogenic VOCs were much higher over Atlanta, often at least 10 times greater than in the northeastern U.S. plumes. WSOC concentrations tend to follow the trends in anthropogenic emissions, being approximately twice as high in the northeastern plumes, where anthropogenic emissions were higher by similar amounts.

A comparison can also be made between ΔWSOC/ΔCO in the two regions. Recall the studies of plume evolution in the northeast (section 4.3.3) show that ΔWSOC/ΔCO increases from near zero close to the urban region to a fairly constant value of 32 ± 4 μg C/m^3/ppmv after approximately 1 to 2 days of advection. For comparison to this number, the ΔWSOC/ΔCO ratio is calculated over Atlanta using two different methods.

In the first analysis, the mean of WSOC and CO measured just above the boundary layer prior to entering and just after leaving the regions of elevated CO concentration is used as the background values to which the higher boundary layer values are compared. A background value of 0.05 μg C/m^3 (half the LOD) is used for WSOC, since the measurements were below the LOD, and 91 ppbv for CO. Variability in CO, indicated by the CO standard deviation, in the regions just above the plume was 5 ppbv, leading to approximately 5% variability in ΔWSOC/ΔCO. The ratios of ΔWSOC and ΔCO relative to this assumed constant background are also shown in Figure 7.2 and are in the range of 30 to 40 μg C/m^3/ppmv.

Alternatively, the ratio of ΔWSOC to ΔCO can also be calculated from the slope of WSOC to CO. These results are shown in Figure 7.3, where only boundary layer data are included (in-cloud sampling is also excluded since the WSOC was scavenged). These

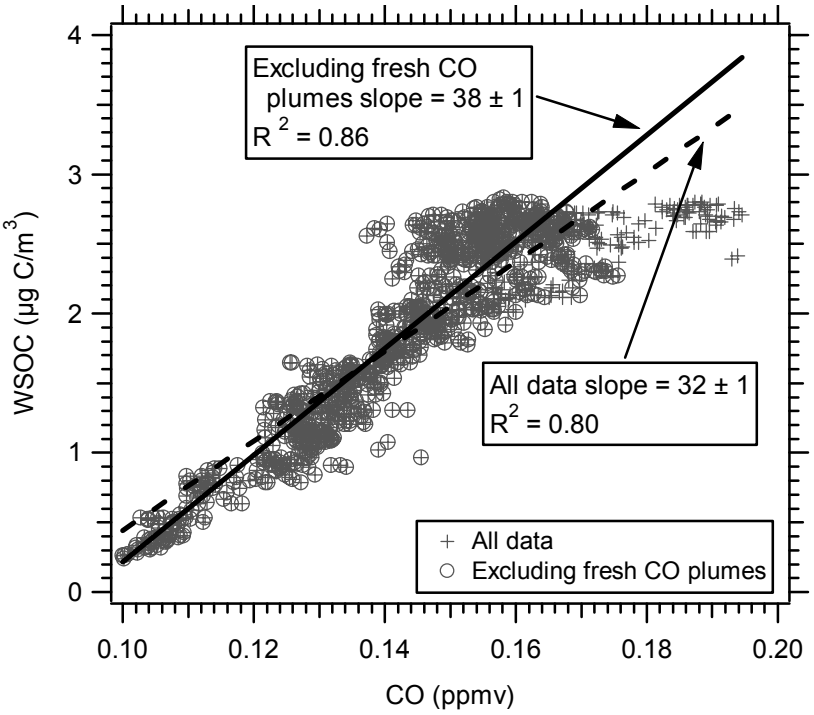

Figure 7.3. Boundary layer WSOC versus CO from the flight over Atlanta and the surrounding region. Data including and excluding the fresh CO plumes (B and C in Figure 7.2) are shown. The slope of WSOC to CO can be used as a second method to calculate the ratio of ΔWSOC to ΔCO.

data have been further subdivided to exclude periods when sampling in the fresh CO plumes identified as B and C in Figure 7.2. For all boundary layer data ΔWSOC/ΔCO is 32 ± 1 µg C/m^3/ppmv, and excluding fresh CO the ratio is 38 ± 1 µg C/m^3/ppmv (± is slope 95% confidence interval).

The two analyses produce similar results and both suggest that ratios over Atlanta and the surrounding region are very similar to 32 ± 4 µg C/m^3/ppmv, the ratio in plumes that had advected for at least one day from urban centers in the northeast. Since the biogenic VOCs are at much higher concentrations in Atlanta compared to the northeast

(Table 7.1) it is anticipated that Atlanta SOA (and hence WSOC) should have a significantly greater contribution of biogenic species compared to the northeast, and hence a substantially higher ΔWSOC to ΔCO ratio. Overall the ratios are the same, and when sampling in fresh CO regions the Atlanta ratio is only ~20% higher. It is possible that the Atlanta WSOC was still chemically evolving and that in more chemically aged air ΔWSOC/ΔCO would be substantially higher, however, estimates of Atlanta WSOC photochemical age based on the toluene to benzene ratio indicate that the age is greater than roughly one day.

7.3.2. Ground-based Measurements of Carbonaceous Aerosol Chemical Components

Integrated filters were collected and analyzed at a number of sites in urban Atlanta and the surrounding region in the summers of 2004 and 2005 to investigate sources of organic aerosols. As discussed in chapter 6, in 2004 a series of measurements (21 total) were made at the Georgia Institute of Technology (GIT) campus over a range of days in June to September. (Note, this includes the period of the NEAQS/ITCT 2004 Atlanta over-flight on 15 August 2004.) In 2005 two sets of simultaneous (paired) measurements were made to investigate spatial distributions. In both experiments one sampler remained at GIT at the same site as the 2004 experiments. In the first experiment, an identical system was situated within a meter of a major expressway (7 traffic lanes in each direction, Interstate-75/85) that runs through Atlanta and which is located approximately 400 m from the GIT sampling site. In the second experiment, conducted a number of weeks later, simultaneous samples were collected during a period

of poor air quality over four consecutive days at GIT and Yorkville, a rural site ~ 80 km west of Atlanta (see Figure 7.1).

The airborne results point to mobile sources for much of the components comprising the fine particle WSOC. This WSOC could be directly emitted by vehicles or through SOA formation of their emissions, or a combination of both. Some studies indicate that WSOC compounds, such as n-alkanoic acids and aromatic aldehydes and acids, are directly emitted by vehicles [*Rogge et al.*, 1993; *Lawrence and Koutrakis*, 1996]. However, comparisons between carbonaceous aerosols measured at the expressway, at GIT, and in Yorkville suggest that only a minor fraction of WSOC was directly emitted, instead most appeared to be formed in the atmosphere, or from reactions in the condensed phase. (Recall that this was also seen in the aircraft data of Figure 7.2, where WSOC tracked the regional CO but not the more variable fresh emissions.) Particulate EC is a known primary component of vehicle emissions, and as expected highest concentrations are observed along the expressway and lowest at the rural Yorkville site (Table 7.2). EC was a factor of about 10 larger at the expressway than at GIT, and a factor of 6 higher at GIT than Yorkville (also see Figure 7.4). Organic carbon is known to be composed of both primary and secondary compounds, and as such exhibits less difference between the various sites. OC was a factor of 1.4 higher at the expressway compared to GIT, and GIT was 1.2 times higher than Yorkville. WSOC showed little variability. Expressway WSOC was 1.1 times higher than GIT, and GIT was 1.07 times higher than Yorkville. A paired t-test on the hypothesis that the WSOC is equal at both sites has an observed significant level (p-value) of 0.039 and 0.017 for the expressway/GIT and Yorkville/GIT experiments, respectively. Side-by-side tests of the

Table 7.2. Mean ± standard deviation from two separate experiments involving simultaneous measurements of carbonaceous aerosol components. In the first experiment four separate daytime (10:00 to 22:00 EDT) integrated filter measurements were conducted simultaneously next to a major expressway (I-75/85) and a site located on the GIT campus ~ 400 m from the expressway site. Sampling was conducted on 15, 16, 17, 18 June 2005. In the second experiment, four 24 hour integrated measurements were made at Yorkville, ~ 80 km west of GIT (see Figure 7.1) starting on 23 July 2005 at 10:00 and ending 27 July 2005 at 10:00 EDT. All concentrations are in μg C/m^3.

	EC	OC	WSOC
Expressway	4.43 ± 1.02	10.82 ± 1.63	4.73 ± 0.69
GIT	0.48 ± 0.10	7.83 ± 1.03	4.33 ± 0.79
Yorkville	0.15 ± 0.01	8.51 ± 1.72	6.26 ± 1.29
GIT	0.90 ± 0.24	10.50 ± 1.75	6.72 ± 1.41

samplers and methods used in these paired experiments indicate an integrated filter WSOC measurement precision on the order of 5%. Overall these results suggest little difference in WSOC between GIT and the other two sites. Thus, it is concluded that most compounds comprising WSOC in this study are linked to mobile sources but are not directly emitted.

The regional nature of the WSOC indicated by the aircraft CO and WSOC measurement is also demonstrated in the group speciated composition results. Figure 7.4 shows the Yorkville/GIT comparison during the four day consecutive measurement period in which air quality generally worsened. Along with EC, OC, and WSOC, comparisons are made between the WSOC fractions WSOCxp_a, WSOCxp_n, and WSOCxrr_a. At the GIT site during this four day experiment, these three groups comprised, on average, 72% of the WSOC (this is discussed further below). These plots show that although primary species, EC and some portion of OC, vary between sites,

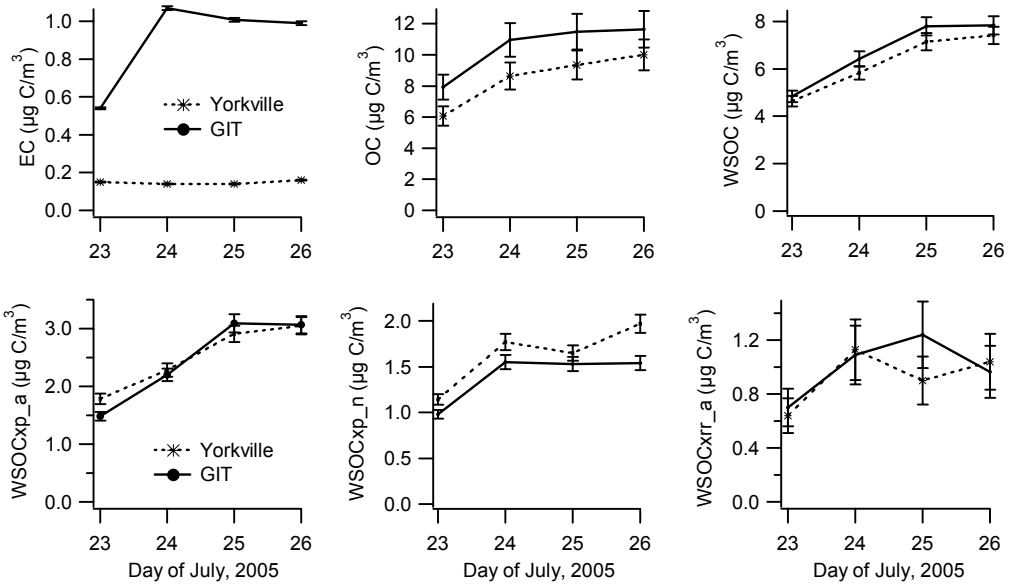

Figure 7.4. Comparison between 24 hour integrated filter measurements at GIT and the Yorkville site. The three WSOC fractions plotted (WSOCxp_a, WSOCxp_n, and WSOCxrr_a) comprise over 70% of WSOC. Uncertainties are based on side-by-side comparisons between the two instruments and extraction methods made prior to the experiment.

WSOC and its major isolated chemical fractions have similar trends in urban Atlanta and at the rural Yorkville site.

Poor air quality during this sampling period was caused by a stationary high-pressure system resulting in hot stagnant conditions (average temperature was 88^{o}F with afternoon temperatures as high as 110^{o}F). Average $PM_{2.5}$ concentrations recorded in Atlanta during the measurement period were 36 µg/m^3, with early morning concentrations greater than 40 µg/m^3 and reaching 71 µg/m^3. Note that these are significantly larger than those recorded during the fly-over in August 2004, however, in

both cases high WSOC concentrations were measured considerable distances from the urban center.

The three major components of WSOC isolated with the XAD-8/SEC method appear to be linked to a common source, or sources. For all the ground-based data collected in both the summer 2004 and 2005 experiments, WSOCxp_a, WSOCxp_n, and WSOCxrr_a have correlations (R^2) versus each other greater than 0.79 (Figure 7.5) and linear regressions have near-zero intercepts. These results imply a common source, or possibly different sources that produce a similar array of chemical fractions in the fine particles. There is, however, no evidence for a strong source for one specific group of these three fractions.

These three chemical fractions of WSOC are also well correlated with WSOC concentrations. For the data in Figure 7.5 the R^2 between WSOC and each fraction is 0.91, 0.81, and 0.84, for WSOCxp_a, WSOCxp_n, and WSOCxrr_a, respectively, and for the sum of these three fractions 0.92 (correlations not shown). In contrast, the fractions WSOCxrr_n, and especially WSOCxru, are not as well correlated with other major WSOC chemical groups, or WSOC, and appear to have different sources. For WSOCxrr_n the R^2 is less than 0.46 when regressed against other chemical fractions, and 0.42 when regressed against WSOC. For WSOCxru, all R^2 values are less than 0.20, and there is no correlation with WSOC ($R^2 = 0.05$).

Poor correlation between WSOCxru and the other major chemical groups of WSOC is intriguing. As mentioned in chapter 5, calibrations of the XAD-8 method suggest that the WSOCxru fraction contains compounds such as organic nitrates, cyclic

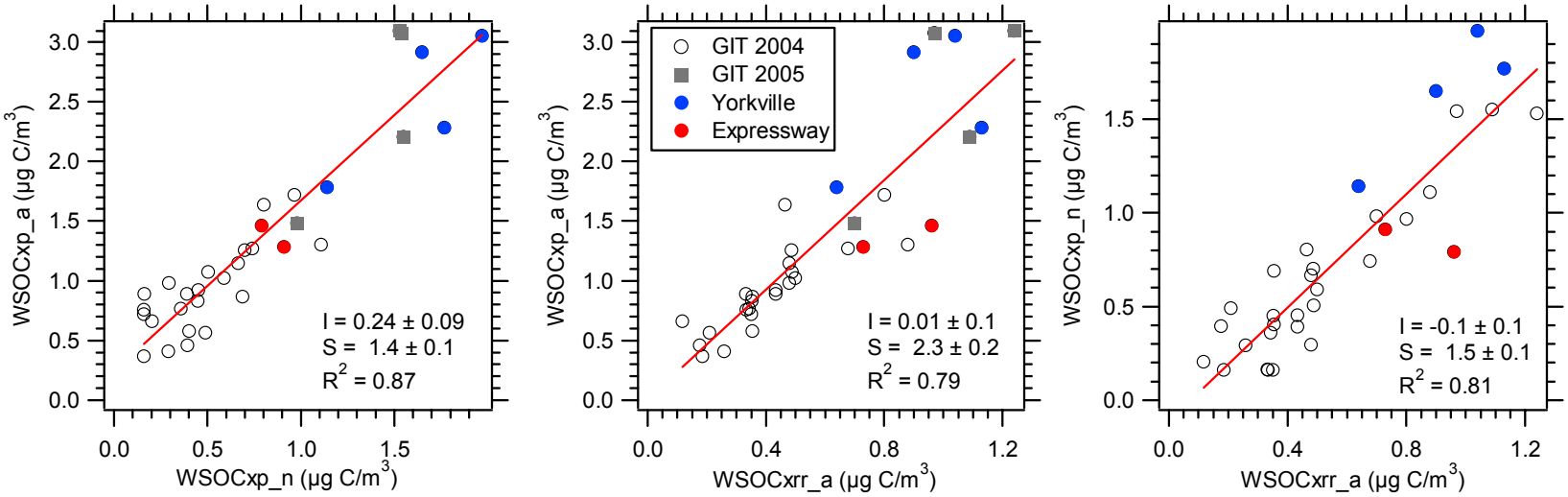

Figure 7.5. Correlation between major fractions of WSOC from 12 and 24 hour integrated filter measurements collected at GIT in 2004 and 2005, Yorkville, and the expressway. Linear regressions are for data at all sites combined, where I is the intercept, S the slope, and the uncertainty is ± one standard deviation.

acids, and aliphatic acids and carbonyls greater than C_3 or C_4, which are compounds often found in aerosols in remote regions with significant biogenic emissions. The low correlation between WSOCxru and the other three major groups (WSOCxp_a, WSOCxp_n, and WSOCxrr_a) is due to WSOCxru concentrations tending to remain unchanged during more polluted conditions when EC, OC, and WSOC all increase in concentration. Table 7.3 compares the mean concentration of the WSOC components from the summer of 2004 GIT data, divided into clean (daily peak O_3 < 85 ppbv) and more polluted conditions (daily peak O_3 > 85 ppbv), and the poor air quality period during the four day Yorkville/GIT measurements in 2005. Table 7.3 shows that the three major isolated fractions of WSOC (WSOCxp_a, WSOCxp_n, WSOCxrr_a) were at higher concentrations during the measurement periods with higher O_3 and $PM_{2.5}$, whereas WSOCxru concentrations were not. As a result, the pie charts of Figure 7.6 show that the three main components of WSOC dominate even more, and WSOCxru becomes a much smaller fraction during polluted conditions. Poor air quality episodes during the summer generally develop due to stagnant conditions associated with high-pressure systems. At these times local anthropogenic emissions may be expected to play a larger role in the formation of secondary organic aerosol, and biogenic precursors a smaller role. This is consistent with the observations of higher EC levels during the polluted events, and higher concentrations of the three major WSOC components (Table 7.3). In contrast, WSOCxru may be comprised of more biogenic SOA products and thus does not significantly change in concentration during stagnant conditions. These observations are fairly robust, similar results are found for additional data not included in this analysis.

Table 7.3. Mean and ± standard deviation of the carbonaceous aerosol, based on 24 hour integrated filter samples collected in the summers of 2004 and 2005 at GIT, as well as daily peak ozone and 24 hour mean $PM_{2.5}$ mass. The 2004 samples were from a range of days in June (7 days), August (13 days) and one day in September. The GIT Polluted 2004 data are three days during the 2004 sampling campaign having daily peak O_3 higher than 85 ppbv. The 2005 data are the GIT component of the Yorkville/GIT paired experiment recorded over four consecutive poor air quality days (July 23 through 27). All carbonaceous aerosol concentrations are in μg C/m^3.

	GIT 2004	GIT Polluted 2004	GIT Polluted 2005
Number of Samples	18	3	4
Daily Peak O_3, ppbv*	55.3 ± 16.4	96.0 ± 20.9	100.3 ± 24.5
$PM_{2.5}$*, μg/m^3	16.0 ± 7.2	31.5 ± 12.5	36.0 ± 14.6
EC	0.49 ± 0.26	1.02 ± 0.01	0.90 ± 0.24
OC	5.84 ± 1.81	11.0 ± 1.4	10.5 ± 1.8
WSOC	2.96 ± 0.69	4.05 ± 0.99	6.72 ± 1.41
WSOCxru	0.56 ± 0.19	0.30 ± 0.30	0.51 ± 0.04
WSOCxp_a (A)	0.82 ± 0.27	1.34 ± 0.59	2.46 ± 0.77
WSOCxp_n (B)	0.42 ± 0.20	0.66 ± 0.40	1.40 ± 0.28
WSOCxp_u	0.46 ± 0.36	0.77 ± 0.08	0.73 ± 0.18
WSOCxrr_a (C)	0.37 ± 0.13	0.46 ± 0.34	1.00 ± 0.23
WSOCxrr_n	0.23 ± 0.10	0.41 ± 0.08	0.42 ± 0.22
WSOCxrr_u	0.07 ± 0.17	0.09 ± 0.12	0.06 ± 0.20
(A + B + C)/WSOC	0.54 ± 0.13	0.57 ± 0.21	0.72 ± 0.05
WSOCxru/WSOC	0.20 ± 0.08	0.09 ± 0.11	0.08 ± 0.03

*GIT ozone and $PM_{2.5}$ data are from the allocated Georgia EPA site in South DeKalb in Atlanta, approximately 20 km southeast of the aerosol measurements.

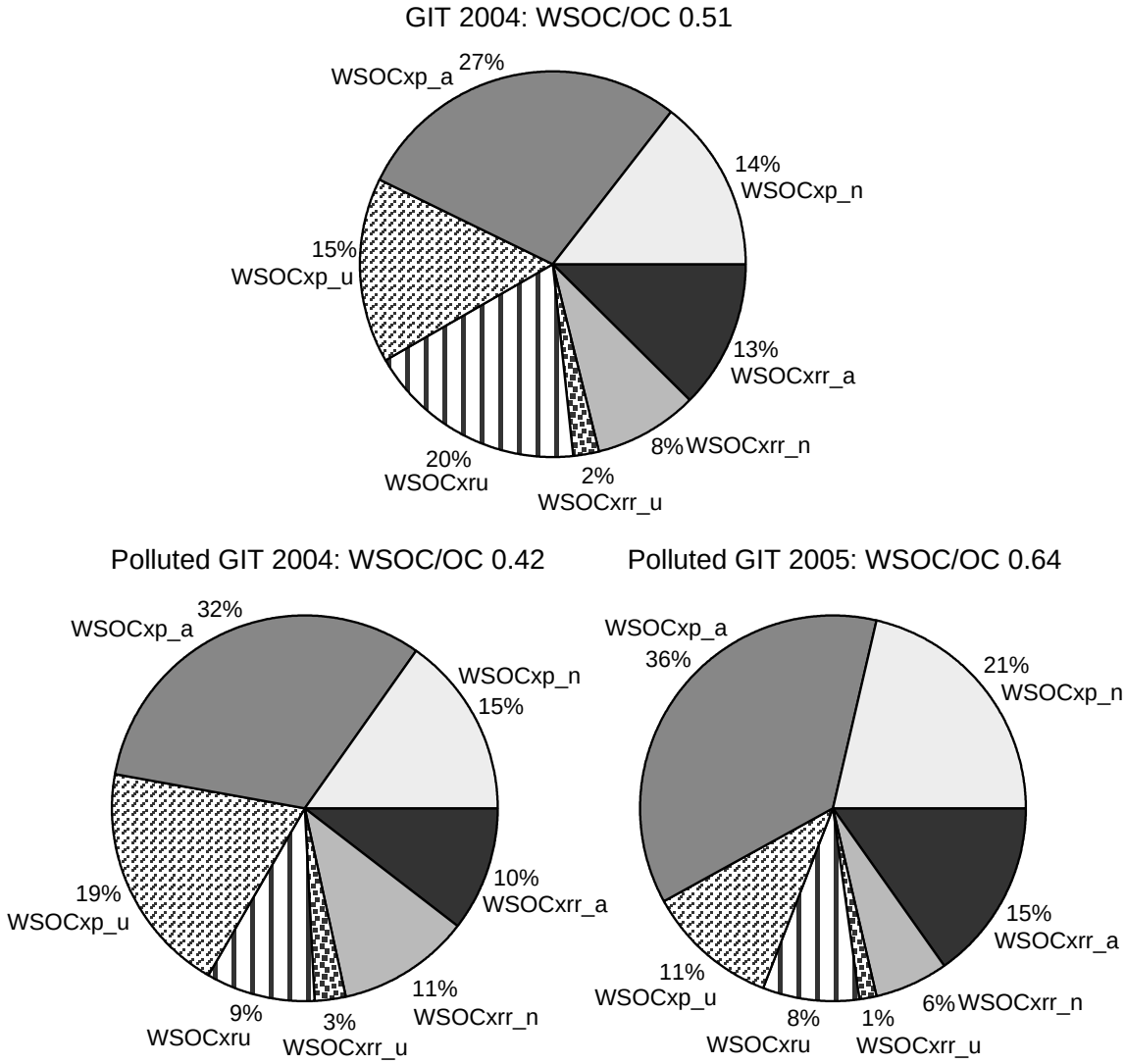

Figure 7.6. Mean XAD-8/SEC isolated fractions of WSOC from 24 hour integrated Hi-Volume $PM_{2.5}$ samples collected at GIT. The three data sets are (a) 18 samples collected in the summer of 2004, (b) 3 samples collected in the summer of 2004 during more polluted conditions, and (c) 4 consecutive day samples during the 2005 Yorkville/GIT comparison, a period of poor air quality. Concentrations are summarized in Table 7.3.

Finally, another consequence of a relatively uniform spatial distribution of WSOC compared to the more variable OC is a spatially variable WSOC to OC ratio. For the two separate paired experiments, on average WSOC/OC was 0.74 in Yorkville compared to 0.64 at GIT, and 0.56 at GIT compared to 0.42 at the expressway site. Higher WSOC to OC ratios recorded at sampling sites further from mobile sources suggest that the ratio is not due mainly to rapid in-situ SOA formation, since WSOC was nearly the same at both paired sites (see Table 7.2), but instead due to lower OC concentrations. Thus it appears that differences in primary OC between the sites is responsible for the spatial variability in WSOC/OC.

7.4. Summary

In conclusion, these data suggest that much of the fine particle WSOC is linked indirectly to vehicle emissions and may be generated via SOA formation. The current view is that aromatic VOCs from mobile sources are mostly responsible for anthropogenic SOA. However, the emissions and current yields used for predicting aromatic SOA formation will likely not account for the observed WSOC concentration, suggesting that other anthropogenic VOCs involving unknown mechanisms may efficiently lead to SOA. As previously mentioned, *de Gouw et al.* [2005] concluded that as plumes aged in the northeastern U.S. the decrease in alkanes was the only VOC with a sufficient mass change to account for the observed increases in the organic aerosol mass. It would seem likely, given the similar ΔWSOC/ΔCO ratios between the northeastern urban cities and Atlanta, that similar processes apply in Atlanta.

It also needs to be considered, as previously mentioned, studies based on radiocarbon analysis suggest that in the south and southeast most of the SOA is biogenic. Perhaps both observations are correct. It could be speculated that the SOA formation in Atlanta involves mainly biogenic VOCs, however, the process is limited by anthropogenic precursors. In other words, there is some anthropogenic component, likely linked to vehicle emissions given the high correlation between WSOC and vehicle tracers (such as an alkane derivative), which must be present for the SOA to occur. More extensive sampling in metropolitan Atlanta with additional measurement techniques should be undertaken to further investigate the extent of SOA formation and the relative roles of anthropogenic versus biogenic emissions.

CHAPTER 8
FUTURE WORK

The PILS-TOC has been shown to provide useful measurements of WSOC both on the ground and when airborne. However, with liquid systems inevitably there is the issue of smearing (i.e., mixing of the liquid sample in the various components of the system). Although due to the difference in sample time this issue is likely to be less of a factor for the ground-based WSOC measurements as opposed to the airborne WSOC measurements. As previously mentioned some measures, such as small bore tubing and small volume debubblers and liquid filters, have been taken. However, there still is room for improvement. One of the easiest solutions may be using the smallest volume possible syringes for the liquid pumping system.

The XAD-8 and SEC speciation methods do seem to provide much useful information about WSOC. However, these methods have really only begun to help in better understanding WSOC. The potential exists to continue to improve these techniques.

The calibrations for the XAD-8 column suggest that the WSOCxru fraction is composed of biogenic SOA compounds. Therefore, it would be ideal if this fraction could actually be determined directly rather than by difference (= WSOCxr – WSOCxrr). It has been suggested that an organic eluent, such as acetonitrile, could be used to recover these WSOCxru compounds. Unfortunately, the TOC analyzer could not be used as the detector if organic solvents are used for this separation. Perhaps making the XAD-8 column smaller would allow the WSOCxru compounds to also be recovered with the inorganic eluent at pH 13.

It would also be more ideal when performing on-line XAD-8 measurements if the WSOCxr fraction could also be determined on-line rather than by difference (= WSOC – WSOCxp). Based on the calibration experiments a minimum mass of 25 μg C needs to be retained on the current XAD-8 column in order to achieve near 100% recovery with pH 13 eluent. A 15 L/min PILS system cannot achieve such detection limits. However, it may be possible to add a concentrator upstream of the PILS in the current set-up to improve the detection limit of the instrument. Another possibility may be, again, reducing the size of the XAD-8 column to retain a smaller minimum mass on the XAD-8 for efficient recovery of the WSOCxr fraction.

The current SEC column requires a minimum analyte concentration of approximately 2 ppm C (2 μg C) for the analysis. Again, this has made on-line determination of the functional groups impossible. On-line measurements of each fraction would be a very useful addition to the present capabilities of the technique. There are two possibilities to investigate. One is a different column and/or resin. Keeping the same type of resin currently used, commercially available high pressure columns may provide significant improvements. They are known to have better separation than hand-packed low pressure columns and also likely would require less mass. Although since the current method uses the SEC column untraditionally, it is not clear that an appropriate high pressure column is available. A different type of resin altogether may provide better separation and/or allow for on-line measurements. The second possibility is that a modified version of the current PILS-TOC system could be used. Again, a concentrator would need to be added upstream of the PILS. For example, a concentrated XAD-8 separated sample could be collected for 1 hour in a sample loop

and then injected onto the SEC column. Therefore, a time-resolved measurement of WSOCxp into functional groups would be obtained.

There is also the possibility to separate the XAD-8 fractions further with other analytical techniques. It has been shown that the WSOCxp fraction is important during PM events. Being able to determine important compounds in this fraction that perhaps are the driving force during these PM events would be a very useful piece of information. Performing LC/MS (liquid chromatography/mass spectroscopy) on the WSOC, WSOCxp, and WSOCxrr could be a first attempt. Sample volume, liquid concentration, and the presence of salts in the sample are not an issue for LC-MS. However, finding an optimum method can be a limitation.

It was shown from performing ^{13}C-NMR on the XAD-8 fractions how the spectra were simplified by performing the separation first. Therefore, the possibility also exists to characterize the fractions obtained by SEC (WSOCxp_a, WSOCxp_n, WSOCxrr_a, and WSOCxrr_n) further by ^{13}C-NMR or techniques such as LC-MS and carbon isotope analysis. Experiments on specific SEC isolated fractions would likely provide even more insights than what can be gained by performing them on the complete sample group. Although a substantial amount of mass may need to be collected since the 1 ml sample injected onto the SEC column is diluted significantly in the eluent flowrate used in the current SEC method and these other techniques do require a higher carbon content than the TOC analyzer.

CHAPTER 9
CONCLUSIONS

The organic carbon (OC) aerosol is chemically complex making it the least understood component of aerosol particles. Since most previous analyses of the organic aerosol have dealt with the development and application of specific speciation methods, only a small fraction of the organic compounds present in the aerosol have been identified or attempted to be quantified. A useful approach, as illustrated in this thesis, is to instead apply methods capable of quantitatively measuring and speciating a large chemical fraction of the aerosol. Approaches aimed at group speciation rather than specific speciation not only provide new insights into the chemical makeup of a large fraction of the ambient organic aerosol, but the isolated fractions can also be analyzed for other properties of interest. The main emphasis of this work is on the fraction of the organic aerosol that is soluble in water (WSOC). WSOC is of interest for a number of reasons, especially since little is known about its chemical nature.

In this work, first, a method for real-time measurements of WSOC is established. Then novel techniques to further speciate and chemically characterize the WSOC are developed. The goals in developing these techniques include assessing various methods, chemically identifying a large portion of the ambient fine particle organic aerosol in urban environments, and investigating possible sources. The major findings of this work are summarized below.

A PILS-TOC (Particle-into-Liquid Sampler-Total Organic Carbon) system allows for quantitative measurements in near real-time of fine particle WSOC aerosols. The PILS captures ambient particles into a flow of purified water, which is then forced

through a liquid filter and the carbonaceous content quantified by a TOC analyzer. This system has a limit of detection of 0.1 μg C/m^3 and uncertainty of approximately ± 10%. The results obtained with this instrument are the first real-time measurements of WSOC on the ground or when airborne.

Using a PILS-TOC at an urban ground-based site in St. Louis, consistently higher WSOC to OC ratios were observed in summer than in autumn. Under episodes when air quality worsened over periods of 5 to 7 days, a regular diurnal pattern in WSOC/OC was observed, ranging from approximately 0.40 at night to 0.80 at mid-day. This trend was similar to other secondarily formed products, such as ozone, and consistent with the notion that at least some fraction of the WSOC was formed in the atmosphere by secondary processes. The elucidation of the subdaily cycle of WSOC allows for a unique observation for an urban site and demonstrates the insights gained from near real-time measurements.

Aircraft measurements made with the PILS-TOC over the northeastern U.S. during the New England Air Quality Study/Intercontinental Transport and Chemical Transformation 2004 program found biomass burning and emissions emanating from urban centers as two main sources of WSOC. Examination of urban plumes suggests WSOC is formed within approximately 1 day of emissions and may be produced from compounds co-emitted with carbon monoxide (CO).

To further speciate the WSOC, XAD-8 resin was found to provide a useful method. XAD-8 can be coupled with a PILS-TOC for on-line speciation measurements or size-exclusion chromatography (SEC) for off-line speciation measurements. The XAD-8 column itself separates the WSOC into its hydrophilic (pentrates the XAD-8 with

near 100% efficiency at pH 2) and hydrophobic (retained by the XAD-8 at pH 2) fractions. Part of the hydrophobic fraction can subsequently be extracted from the XAD-8 with high efficiently at pH 13 and is referred to as the recovered hydrophobic fraction. Calibrations with atmospherically relevant standards suggest hydrophilic compounds include aliphatic acids and carbonyls with less than 4 or 5 carbons, saccharides, and amines. Recovered hydrophobic compounds include aromatic acids and phenols (or other aromatic-like compounds with similar properties). Unrecovered hydrophobic compounds include aliphatic acids and carbonyls with greater than 3 or 4 carbons, organic nitrates, and cyclic acids. SEC, if used, further resolves the XAD-8 hydrophilic and recovered hydrophobic fractions into acidic, neutral, and basic functional groups. Although other investigators have developed methods to speciate WSOC, the key to this approach is no organic eluents are needed and therefore quantitative data can be obtained directly from either the on-line or off-line separation using the TOC analyzer.

On-line measurements of WSOC and the XAD-8 isolated hydrophilic and hydrophobic WSOC fractions in urban St. Louis and Atlanta were able to investigate daily and seasonal trends in WSOC, hydrophilic WSOC, and hydrophobic WSOC. Both the WSOC to OC and hydrophilic WSOC to OC ratios increase from winter to summer and are found to be greatest in an Atlanta summer PM event under stagnant conditions. Mainly a greater portion of hydrophilic compounds cause this increase in the WSOC fraction. These results are suggestive of an increase in summertime SOA production leading to a higher fraction of WSOC, and that most of these compounds are hydrophilic.

Based on the analysis of SEC fractions from urban Atlanta summer, hydrophilic aliphatic and recovered hydrophobic acids appear to account for 20% μg C/μg C of the

OC and are correlated with each other ($R^2 = 0.74$), with hydrophilic neutrals ($R^2 = 0.61$), and with gaseous 24 hour averaged VOCs (Volatile Organic Compounds) expected from mobile sources (e.g., isopentane $R^2 = 0.67$). In biomass burning samples, hydrophilic neutrals (e.g., saccharides) and recovered hydrophobic neutrals dominate with minor fractions of recovered hydrophobic and hydrophilic aliphatic acids. Atlanta winter samples tend to be a combination of summer and biomass samples.

Combined speciation and airborne WSOC measurements over Atlanta and its surrounding region seem to indicate that the source of WSOC is indirectly linked to vehicle emissions. This is supported by the comparison of aircraft measurements of urban plumes over metropolitan Atlanta and the northeastern U.S. which show similar ratios of ΔWSOC/ΔCO even though Atlanta has much higher concentrations of biogenic VOCs. Additionally, across Atlanta and its surrounding regions, WSOC is correlated with CO and appears to be comprised of three major chemical groups that are linked to a similar source and increase in concentration under more polluted conditions.

Although there is still much to be learned about the organic aerosol, overall, this research shows that in addition to biomass burning, the other main source of WSOC is secondary organic aerosol. From quantitative real-time measurements in urban areas, WSOC appears to track other photochemically produced compounds and increases with plume age. The application of the speciation methods to the organic aerosol (especially in urban Atlanta) suggests that SOA is mainly composed of small-chain aliphatic compounds indirectly linked to vehicle emissions.

APPENDIX A
CONCENTRATION CALCULATIONS

This appendix summarizes the equations used to calculate various parameters presented in this thesis. For each equation a sample calculation is performed using data from actual ambient samples presented in this thesis.

A.1. Calculations for On-line Measurements

The following equations are used for the data presented in chapters 3, 4, 5, and 7.

A.1.1 OC and/or EC

Determined by the Sunset Labs calculation software.

A.1.2. WSOC and/or WSOCxp

The concentrations of WSOC and WSOCxp in air are calculated using the difference in the Total and Filtered (background) air liquid concentration times the volumetric flowrate at the impactor, which includes a dilution factor, all divided by the flowrate of air. The dilution factor comes about from the design of the PILS. Liquid is added to the sample from condensing steam onto the impactor plate and the drops themselves. In a PILS-IC system, the dilution was accurately determined by spiking the transport flow with lithium. Measuring the concentration of lithium upstream and downstream of the impactor provided a measure of the dilution. A similar approach cannot be used to measure the dilution factor in the PILS-TOC system since the TOC analyzer makes a bulk measurement of organic carbon. However, the dilution by a 15 L/min PILS system is

usually around 17% +/- 0.5%. This is based on previous studies where a 15 L/min PILS-IC was operated identically to the WSOC system. Since the flowrate of liquid going over the impactor in the PILS-IC is known to be 0.17 ml/min, the volume of liquid added by the condensing steam and drops themselves can be determined. It can be assumed that this additional volume of water in the PILS-IC is the same for the PILS-TOC since both systems are run in the same manner with the exception of the higher liquid flow rate over the impactor in the PILS-TOC. Therefore, the volumetric flowrate is the flowrate of DI water over the impactor (0.61 ml/min) plus the volume of additional liquid from the condensing steam and drops themselves (((1.17 * 0.17 ml/min) – 0.17 ml/min)).

$$[\text{WSOC}] = \frac{\text{volumetric flowrate at impactor} \times \left(\begin{array}{c} \text{Total liquid concentration -} \\ \text{Filtered air liquid concentration} \end{array} \right)}{\text{air flowrate}}$$

$$[\text{WSOC}] = \frac{(0.61\,\text{ml/min} + ((1.17 \times 0.17\,\text{ml/min}) - 0.17\,\text{ml/min})) \times 100\,\text{ppb C}}{15\,\text{L/min}}$$

$$[\text{WSOC}] = 4.26\,\mu\text{g C/m}^3$$

A.1.3. WSOCxr

$$[\text{WSOCxr}] = [\text{WSOC}] - [\text{WSOCxp}]$$

$$[\text{WSOCxr}] = 4.26\,\mu\text{g C/m}^3 - 2.69\,\mu\text{g C/m}^3$$

$$[\text{WSOCxr}] = 1.57\,\mu\text{g C/m}^3$$

Note, generally the WSOC data were linearly interpolated since the WSOC and WSOCxp measurements were made sequentially, not simultaneously. The WSOCxp concentration used in the sample calculation is a typical ambient concentration presented in chapter 5.

A.1.4. WIOC

$$[\text{WIOC}] = [\text{OC}] - [\text{WSOC}]$$

$$[\text{WIOC}] = 9.04\ \mu\text{g C/m}^3 - 4.26\ \mu\text{g C/m}^3$$

$$[\text{WIOC}] = 4.78\ \mu\text{g C/m}^3$$

A.2. Calculations for Integrated Filter Measurements

The following equations are used for the data presented in chapters 6 and 7.

A.2.1. OC and/or EC

$$[\text{OC}] = \frac{\text{mass per punch} \times \text{area of filter}}{\text{air flowrate} \times \text{integration time}}$$

$$[\text{OC}] = \frac{35.9\ \mu\text{g C/cm}^2 \times 400.50\ \text{cm}^2}{1104\ \text{L/min} \times 1440\ \text{min} \times \frac{1000\ \text{cm}^3}{1\ \text{L}} \times \left(\frac{1\ \text{m}}{100\ \text{cm}}\right)^3}$$

$$[\text{OC}] = 9.04\ \mu\text{g C/cm}^3$$

A.2.2. WSOC and/or WSOCxp

$$[\text{WSOC}] = \left(\frac{\text{liquid concentration} \times \text{extraction volume}}{\text{air flowrate} \times \text{integration time}} \right) \times \frac{\text{total number of filter pieces}}{\text{number of filter pieces extracted}}$$

$$[\text{WSOC}] = \left(\frac{13050 \text{ ppb C} \times 125 \text{ ml}}{1104 \text{ L/min} \times 1440 \text{ min}} \right) \times \frac{4}{1}$$

$$[\text{WSOC}] = 4.10 \text{ µg C/m}^3$$

A.2.3. WSOCxr

$$[\text{WSOCxr}] = [\text{WSOC}] - [\text{WSOCxp}]$$

$$[\text{WSOCxr}] = 4.10 \text{ µg C/m}^3 - 2.69 \text{ µg C/m}^3$$

$$[\text{WSOCxr}] = 1.41 \text{ µg C/m}^3$$

Note, the WSOCxp concentration used in the sample calculation is a typical ambient concentration presented in chapter 6.

A.2.4. WSOCxrr and WSOCxru

First, the mass of carbon expected to be and actually retained on the XAD-8 are determined.

$$\text{expected retained mass} = \left(\text{WSOC liquid concentration - WSOCxp liquid concentration}\right) \times \text{sample flowrate over XAD - 8} \times \text{length of time sample over XAD - 8}$$

$$\text{expected retained mass} = (13050 \text{ ppb C} - 8573 \text{ ppb C}) \times 1.2 \text{ ml/min} \times 30 \text{ min} \times \frac{1\text{L}}{1000 \text{ ml}}$$

$$\text{expected retained mass} = 161 \text{ μg C}$$

$$\text{actual retained mass} = \text{WSOCxrr liquid concentration} \times \left(\begin{array}{c}\left(\begin{array}{c}\text{NaOH flowrate over XAD - 8} \times \\ \text{time collect WSOCxrr}\end{array}\right) \\ + \text{volume HCl added to adjust pH}\end{array}\right)$$

$$\text{actual retained mass} = 11300 \text{ ppb C} \times \left(\left(1.2 \text{ ml/min} \times 5 \text{ min}\right) + 4 \text{ ml}\right) \times \frac{1\text{ L}}{1000 \text{ ml}}$$

$$\text{actual retained mass} = 113 \text{ μg C}$$

Then the ratio of the actual to expected retained mass is used to determine WSOCxrr and WSOCxru from WSOCxr.

$$[\text{WSOCxrr}] = \frac{\text{actual retained mass}}{\text{expected retained mass}} \times [\text{WSOCxr}]$$

$$[\text{WSOCxrr}] = \frac{113 \text{ μg C}}{161 \text{ μg C}} \times 1.41 \text{ μg C/m}^3$$

$$[\text{WSOCxrr}] = 0.99 \text{ μg C/m}^3$$

$$[\text{WSOCxru}] = \left(1 - \frac{\text{actual retained mass}}{\text{expected retained mass}}\right) \times [\text{WSOCxr}]$$

$$[\text{WSOCxru}] = \left(1 - \frac{113\,\mu\text{g C}}{161\,\mu\text{g C}}\right) \times 1.41\,\mu\text{g C/m}^3$$

$$[\text{WSOCxru}] = 0.42\,\mu\text{g C/m}^3$$

A.2.5. Integration of SEC chromatograms

A.2.5.1. WSOC and/or WSOCxp SEC Integral

$$[\text{WSOC}]\,\text{SEC Integral} = \sum_{i=t_i}^{t_f} \left(\left(\frac{\text{eluent flowrate} \times \text{TOC Analyzer measurement interval} \times (\text{WSOC liquid concentration})_i \times \text{extraction volume}}{\text{sample loop volume} \times \text{air flowrate} \times \text{integration time}} \right) \times \frac{\text{total number of filter pieces}}{\text{number of filter pieces extracted}} \right)$$

$$[\text{WSOC}]\,\text{SEC Integral} = \sum_{i=t_i}^{t_f} \left(\left(\frac{1.3\,\text{ml/min} \times 3\,\text{s} \times \frac{1\,\text{min}}{60\,\text{s}} \times (\text{WSOC liquid concentration})_i \times 125\,\text{ml}}{1\,\text{ml} \times 1104\,\text{L/min} \times 1440\,\text{min}} \right) \times \frac{4}{1} \right)$$

$$= 4.58\,\mu\text{g C/m}^3$$

where t_i is when concentration initially starts to increase from baseline and t_f is when concentration returns to baseline.

A.2.5.2. WSOCxrr SEC Integral

$$[\text{WSOCxrr}]\,\text{SEC Integral} = \sum_{i=t_i}^{t_f} \left(\left(\begin{array}{c} \text{eluent flowrate} \times \text{TOC Analyzer measurement interval} \\ \times \left(\text{WSOC liquid concentration}\right)_i \\ \times \text{extraction volume} \times \\ \left(\left(\begin{array}{c} \text{NaOH flowrate over XAD - 8} \\ \times \text{time collect WSOCxrr} \end{array} \right) + \\ \text{volume HCl added to adjust pH} \end{array} \right) \\ \hline \begin{array}{c} \text{sample loop volume} \times \text{air flowrate} \\ \times \text{integration time} \\ \times \text{sample flowrate over XAD - 8} \\ \times \text{length of time sample over XAD - 8} \end{array} \end{array} \right) \times \frac{\text{total number of filter pieces}}{\text{number of filter pieces extracted}} \right)$$

$$[\text{WSOCxrr}]\,\text{SEC Integral} = \sum_{i=t_i}^{t_f} \left(\left(\begin{array}{c} 1.3\ \text{ml/min} \times 3\ \text{s} \times \frac{1\ \text{min}}{60\ \text{s}} \\ \times \left(\text{WSOC liquid concentration}\right)_i \\ \times 125\ \text{ml} \times \left(\left(1.2\ \text{ml/min} \times 5\ \text{min}\right) + 4\ \text{ml} \right) \\ \hline 1\ \text{ml} \times 1104\ \text{L/min} \times 1440\ \text{min} \times 1.2\ \text{ml/min} \times 30\ \text{min} \end{array} \right) \times \frac{4}{1} \right)$$

$$= 0.76\ \mu\text{g C/m}^3$$

where t_i is when concentration initially starts to increase from baseline and t_f is when concentration returns to baseline.

A.2.5.3. WSOCxp_a, WSOCxp_n, WSOCxp_b, WSOCxrr_a, and WSOCxrr_n

Chromatographic peaks that elute first (WSOCxp_a and WSCOxrr_a) were fit with a Gaussian function using data from the leading edge to slightly following the maximum value. The second peak (WSOCxp_n and WSOCxrr_n) was taken as the difference in the ambient chromatogram and the Gaussian function. Bases (WSOCxp_b), if they exist, were subtracted from the second peak by fitting with a linear baseline. More information can be found in chapter 6.

A.2.5.4. WSOCxp_u and WSOCxrr_u

$$[\text{WSOCxp\_u}] = [\text{WSOCxp}] - [\text{WSOCxp\_a}] - [\text{WSOCxp\_n}] - [\text{WSOCxp\_b}]$$

$$[\text{WSOCxp\_u}] = 2.69\ \mu g\ C/m^3 - 1.07\ \mu g\ C/m^3 - 0.50\ \mu g\ C/m^3 - 0.02\ \mu g\ C/m^3$$

$$[\text{WSOCxp\_u}] = 1.10\ \mu g\ C/m^3$$

$$[\text{WSOCxrr\_u}] = [\text{WSOCxrr}] - [\text{WSOCxrr\_a}] - [\text{WSOCxrr\_n}]$$

$$[\text{WSOCxrr\_u}] = 0.99\ \mu g\ C/m^3 - 0.49\ \mu g\ C/m^3 - 0.27\ \mu g\ C/m^3$$

$$[\text{WSOCxrr\_u}] = 0.23\ \mu g\ C/m^3$$

Note, the concentrations of WSOCxp_a, WSOCxp_n, WSOCxp_b, WSOCxrr_a, and WSOCxrr_n used in the sample calculations are typical ambient concentrations presented in chapter 6.

A.2.6. WIOC

$$[\text{WIOC}] = [\text{OC}] - [\text{WSOC}]$$

$$[\text{WIOC}] = 9.04\ \mu\text{g C/m}^3 - 4.26\ \mu\text{g C/m}^3$$

$$[\text{WIOC}] = 4.78\ \mu\text{g C/m}^3$$

REFERENCES

Andracchio, A., C. Cavicchi, D. Tonelli, and S. Zappoli, A new approach for the fractionation of water-soluble organic carbon in atmospheric aerosols and cloud drops, *Atmos. Environ., 36*, 5097-5107, 2002.

Andrews, E., P. Saxena, S. Musarra, L.M. Hildemann, P. Koutrakis, P.H. McMurry, I. Olmez, and W.H. White, Concentration and composition of atmospheric aerosols from the 1995 SEAVS experiment and a review of the closure between chemical and gravimetric measurements, *J. Air and Waste Manage. Assoc., 50*, 648-664, 2000.

Anttila, P., T. Hyötyläinen, A. Heikkilä, M. Jussila, J. Finell, M. Julmala, and M.-L. Riekkola, Determination of organic acids in aerosol particles from a coniferous forest by liquid chromatography-mass spectrometry, *J. Sep. Sci., 28*, 337-346, 2005.

Bae, M.S., J.J. Schauer, J.T. DeMinter, and J.R. Turner, Hourly and daily patterns of particle-phase organic and elemental carbon concentrations in the urban atmosphere, *J. Air and Waste Manage. Assoc., 54*, 823-833, 2004.

Bahreini, R., J.L. Jimenez, J. Wang, R.C. Flagan, J.H. Seinfeld, J.T. Jayne, and D.R. Worsnop, Aircraft-based aerosol mass spectrometer measurements of particle size and composition during Ace-Asia, *J. Geophys. Res., 108*(8645), 10.1029/2002JD003226, 2003.

Baumann, K., F. Ift, J.Z. Zhao, and W.L. Chameides, Discrete measurements of reactive gases and fine particle mass and composition during the 1999 Atlanta Supersite Experiment, *J. Geophys. Res., 108*(D7), 8416, doi:10.1029/2001JD001210, 2003.

Berresheim, H., P. Wine, and D. Davis, Sulfur in the Atmosphere in *Composition, Chemistry, and Climate of the Atmosphere*, edited by H.B. Singh, Van Nostrand Reinhold, New York, 1995.

Birch, M.E. and R.A. Cary, Elemental carbon-based method for monitoring occupational exposures to particulate diesel exhaust, *Aerosol Sci. Technol., 25*, 221-241, 1996.

Brock, C.A., F. Schröder, B. Kärcher, A. Petzold, R. Busen, and M. Fiebig, Ultrafine particle size distributions measured in aircraft exhaust plumes, *J. Geophys. Res., 105*(D21), 26555-26567, 2000.

Brock, C.A., P.K. Hudson, E.R. Lovejoy, A. Sullivan, J.B. Nowak, L.G. Huey, O.R. Copper, D.J. Cziczo, J. de Gouw, F.C. Fehsenfeld, J.S. Holloway, G. Hübler, B.G. LaFleur, D.M. Murphy, J.A. Neuman, D.K. Nicks, Jr., D.A. Orsini, D.D. Parrish, T.B. Ryerson, D.J. Tanner, C. Warneke, R.J. Weber, and J.C. Wilson, Particle characteristics following cloud-modified transport from Asia to North America, *J. Geophys. Res., 109*, D23S26, doi:10.1029/2003JD004198, 2004.

Brock, C.A., R.A. Washenfelder, M. Trainer, T.B. Ryerson, J.C. Wilson, J.M. Reeves, L.G. Huey, J.S. Holloway, D.D. Parrish, G. Hubler, and F.C. Fehsenfeld, Particle growth in the plumes of coal-fired power plants, *J. Geophys. Res.*, *107*, 10.1029/2001JD001062, 2002.

Chang, H., P. Herckes, and J.L. Collett Jr., On the use of anion exchange chromatography for the characterization of water soluble organic carbon, *Geophys. Res. Lett., 32*, L01810, doi:10.1029/2004GL021322, 2005.

Clesceri, L.S., A.E. Greenberg, and R.R. Trussell, *Standard Methods for Examination of Water and Wastewater*, American Public Health Assoc., American Water Works Assoc., and Water Pollution Control Federation, Washington D.C., 1989.

de Gouw, J.A., A.M. Middlebrook, C. Warneke, P.D. Goldan, W.C. Kuster, J.M. Roberts, F.C. Fehsenfeld, D.R. Worsnop, M.R. Canagaratna, A.A.P. Pszenny, W.C. Keene, M. Marchewka, S.B. Bertman, and T.S. Bates, Budget of organic carbon in a polluted atmosphere: Results from the New England Air Quality Study in 2002*, J. Geophys. Res., 110*, D16305, doi:10.1029/2004JD005623, 2005.

de Gouw, J.A., C. Warneke, D.D. Parrish, J.S. Holloway, M. Trainer, and F.C. Fehsenfeld, Emission sources and ocean uptake of acetonitrile (CH_3CN) in the atmosphere, *J. Geophys. Res., 108*(D11), 4329, doi:10.1029/2002JD002897, 2003b.

de Gouw, J.A., C. Warneke, T. Karl, G. Eerdekens, C. van der Veen, and R. Fall, Sensitivity and specificity of atmospheric trace gas detection by proton-transfer-reaction mass spectrometry, *Int. J. Mass Spectrom., 223-224*, 365-382, 2003a.

Decesari, S., M.C. Facchini, E. Matta, F. Lettini, M. Mircea, S. Fuzzi, E. Tagliavini, and J.-P. Putaud, Chemical features and seasonal variation of fine aerosol water-soluble organic compounds in the Po Valley, Italy, *Atmos. Environ., 35*, 3691-3699, 2001.

Decesari, S., M.C. Facchini, E. Matta, M. Mircea, S. Fuzzi, A.R. Chughtai, and D.M. Smith, Water soluble organic compounds formed by oxidation of soot, *Atmos. Environ., 36*, 1827-1832, 2002.

Decesari, S., M.C. Facchini, S. Fuzzi, and E. Tagliavini, Characterization of water-soluble organic compounds in atmospheric aerosol: A new approach, *J. Geophys. Res., 105*, 1481-1489, 2000.

Draxler, R.R. and G.D. Rolph, HYSPLIT (HYbrid Single-Particle Lagrangian Integrated Trajectory) Model access via NOAA ARL READY Website (http://www.arl.noaa.gov/ready/hysplit4.html), NOAA Air Resources Laboratory, Silver Spring, MD, 2003.

Eatough, D.J., A. Wadsworth, D.A. Eatough, J.W. Crawford, L.D. Hansen, and E.A. Lewis, A multiple system, multi-channel diffusion denuder sampler for the determination of fine-particulate organic material in the atmosphere, *Atmos. Environ., 27A*, 1213-1219, 1993.

Edney, E.O., T.E. Kleindienst, M. Jaoui, M. Lewandowski, J.H. Offenberg, W. Wang, and M. Claeys, Formation of 2-methyl tetrols and 2-methylglyceric acid in secondary organic aerosol from laboratory irradiated isoprene/NO_x/SO_2/air mixtures and their detection in ambient $PM_{2.5}$ samples collected in the eastern United States, *Atmos. Environ., 39*, 5281-5289, 2005.

Eller, P.M. and M.E. Cassinelli (Eds.), *NIOSH Manual of Analytical Methods, 4th Edition (1st Supplement)*, National Institute for Occupational Safety and Health, Cincinnati, 1996.

EPA, U.S. Environmental Protection Agency, "National Air Pollution Emission Trends, 1900-1996," EPA-454/R-97-011, December 1997.

EPA, U.S. Environmental Protection Agency, "The particle pollution report: Current understanding of air quality and emissions through 2003," EPA-454-R-04-002, 2004.

Facchini, M.C., M. Mircea, S. Fuzzi, and R.J. Charlson, Cloud albedo enhancement by surface-active organic solutes in growing droplets, *Nature, 401*, 257-259, 1999.

Facchini, M.C., S. Decesari, M. Mircea, S. Fuzzi, and G. Loglio, Surface tension of atmospheric wet aerosol and cloud/fog droplets in relation to their organic carbon content and chemical composition, *Atmos. Environ., 34*, 4853-4857, 2000.

Finlayson-Pitts, B.J. and J.N. Pitts, Jr., *Chemistry of the Upper and Lower Atmosphere Theory, Experiments, and Applications*, Academic Press, New York, 2000.

Forstner, H.J.L, R.C. Flagan, and J.H. Seinfeld, Molecular speciation of secondary organic aerosol from the higher alkenes: 1-octene and 1-decene, *Atmos. Environ., 31*, 1953-1964, 1997a.

Forstner, H.J.L., J.H. Seinfeld, and R.C. Flagan, Secondary Organic Aerosol from the Photooxidation of Aromatic Hydrocarbons: Molecular Composition, *Environ. Sci. Technol., 31*, 1345-1358, 1997b.

Fraser, M.P., G.R. Cass, and B.R.T. Simoneit, Air Quality Model Evaluation Data for Organics. 6. C_3-C_{24} Organic Acids, *Environ. Sci. Tech., 37*, 446-453, 2003.

Gill, P.S., T.E. Graedel, and C.J. Weschler, Organic Films on Atmospheric Aerosol Particles, Fog Droplets, Cloud Droplets, Raindrops, and Snowflakes, *Rev. Geophys. Space Phys., 21*, 903-920, 1983.

Glasius, M., M. Lahaniati, A. Calogirou, D.D. Bella, N.R. Jensen, J. Hjorth, D. Kotzias, and B.R. Larsen, Carboxylic Acids in Secondary Aerosols from Oxidation of Cyclic Monoterpenes by Ozone, *Environ. Sci. Technol., 34*, 1001-1010, 2000.

Graham, B., O.L. Mayol-Bracero, P. Guyon, G.C. Roberts, S. Decesari, M.C. Facchini, P. Artaxo, W. Maenhaut, P. Koll, and M.O. Andreae, Water-soluble organic compounds in biomass burning aerosols over Amazonia 1. Characterization by

NMR and GC-MS, *J. Geophys. Res., 107*, 8047, doi: 10.1029/2001JD000336, 2002.

Griffin, R.J., D.R. Crocker III, R.C. Flagan, and J.H. Seinfeld, Organic aerosol formation from the oxidation of biogenic hydrocarbons, *J. Geophys. Res., 104*(D3), 3555-3568, doi:10.1029/1998JD100049, 1999.

Grosjean, D. and J.H. Seinfeld, Parameterization of the Formation Potential of Secondary Organic Aerosols, *Atmos. Environ., 23*, 1733-1747, 1989.

Grosjean, D. and S.K. Friedlander, Formation of organic aerosols from cyclic olefins and diolefins, *Adv. Environ. Sci. Technol., 9*, 435-473, 1980.

Grosjean, D., *In Situ*, Organic Aerosol Formation during a Smog Episode: Estimated Production and Chemical Functionality, *Atmos. Environ., 26A*, 953-963, 1992.

Hamilton, J., P. Webb, A. Lewis, J. Hopkins, S. Smith, and P. Davy, Partially oxidised organic components in urban aerosol using GCxGC-TOF/MS, *Atmos. Chem. Phys. Discuss., 4*, 1393-1423, 2004.

Harley, R.A., M.P. Hannigan, M.P., and G.R. Cass, Respeciation of organic gas emissions and the detection of excess unburned gasoline in the atmosphere, *Environ. Sci. Technol., 26*, 2395-2408, 1992.

Hatakeyama, S., M. Ohno, J. Weng, H. Takagi, and H. Akimoto, Mechanism for the formation of gaseous and particulate products from ozone-cycloalkene reactions in air, *Environ. Sci. Technol., 21*, 52-57, 1987.

Hatakeyama, S., T. Tanonaka, J. Weng, H. Bandow, H. Takagi, and H. Akimoto, Ozone-cyclohexene reaction in air: quantitative analysis of particulate products and the reaction mechanism, *Environ. Sci. Technol., 19*, 935-942, 1985.

Havers, N., P. Burba, J. Lambert, and D. Klockow, Spectroscopic Characterization of Humic-Like Substances in Airborne Particulate Matter, *J. Atmos. Chem., 29*, 45-54, 1998.

Hedges, J.I., J.A. Baldock, Y. Gelinas, C. Lee, M.L. Peterson, and S.G. Wakeham, The biochemical and elemental compositions of marine plankton: A NMR perspective, *Marine Chemistry, 78*, 47-63, 2002.

Her, N., G. Amy, D. Foss, J. Cho, Y. Yoon, and P. Kosenka, Optimization of Method for Detecting and Characterizing NOM by HPLC – Size Exclusion Chromatography with UV and On-Line DOC Detection, *Environ. Sci. Technol., 36*, 1069-1076, 2002a.

Her, N., G. Amy, D. Foss, J. Cho, Y. Yoon, and P. Kosenka, Optimization of Method for Detecting and Characterizing NOM by HPLC – Size Exclusion Chromatography with UV and On-Line DOC Detection, *Environ. Sci. Technol., 36*, 1069-1076, 2002b.

Hoffmann, T., J.R. Odum, F. Bowman, D. Collins, D. Klockow, D., R.C. Flagan, and J.H. Seinfeld, Formation of organic aerosols from the oxidation of biogenic hydrocarbons, *J. Atmos. Chem., 26*, 189-222, 1997.

Holloway, J.S., R.O. Jakoubek, D.D. Parrish, C. Gerbig, A. Volz-Thomas, S. Schmitgen, A. Fried, B. Wert, B. Henry, and J.R. Drummond, Airborne intercomparison of vacuum ultraviolet fluorescence and tunable diode laser absorption measurements of tropospheric carbon monoxide, *J. Geophys. Res., 105*(D19), 24251-24261, 2000.

Huebert, B., T. Bertram, J. Kline, S. Howell, D. Eatough, and B. Blomquist, Measurements of organic and elemental carbon in Asian outflow during ACE-Asia from the NSF/NCAR C-130, *J. Geophys. Res., 109*, D19S11, doi:10.1029/2004JD004700, 2004.

Jacobson, M.C., H.-C. Hansson, K.J. Noone, and R.J. Charlson, Organic atmospheric aerosols: Review and state of the science, *Reviews of Geophys.*, *38*, 267-294, 2000.

Jang, M. and R.M. Kamens, Characterization of Secondary Aerosol from the Photooxidation of Toluene in the Presence of NO_x and 1-Propene, *Environ. Sci. Technol., 35*, 3626-3639, 2001.

Jang, M. and S.R. McDow, Products of Benz[*a*]anthracene Photodegradation in the Presence of Known Organic Constituents of Atmospheric Aerosols, *Environ. Sci. Technol., 31*, 1046-1053, 1997.

Kalberer, M., D. Paulsen, M. Sax, M. Steinbacher, J. Dommen, A.S.H. Prevot, R. Fisseha, E. Weingartner, V. Frankevich, R. Zenobi, and U. Baltensperger, Identification of Polymers as Major Components of Atmospheric Organic Aerosols, *Science, 303*, 1659-1662, 2004.

Kanakidou, M., J.H. Seinfeld, S.N. Pandis, I. Barnes, F.J. Dentener, M.C. Facchini, R. Van Dingenen, B. Ervens, A. Nenes, C.J. Nielsen, E. Swietlicki, J.P. Putaud, Y. Balkanski, S. Fuzzi, J. Horth, G.K. Moortgat, R. Winterhalter, C.E.L. Myhre, K. Tsigaridis, E. Vignati, E.G. Stephanou, and J. Wilson, Organic aerosol and global climate modelling: a review, *Atmos. Chem. Phys., 5*, 1053-1123, 2005.

Kawamura, K. and F. Sakaguchi, Molecular distributions of water soluble dicarboxylic acids in marine aerosols over the Pacific Ocean including tropics, *J. Geophys. Res., 104*, 3501-3509, 1999.

Kawamura, K. and K. Ikushima, Seasonal Changes in the Distribution of Dicarboxylic Acids in the Urban Atmosphere, *Environ. Sci. Technol., 27*, 2227-2235, 1993.

Kawamura, K., L. Ng, and I.R. Kaplan, Determination of organic acids (C_1-C_{10}) in the atmosphere motor exhausts, and engine oils, *Environ. Sci. Technol., 19*, 1082-1086, 1985.

Kawamura, K., N. Umemoto, M. Mochida, T. Bertram, S. Howell, and B.J. Huebert, Water-soluble dicarboxylic acids in the tropospheric aerosols collected over east Asia and western North Pacific by ACE-Asia C-130 aircraft, *J. Geophys. Res., 108*(D23), 8639, doi:10.1029/2002JD003256, 2003.

Khwaja, H.A., Atmospheric concentrations of carboxylic acids and related compounds at a semiurban site, *Atmos. Environ., 29*, 127-139, 1995.

Kirchstetter, T.W., R.A. Harley, N.M. Kreisberg, M.R. Stolzenburg, and S.V. Hering, On-road measurement of fine particle and nitrogen oxide emissions from light- and heavy-duty motor vehicles, *Atmos. Environ., 33*, 2955-2968, 1999.

Kirchstetter, T.W., T. Novakov, P.V. Hobbs, and B. Magi, Airborne measurements of carbonaceous aerosols in southern Africa during the dry biomass burning season, *J. Geophys. Res., 108*(D13), 8476, doi:10.1029/2002JD002171, 2003.

Kiss, G., E. Tombácz, B. Varga, T. Alsberg, and L. Persson, Estimation of the average molecular weight of humic-like substances isolated from fine atmospheric aerosol, *Atmos. Environ., 37*, 3783-3794, 2003.

Kiss, G., B. Varga, I. Galambos, and I. Ganszky, Characterization of water-soluble organic matter isolated from atmospheric fine aerosol, *J. Geophys., Res., 107*(D21), 8339, doi:10.1029/2001JD000603, 2002.

Krivácsy, Z., A. Gelencsér, G. Kiss, E. Mészáros, A. Molnár, A. Hoffer, T. Mészáros, Z. Sárvári, D. Temesi, B. Varga, U. Baltensperger, S. Nyeki, and E. Weingartner, Study of Chemical Character of Water Soluble Organic Compounds in Fine Atmospheric Aerosol at the Jungfraujoch, *J. Atmos. Chem., 39*, 235-259, 2001.

Krivácsy, Z., Gy. Kiss, B. Varga, I. Galambos, Zs. Sárvári, A. Gelencsér, Á. Molnár, S. Fuzzi, M.C. Facchini, S. Zappoli, A. Andracchio, T. Alsberg, H.C. Hansson, and L. Persson, Study of humic-like substances in fog and interstitial aerosol by size-exclusion chromatography and capillary electrophoresis, *Atmos. Environ., 34*, 4273-4281, 2000.

Kroll, J.H., N.L. Ng, S.M. Murphy, R.C. Flagan, and J.H. Seinfeld, Secondary organic aerosol formation from isoprene photooxidation under high-NOx conditions, *Geophys. Res. Lett., 32*, L18808, doi:10.1029/2005GL023637, 2005.

Lawrence, J. and P. Koutrakis, Measurement and speciation of gas and particulate phase organic acidity in an urban environment 2. Speciation, *J. Geophys. Res., 101*, 9171-9184, 1996.

Lemire, K.R., D.T. Allen, G.A. Klouda, and C.W. Lewis, Fine particulate matter source attribution for southeast Texas using $^{14}C/^{13}C$ ratios, *J. Geophys. Res., 107*(D22), 4613, doi:10.1029/2002JD002339, 2002.

Lim, H.-J. and B.J. Turpin, Origins of primary and secondary organic aerosol in Atlanta: Results of Time-Resolved Measurements during the Atlanta Supersite Experiment, *Environ. Sci. Technol., 36,* 4489-4496, 2002.

Lim, H.-J., B.J. Turpin, E. Edgerton, S.V. Hering, G. Allen, H. Maring, and P. Solomon, Semi-continuous aerosol carbon measurements: Comparison of Atlanta Supersite measurements, *J. Geophys. Res., 108*, 8419, 10.1029/2001JD001214, 2003.

Limbeck, A., M. Kulmala, and H. Puxbaum, Secondary organic aerosol formation in the atmosphere via heterogeneous reaction of gaseous isoprene on acidic particles, *Geophys. Res. Lett., 30*(19), 1996, doi:10.1029/2003GL017738, 2003.

Maria, S.F., L.M. Russell, B.J. Turpin, and R.J. Porcja, FTIR measurements of functional group and organic mass in aerosol samples over the Caribbean, *Atmos. Environ., 36*, 5185-5196, 2002.

Maria, S.F., L.M. Russell, B.J. Turpin, R.J. Porcja, T.L. Campos, R.J. Weber, and B.J. Huebert, Source signatures of carbon monoxide and organic functional groups in Asian Pacific Regional Aerosol Characterization Experiment (ACE-Asia) submicron aerosol types, *J. Geophys. Res., 108*(D23), 8637, doi:10.1029/2003JD003703, 2003.

Marple, V.A., K.L. Rubow, and S.M. Behm, A microorifice uniform deposit impactor (MOUDI): description, calibration, and use, *Aerosol Sci. Technol., 14*, 434-446, 1991.

Mayol-Bracero, O.L., P. Guyon, B. Graham, G.C. Roberts, M.O. Andreae, S. Decesari, M.C. Facchini, S. Fuzzi, and P. Artaxo, Water-soluble organic compounds in biomass burning aerosols over Amazonia 2. Apportionment of the chemical composition and importance of the polyacidic fraction, *J. Geophys. Res.*, *107,* 891, 10.1029/2001JD000522, 2002b.

Mayol-Bracero, O.L., R. Gabriel, M.O. Andreae, T.W. Kirchstetter, T. Novakov, J. Ogren, P. Sheridan, and D.G. Streets, Carbonaceous aerosols over the Indian Ocean during the Indian Ocean Experiment (INDOEX): Chemical characterization, optical properties, and probable sources, *J. Geophys. Res., 107*(D19), 8030, doi:10.1029/2000JD000039, 2002a.

McDow, S.R. and J.J. Huntzicker, Vapor absorption artifact in the sampling of organic aerosol: Face velocity effects, *Atmos. Environ., Part A, 24*, 2563-2571, 1990.

Mochida, M., K. Kawamura, N. Umemoto, M. Kobayashi, S. Matsunaga, H.-J. Lim, B.J. Turpin, T.S. Bates, and B.R.T. Simoneit, Spatial distributions of oxygenated organic compounds (dicarboxylic acids, fatty acids, and levoglucosan) in marine aerosols over the western Pacific and off the coast of East Asia: Continental outflow of organic aerosols during the ACE-Asia campaign, *J. Geophys. Res., 108*(D23), 8638, doi:10.1029/2002JD003249, 2003.

Mukai, A. and Y. Ambe, Characterization of humic acid-like brown substance in airborne particulate matter and tentative identification of its origin, *Atmos. Environ., 20,* 813-819, 1986.

Narukawa, M., K. Kawamura, N. Takeuchi, and T. Nakajima, Distribution of dicarboxylic acids and carbon isotope compositions in aerosols from 1997 Indonesian forest fires, *Geophys. Res. Lett., 26*, 3101-3104, 1999.

Novakov, T. and C.E. Corrigan, Cloud condensation nucleus activity of the organic component of biomass smoke particles, *Geophys. Res. Lett., 16*, 2141-2144, 1996.

Novakov, T. and J.E. Penner, Large contribution of organic aerosols to cloud-condensation-nuclei concentrations, *Nature, 365*, 823-826, 1993.

Novakov, T., D.A. Hegg, and P.V. Hobbs, Airborne measurements of carbonaceous aerosols on the East Coast of the United States, *J. Geophys. Res., 102*(D25), 30023-30030, 1997.

Odum, J.R., T.P.W. Jungkamp, R.J. Griffin, R.C. Flagan, and J.H. Seinfeld, The atmospheric aerosol-forming potential of whole gasoline vapor, *Science, 276*, 96-99, 1997.

Orsini, D.A., Y. Ma, A. Sullivan, B. Sierau, K. Baumann, and R.J. Weber, Refinements to the particle-into-liquid sampler (PILS) for ground and airborne measurements of water-soluble aerosol composition, *Atmos. Environ., 37*, 1243-1259, 2003.

Palen, E.J., D.T. Allen, S.N. Pandis, S.E. Paulson, J.H. Seinfeld, and R.C. Flagan, Fourier Transform Infrared Analysis of Aerosol Formed in the Photo-oxidation of Isoprene and ß-Pinene, *Atmos. Environ., 26A*, 1239-1251, 1992.

Pandis, S.N., S.E. Paulson, J.H. Seinfeld, and R.C. Flagan, Aerosol formation in the photooxidation of isoprene and ß-pinene, *Atmos. Environ., 25A*, 997-1008, 1991.

Rogge, W.F., L.M. Hildemann, M.A. Mazurek, G.R. Cass, and B.R.T. Simoneit, B.R.T., Sources of fine organic aerosol. 2. Noncatalyst and catalyst-equipped automobiles and heavy-duty diesel trucks, *Environ. Sci. Technol., 27*, 636-651, 1993.

Rolph, G.D., Real-time Environmental Applications and Display sYstem (READY) Website (http://www.arl.noaa.gov/ready/hysplit4.html), NOAA Air Resources Laboratory, Silver Spring, MD, 2003.

Russell, M. and D.T. Allen, Predicting secondary organic aerosol formation rates in southeast Texas, *J. Geophys. Res., 110*, D07S17, doi:10.1029/2004JD004722, 2005.

Sannigrahi, P., A.P. Sullivan, R.J. Weber, and E.D. Ingall, Characterization of water-soluble organic carbon in urban atmospheric aerosols using solid-state ^{13}C NMR spectroscopy, *Environ. Sci. Technol., 40*, 666-672, 2006.

Sannigrahi, P., E.D. Ingall, and R. Benner, Cycling of dissolved and particulate organic matter at station Aloha: Insights from ^{13}C NMR spectroscopy coupled with elemental, isotopic and molecular analyses, *Deep Sea Research I, 52*, 1429-1444, 2005.

Saxena, P. and L.M. Hildemann, Water-soluble organics in atmospheric particles: A critical review of the literature and application of thermodynamics to identify candidate compounds, *J. Atmos. Chem., 24*, 57-109, 1996.

Saxena, P., L.M. Hildemann, P.H. McMurry, and J.H. Seinfeld. Organics alter hygroscopic behavior of atmospheric particles, *J. Geophys. Res., 100*, 18755-18770, 1995.

Schauer, J.J., W.F. Rogge, L.M. Hildemann, M.A. Mazurek, G.R. Cass, and B.R.T. Simoneit, Source Apportionment of Airborne Particulate Matter Using Organic Compounds as Tracers, *Atmos. Environ., 30*, 3837-3855, 1996.

Seinfeld, J.H. and S.N. Pandis, *Atmospheric Chemistry and Physics: From Air Pollution to Climate Changes*, John Wiley & Sons, New York, 1998.

Sheesley, R.J., J.J. Schauer, E. Bean, and D. Kenski, Trends in secondary organic aerosol at a remote site in Michigan's Upper Peninsula, *Environ. Sci. Technol., 38,* 6491-6500, 2004.

Simoneit, B.R.T., Biomass burning – a review of organic tracers for smoke from incomplete combustion, *Applied Geochem., 17*, 129-162, 2002.

Sorooshian, A., F.J. Brechtel, Y. Ma, R.J. Weber, A. Corless, R.C. Flagan, and J.H. Seinfeld, Modeling and characterization of a modified Particle-into-Liquid Sampler (PILS) optimized for aircraft sampling, *J. Geophys. Res.,* submitted, 2005.

Specht, C.H. and F.H. Frimmel, Specific Interactions of Organic Substances in Size-Exclusion Chromatography, *Environ. Sci. Technol., 34*, 2361-2366, 2000.

Stohl, A., S. Eckhardt, C. Forster, P. James, N. Spichtinger, and P. Seibert, A replacement for simple back trajectory calculations in the interpretation of atmospheric trace substance measurements, *Atmos. Environ., 36*, 4635-4648, 2002.

Thurman, E.M. and R.L. Malcolm, Preparative Isolation of Aquatic Humic Substances, *Environ. Sci. Technol., 15*, 463-466, 1981.

Turpin, B.J., J.J. Huntzicker, and S.V. Hering, Investigation of organic aerosol sampling artifacts in the Los Angeles basin, *Atmos. Environ., 28*, 3061-3071, 1994.

Weber, R., D. Orsini, M. Bergin, C.S. Kiang, M. Chang, J. St. John, C. Carrico, Y.-N. Lee, P. Dasgupta, J. Slanina, B. Turpin, E. Edgerton, S. Hering, G. Allen, P. Solomon, and W. Chameides, Short-Term Temporal Variation In PM2.5 Mass

And Chemical Composition During The Atlanta Supersite Experiment, 1999, *J. Air and Waste Manage. Assoc., 53*, 84-91, 2003.

Weber, R.J., D. Orsini, Y. Daun, Y.-N. Lee, P. Klotz, and F. Brechtel, A particle-in-liquid collector for rapid measurement of aerosol chemical composition, *Aerosol Sci. Tech., 35*, 718-727, 2001.

Wilson, J.C., B.G. Lafleur, H. Hilbert, W.R. Seebaugh, J. Fox, D.W. Gesler, C.A. Brock, B.J. Huebert, and J. Mullen, Function and Performance of a Low Turbulence Inlet for Sampling Supermicron Particles from Aircraft Platforms, *Aerosol Sci. Technol., 38*, 790-802, 2004.

Wilson, M.A., *NMR techniques and applications in geochemistry and soil chemistry*, Pergamon, Oxford, 1987.

Zappoli, S., A. Andracchio, S. Fuzzi, M.C. Facchini, A. Gelencsér, G. Kiss, Z. Krivácsy, A. Molnár, E. Mészáros, H.-C. Hansson, K. Rosman, and Y. Zebühr, Inorganic, organic and macromolecular components of fine aerosol in different areas of Europe in relation to their water solubility, *Atmos. Environ., 33*, 2733-2743, 1999.

Zhang, Q., C. Anastasio, and M. Jimenez-Cruz, Water-soluble organic nitrogen in atmospheric fine particle ($PM_{2.5}$) from northern California, *J. Geophys. Res., 107*(D11), AAC, doi:10.1029/2001JD000870, 2002.